Asian Journal of Natural Product Biochemistry

| Asian J Nat Prod Biochem | vol. 23 | no. 2 | December 2025 |
| ISSN 2775-4189| E-ISSN 2775-4197 |

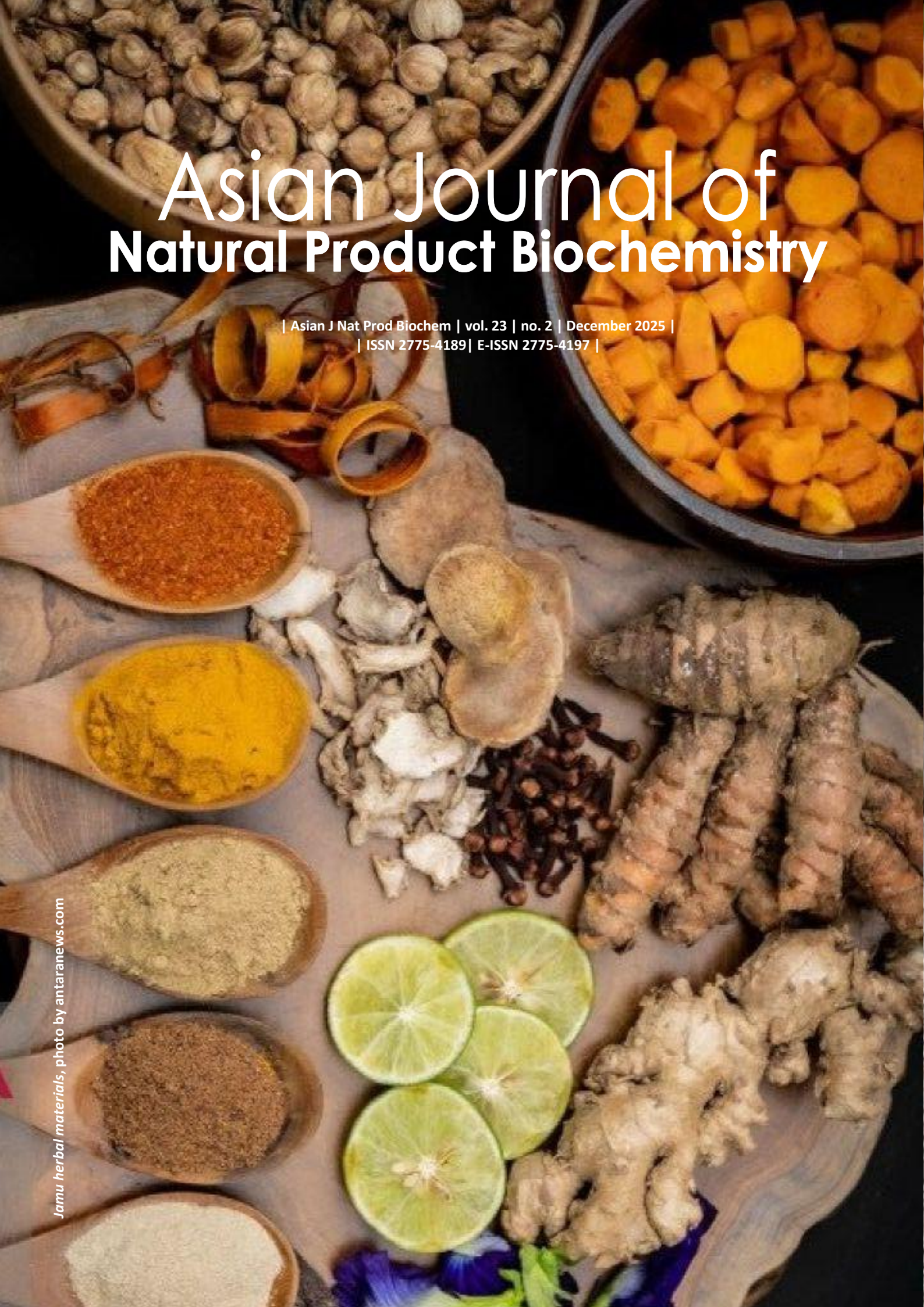

Jamu herbal materials, photo by antaranews.com

Asian Journal of Natural Product Biochemistry

| Asian J Nat Prod Biochem | vol. 23 | no. 2 | December 2025 |

Published semiannually **PRINTED IN INDONESIA**

ISSN: 2775-4189 E-ISSN: 2775-4197

9 772775 418458 9 772775 419455

Asian Journal of Natural Product Biochemistry

| Asian J Nat Prod Biochem | vol. 23 | no. 2 | December 2025 |

ONLINE
http://smujo.id/jnpb

p-ISSN
2775-4189

e-ISSN
2775-4197

PUBLISHER
Smujo International

ASSOCIATION
Society for Indonesian Biodiversity

INSTITUTION
Universitas Sebelas Maret, Surakarta, Indonesia

OFFICE ADDRESS
Jl. Ir. Sutami 36A, Surakarta 57126, Central Java, Indonesia. Tel./fax. +62-271-663375, email: editors@smujo.id

PERIOD OF ISSUANCE
June, December

Society for Indonesia Biodiversity

Universitas Sebelas Maret Surakarta, Indonesia

Published by Smujo International for The Society for Indonesian Biodiversity and Sebelas Maret University, Surakarta, Indonesia

GUIDANCE FOR AUTHORS

Aims and Scope *Asian Journal of Natural Product Biochemistry* (**Asian J Nat Prod Biochem**) (*formerly Biofarmasi*) encourages submission of manuscripts dealing with all important contributions to natural product chemistry, include bioactivity compounds of land and sea and of plants, microbes and animals; activities of antimicrobial, antiviral, antiparasite, anti-cancer, etc.; ethnopharmacology, ethnomedicines and medical application; plant-derived drugs and pharmaceutical formulations and evaluation; as well as biochemistry, chemistry, biotechnology, physiology, cell structures, pharmacology, toxicology, and chemical ecology of natural products.

Article types The journal seeks for: (i) **Research papers**, (ii) **Reviews**, and (iii) **Short communications**. Original full-length research manuscripts are limited to 8,000 words (including tables and figures) or proportional to articles in this publication number (beyond that, it should be with notice). Review articles are also limited to 8,000 words, while Short communications should be less than 2,500 words, except for pre-study (can be more).

Submission: The journal only accepts online submissions through the open journal system **(https://smujo.id/jnpb/about/submissions)** or, for login problems, email the editors at unsjournals@gmail.com (or editors@smujo.id). Submitted manuscripts should be the original works of the author(s). Please ensure that the manuscript is submitted using the template, which can be found at (https://biodiversitas.mipa.uns.ac.id/D/template.doc). The manuscript must be accompanied by a cover letter containing the article title, the first name and last name of all the authors, and a paragraph describing the claimed novelty of the findings versus current knowledge. Please also provide a list of five potential reviewers in your cover letter. They should come from outside your institution and better from three different countries. Submission of a manuscript implies the submitted work has not been published (except as part of a thesis or report, or abstract) and is not being considered for publication elsewhere. When a group writes a manuscript, all authors should read and approve the final version of the submitted manuscript and its revision; and agree on the submission of manuscripts for this journal. All authors should have made substantial contributions to the concept and design of the research, acquisition of the data and its analysis, drafting the manuscript, and correcting the revision. All authors must be responsible for the work's quality, accuracy, and ethics.

Ethics Author(s) must be obedient to the law and/or ethics in treating the object of research and pay attention to the legality of material sources and intellectual property rights.

Copyright If the manuscript is accepted for publication, the author(s) still hold the copyright and retain publishing rights without restrictions. For the new invention, authors must manage its patent before publication.

Open Access The journal is committed to free-open access that does not charge readers or their institutions for access. Readers are entitled to read, download, copy, distribute, print, search, or link to the full texts of articles, as long as not for commercial purposes. The license type is CC-BY-NC-SA.

Acceptance Only articles written in US English are accepted for publication. Manuscripts will be reviewed by editors and invited reviewers (double-blind review) according to their disciplines. Authors will generally be notified of acceptance, rejection, or need for revision within 1 to 2 months of receipt. Manuscripts will be rejected if the content does not align with the journal scope, does not meet the standard quality, is in an inappropriate format, or contains complicated grammar, dishonesty (i.e., plagiarism, duplicate publications, fabrication of data, citations manipulation, etc.), or ignoring correspondence in three months. The primary criteria for publication are scientific quality and significance. **Uncorrected proofs** will be sent to the corresponding author by system or email as .doc or .docx files for checking and correcting typographical errors. The corrected proofs should be returned in 7 days to avoid publication delays. The accepted papers will be published online in chronological order at any time but printed at the end of each month.

Free of charge This publication is dedicated entirely to the advancement of science and technology, therefore author(s), or author institution(s) are not subject to publication fees. **Reprints** The sample journal reprint is only available by special request. Additional copies may be purchased when ordering by email and sending back the uncorrected proofs.

Manuscript preparation Manuscript is typed on A4 (210x297 mm^2) paper size, in a single column, single space, 10-point (10 pt) Times New Roman font. The margin text is 3 cm from the top, 2 cm from the bottom, and 1.8 cm from the left and right. Smaller lettering sizes can be applied in presenting tables and figures (9 pt). Word processing program or additional software can be used; however, it must be PC compatible, use the template, and be Microsoft Word based (.doc or .rtf; not .docx). **Scientific names** of species (incl. subspecies, variety, etc.) should be written in italics, except in italicized sentences. Scientific names (genus, species, author) and cultivar or strain should be mentioned completely for the first time mentioning it in the body text, especially for taxonomic manuscripts. The genus name can be shortened after the first mention, except in early sentences, or where this may generate confusion; name of the author can be eliminated after the first mention. For example, *Rhizopus oryzae* L. UICC 524 can be written hereinafter as *R. oryzae* UICC 524. Using trivial names should be avoided. **Biochemical and chemical nomenclature** should follow the order of the IUPAC-IUB. For DNA sequences, it is better to use Courier New font. Standard chemical abbreviations can be applied for common and clear used, for example, completely written butilic hydroxyl toluene (BHT) to be BHT hereinafter. **Metric measurements** should use IS denominations, and other systems should use equivalent values with the denomination of IS mentioned first. A dot should not follow abbreviations like g, mg, mL, etc. Minus index (m^{-2}, L^{-1}, h^{-1}) suggested being used, except in things like "per-plant" or "per-plot." **Mathematical equations** can be written down in one column with text; in that case, they can be written separately. **Numbers** one to ten are written in words, except if it relates to measurement, while values above them are written in number, except in early sentences. The fraction should be expressed in decimal. In the text, it should be used "%" rather than "percent." Avoid expressing ideas with complicated sentences and verbiage/phrasing, and use efficient and effective sentences.

The title of the article should be written in compact, clear, and informative sentence, preferably not more than 20 words. Name of author(s) should be completely written, especially for the first and the last name. **Name and institution** address should also be completely written with street name and number (location), postal code, telephone number, facsimile number, and email address. We choose local names in Bahasa Indonesia for universities in Indonesia. The mention of "strata" program, should be avoided. Manuscript written by a group, author for correspondence along with address is required (marked with "♥"). **The title page** (first page) should include title of the article, full name(s), institution(s) and address(es) of the author(s); the corresponding authors detailed postage and e-mail addresses (P), and phone (O) and fax numbers (O).

Abstract A concise abstract is required (about 200 words). The abstract should be informative and state briefly the aim of the research, the principal results and major conclusions. An abstract is often presented separately from the article, thus it must be able to stand alone (completely self-explanatory). References should not be cited, but if essential, then cite the author(s) and year(s). Abbreviations should be avoided, but if essential, they must be defined at their first mention. **Keywords** are about five words, covering scientific and local name (if any), research themes, and special methods used; and sorted from A to Z. **Abbreviations** (if any): All important abbreviations must be defined at their first mention there. **Running title** is about five words.

Introduction is about 600 words, covering the aims of the research and provide an adequate background, avoiding a detailed literature survey or a summary of the results. **Materials and Methods** should emphasize on the procedures and data analysis. **Results and Discussion** should be written as a series of connecting sentences, however, for a manuscript with long discussion should be divided into subtitles. Thorough discussion represents the causal effect mainly explains why and how the results of the research were taken place, and do not only re-express the mentioned results in the form of sentences. **Concluding** sentence should be given at the end of the discussion. **Acknowledgements** are expressed in a brief; all sources of institutional, private and corporate financial support for the work must be fully acknowledged, and any potential conflicts of interest are noted.

Figures and Tables of a maximum of three pages should be clearly presented. The title of a picture is written down below the picture, while the title of a table is written above the table. Colored figures can only be accepted if the information in the manuscript can lose without those images; the chart is preferred to use black and white images. The author could consign any picture or photo for the front cover, although it does not print in the manuscript. All images property of others should be mentioned the source. Author is suggested referring to Wikipedia for international boundaries and Google Earth for satellite imagery. If not specifically mentioned, it is assumed to refer to these sources. **There is no appendix**, all data or data analysis is incorporated into Results and Discussions. For broad data, it can be displayed on the website as a supplement.

References Preferably 80% of it comes from scientific journals published in the last 10 years. In the text, give the author names followed by the year of publication and arrange from oldest to newest and from A to Z; in citing an article written by two authors, both of them should be mentioned; however, for three and more authors only the first author is mentioned followed by et al. For example, Saharjo and Nurhayati (2006) or (Boonkerd 2003a, b, c; Sugiyarto 2004; El-Bana and Nijs 2005; Balagadde et al. 2008; Webb et al. 2008). Extent citation should be avoided, as shown with the word "cit." Reference to unpublished data and personal communication should not appear in the list but should be cited in the text only (e.g., Rifai MA 2007, pers. com. (personal communication); Setyawan AD 2007, unpublished data). In the reference list, the references should be listed in alphabetical order. Names of journals should be abbreviated. Always use the standard abbreviation of a journal's name according to the **ISSN List of Title Word Abbreviations** (www.issn.org/2-22661-LTWA-online.php). Please include DOI links for journal papers. The following examples are for guidance.

Journal:

Saharjo BH, Nurhayati AD. 2006. Domination and composition structure change at hemic peat natural regeneration following burning; a case study in Pelalawan, Riau Province. Biodiversitas 7: 154-158. DOI: 10.13057/biodiv/d070213.

The usage of "et al." in long author lists will also be accepted:

Smith J, Jones M Jr, Houghton L et al. 1999. Future of health insurance. N Engl J Med 965: 325-329. DOI: 10.10007/s002149800025.

Book:

Rai MK, Carpinella C. 2006. Naturally Occurring Bioactive Compounds. Elsevier, Amsterdam.

Chapter in the book:

Webb CO, Cannon CH, Davies SJ. 2008. Ecological organization, biogeography, and the phylogenetic structure of rainforest tree communities. In: Carson W, Schnitzer S (eds.). Tropical Forest Community Ecology. Wiley-Blackwell, New York.

Abstract:

Assaeed AM. 2007. Seed production and dispersal of *Rhazya stricta*. 50th annual symposium of the International Association for Vegetation Science, Swansea, UK, 23-27 July 2007.

Proceeding:

Alikodra HS. 2000. Biodiversity for development of local autonomous government. In: Setyawan AD, Sutarno (eds.). Toward Mount Lawu National Park; Proceeding of National Seminary and Workshop on Biodiversity Conservation to Protect and Save Germplasm in Java Island. Universitas Sebelas Maret, Surakarta, 17-20 July 2000. [Indonesian]

Thesis, Dissertation:

Sugiyarto. 2004. Soil Macro-invertebrates Diversity and Inter-Cropping Plants Productivity in Agroforestry System based on Sengon. [Dissertation]. Universitas Brawijaya, Malang. [Indonesian]

Information from the internet:

Balagadde FK, Song H, Ozaki J, Collins CH, Barnet M, Arnold FH, Quake SR, You L. 2008. A synthetic *Escherichia coli* predator-prey ecosystem. Mol Syst Biol 4: 187. DOI: 10.1038/msb.2008.24. www.molecularsystembiology.com.

THIS PAGE INTENTIONALLY LEFT BLANK

ASIAN J NAT PROD BIOCHEM
Volume 23, Number 2, December 2025
Pages: 93-100

P-ISSN: 2775-4189
E-ISSN: 2775-4197
DOI: 10.13057/biofar/f230201

Effect of *Momordica charantia* and *Ocimum basilicum* on *KRAS* expression in AOM-induced colon cancer in rats

CHRISTOPHER AKINWANDE OKELOLA[1,♥], KUBURAT TEMITOPE ODUFUWA[2,♥♥], ESTHER NKECHI EZIMA[2], BUKUNOLA OLUYEMISI ADEGBESAN[2], TAIWO HASSAN BELLO[2]

[1]Department of Cell Biology and Genetics, Faculty of Science, University of Lagos. Akoka-Yaba, Lagos, Nigeria.
Tel: +234-803-473-9936, ♥email: cokelola@unilag.edu.ng
[2]Department of Biochemistry, Faculty of Basic Medical Sciences, Olabisi Onabanjo University, Ago-Iwoye, OgunState.
♥♥email: odufuwa.temitope@oouagoiwoye.edu.ng

Manuscript received: 6 June 2025. Revision accepted: 17 July 2025.

Abstract. *Okelola CA, Odufuwa KT, Ezima EN, Adegbesan BO, Bello TH. 2025. Effect of* Momordica charantia *and* Ocimum basilicum *on KRAS expression in aom-induced colon cancer in rats. Asian J Nat Prod Biochem 23: 93-100. KRAS* is one of the most frequently mutated oncogenes in colorectal cancer (CRC), contributing to tumor progression and therapeutic resistance. In light of increasing interest in phytotherapy, this study investigated the modulatory effects of aqueous extracts of *Momordica charantia* and *Ocimum basilicum* on *KRAS* gene expression in azoxymethane (AOM)-induced colon cancer in rats. Forty adult male Wistar rats were randomly assigned into five groups (n = 8 per group): three treatment groups (receiving 50, 100, and 200 mg/kg/day of the extract), an AOM-only negative control, and a distilled water-treated normal control. AOM was administered at 20 mg/kg/week for four weeks to induce colon carcinogenesis. After treatment, colon tissues were harvested for histological examination and *KRAS* gene expression analysis using quantitative real-time PCR (qRT-PCR). Phytochemical screening confirmed the presence of alkaloids, flavonoids, saponins, and phenols in the extracts. Histological evaluation revealed dose-dependent protection in extract-treated groups, with restoration of mucosal structure and reduced atypical features. qRT-PCR showed significant downregulation of *KRAS* gene expression in the high-dose group (200 mg/kg), with a 2.8-fold reduction compared to the AOM-only group ($p < 0.01$). The medium-dose group showed a moderate 1.6-fold reduction, while the low-dose group exhibited slight upregulation of *KRAS* expression. These findings suggest that aqueous extracts of *M. charantia* and *O. basilicum* exert chemopreventive effects in AOM-induced colon cancer, likely through phytochemical-mediated downregulation of oncogenic *KRAS* expression and preservation of colon histoarchitecture. The study supports the potential use of these plants as complementary agents in colorectal cancer therapy.

Keywords: AOM, colon cancer, *KRAS*, *Momordica charantia*, *Ocimum basilicum*, qPCR

INTRODUCTION

Colon cancer is a leading cause of cancer-related morbidity and mortality worldwide, ranking third in incidence and second in cancer-related deaths (Ferlay et al. 2021). Most cases begin as adenomatous polyps, which may progress into malignant tumors through a series of genetic and epigenetic alterations (Taufik et al. 2019). Risk factors include dietary patterns, chronic inflammation, and genetic predispositions. Though colon cancer is traditionally a disease of older adults, recent trends show increasing incidence among younger populations.

A crucial factor in colon cancer pathogenesis is the activation of oncogenes and inactivation of tumor suppressor genes. Among these, the *KRAS* gene (Kirsten rat sarcoma viral oncogene homolog) plays a central role. It encodes a GTPase involved in cell proliferation, survival, and differentiation. Mutations in *KRAS* particularly in codons 12, 13, and 61 lead to continuous activation of the RAS/RAF/MEK/ERK and PI3K/AKT signaling pathways, resulting in uncontrolled cell growth and resistance to apoptosis (Ryan and Corcoran 2018; Li et al. 2022). Approximately 40% of colorectal cancers harbor *KRAS* mutations, which are also predictive of poor response to anti-EGFR therapies like cetuximab (Canon et al. 2019). Kirsten rat sarcoma (*KRAS*) encodes a key signaling protein often mutated in colorectal cancer. While new targeted agents, such as *KRAS* G12C inhibitors, have shown efficacy in subsets of colorectal cancer patients, their applicability remains limited—fueling interest in plant-derived compounds, which provide low-toxicity, multi-pathway anticancer effects (Khan et al. 2023; Ros et al. 2024).

Phytochemicals such as flavonoids, terpenes, saponins, and alkaloids possess antioxidant, anti-inflammatory, and antiproliferative properties. These bioactives can modulate multiple signaling pathways and have shown potential in cancer prevention and treatment (Egbuna et al. 2021; Islam et al. 2022). Two plants of particular interest are *Momordica charantia* (bitter melon) and *Ocimum basilicum* (sweet basil).

Momordica charantia, widely used in traditional medicine, contains active compounds like charantin and momordicine that have been shown to inhibit tumor growth and induce apoptosis (Ahmad et al. 2016; La Torre et al. 2020). *Ocimum basilicum* contains essential oils and flavonoids, including eugenol and linalool, with demonstrated anticancer effects (Shenoy et al. 2016;

Eftekhar et al. 2019). Shenoy et al. (2016) reported that methanolic extracts of *O. basilicum* suppressed colon cancer cell growth by inducing oxidative stress and apoptosis. Minari et al. (2018) also found that combining these plants provided protective effects in chemically induced carcinogenesis models.

Studies have shown that *M. charantia* exhibits antiproliferative, pro-apoptotic, and anti-inflammatory effects in various cancer models. Specifically, bioactive constituents such as momordicin, charantin, and triterpenoids have demonstrated the ability to inhibit cancer cell growth and modulate oncogenic signaling (Kaur et al. 2016; Lin et al. 2021). Similarly, *O. basilicum* is rich in flavonoids, phenolics, and essential oils like eugenol and methyl chavicol, which possess cytotoxic, antioxidant, and anti-inflammatory properties (Kooti et al. 2020; Morshed et al. 2022). These compounds have been shown to suppress tumor growth in colorectal and other gastrointestinal cancer models.

However, despite individual reports on the anticancer effects of these plants, there is limited evidence on their combined use, particularly in relation to *KRAS* gene modulation in colorectal cancer. The current study addresses this critical gap by evaluating the synergistic effect of aqueous extracts of *M. charantia* and *O. basilicum* on *KRAS* gene expression, histopathological changes, and weight trends in an AOM-induced colon cancer model in rats. By investigating their combinatory potential, this study aims to advance the understanding of plant-based gene modulation strategies in colorectal carcinogenesis.

MATERIALS AND METHODS

Study area

This study was conducted at the Animal Research Laboratory and Molecular Biology Unit of the Department of Biochemistry, Olabisi Onabanjo University, Ago-Iwoye, Ogun State, Nigeria. The area is located in the humid tropics of southwestern Nigeria with average ambient temperatures of 25-30°C, suitable for maintaining laboratory animal models.

Collection and identification of plant materials

Plants of *M. charantia* and *O. basilicum* were collected in April 2024 from local farms in Sagamu and Ijebu-Ode, Ogun State, Nigeria. The plant materials were authenticated at the Department of Botany, Olabisi Onabanjo University, Ago-Iwoye, Nigeria, and voucher specimens were deposited for future reference.

Preparation of aqueous extracts

Plants were washed, shade-dried for 14 days, and ground into fine powder using an electric blender. The powdered samples were soaked in distilled water (aqueous extraction) in a ratio of 1:10 (w/v) in stoppered glass containers. The mixtures were stirred intermittently and kept at room temperature for 48 hours. They were then filtered through muslin cloth followed by 200 mm mesh filtration. The resulting filtrates were concentrated using a rotary evaporator at 45°C and dried to a paste-like consistency. Extracts were stored at 4°C and reconstituted into appropriate doses for experimental use.

Phytochemical analysis

Qualitative and quantitative phytochemical analyses of the aqueous extracts were carried out according to standard methods described by Vimala et al. (2012), Ejikeme et al. (2016), and the AOAC (2015).

Animal material and ethical compliance

Forty adult male Wistar rats (weighing 180-220 g) were obtained from the Nigerian Institute of Medical Research (NIMR), Lagos. The animals were housed in standard plastic cages in a well-ventilated room at 25°C, with relative humidity between 61-95% and a 12-hour light/dark cycle. They were fed standard laboratory chow and had access to water ad libitum. Animal care and use conformed to institutional ethical guidelines and the World Medical Association (WMA) Declaration of Helsinki (2008) on the ethical treatment of laboratory animals.

Experimental design

Azoxymethane (AOM) was used to induce colon cancer in rats (Table 1). AOM was administered orally at a dose of 20 mg/kg/week for 4 consecutive weeks. Concurrently, rats were administered daily oral doses of the aqueous plant extracts at 50, 100, and 200 mg/kg for four weeks likewise. The extract doses were selected based on previously published LD50 data (Arthur et al. 2011).

At the end of the experimental period, rats were sacrificed via cervical dislocation. Colon tissues were collected; portions were fixed in 10% neutral buffered formalin for histological evaluation, while others were frozen for gene expression analysis.

RNA extraction and cDNA synthesis

Total RNA was extracted from colon tissues using TRIzol reagent (Invitrogen). RNA concentration and purity were determined spectrophotometrically at 260/280 nm. Reverse transcription was performed using a commercial cDNA synthesis kit according to the manufacturer's protocol.

Table 1. Experimental design

The rats were randomly divided into five groups (n = 8 per group)
Group RA: AOM (20 mg/kg/week) + 200 mg/kg/day extract
Group RB: AOM (20 mg/kg/week) + 100 mg/kg/day extract
Group RC: AOM (20 mg/kg/week) + 50 mg/kg/day extract
Group NC (Negative Control): AOM only
Group PC (Positive Control): Distilled water only

Note: AOM: Azoxymethane

Table 2. Primer used in rt - qpcr

Genes	Primer	Bases	Annealing	Cycles
GAPDH	S: 5' -GAGAGCCTTGGCATCCCTAT 3'	20	55C	40
	AS: 5'GATGCGGAAGTTGGGTGTTT-3'	20		
KRAS	S: 5`GGTGAGTTTGTATTAAAAGGTACTGG 3'	26	55C	40
	AS: 5`-TCCTGCACCAGTAATATGCA-3'	20		

At the end of the experimental period, rats were sacrificed via cervical dislocation. Colon tissues were collected; portions were fixed in 10% neutral buffered formalin for histological evaluation, while others were frozen for gene expression analysis.

RNA extraction and cDNA synthesis

Total RNA was extracted from colon tissues using TRIzol reagent (Invitrogen). RNA concentration and purity were determined spectrophotometrically at 260/280 nm. Reverse transcription was performed using a commercial cDNA synthesis kit according to the manufacturer's protocol.

Quantitative real-time PCR (qPCR)

KRAS gene expression was quantified using SYBR Green-based qPCR on a StepOnePlus™ Real-Time PCR System (Applied Biosystems). GAPDH (Glyceraldehyde-3-phosphate dehydrogenase) was used as an internal control (Table 2). Primers were validated for specificity and efficiency (95-105%). The 2^−ΔΔCt method (Livak and Schmittgen 2001) was used to calculate relative expression levels.

Statistical analysis

All data were expressed as mean ± standard error of the mean (SEM). Two-way analysis of variance (ANOVA) was used to assess statistical significance across groups, followed by Tukey's post hoc test for multiple comparisons. GraphPad Prism 9.0 software was used for analysis, and $p < 0.05$ was considered statistically significant.

RESULTS AND DISCUSSION

The qualitative phytochemical screening of the aqueous extract of *O. basilicum* revealed the presence of ten bioactive constituents (Table 3). Alkaloids, saponins, and phenols were found in high abundance (++), while tannins, phlobatannins, terpenoids, cardiac glycosides, steroids, reducing sugars, and flavonoids were moderately present (+). Similarly, the extract of *M. charantia* tested positive for the same ten phytochemical classes (Table 4). Alkaloids and phenols demonstrated high abundance (++), with saponins showing a relatively strong positive reaction, consistent with their water solubility. The remaining phytochemicals exhibited moderate presence (+) across the extract.

Quantitative phytochemical analysis of *O. basilicum* extract (Table 5) showed that alkaloids (58.28 ± 0.01 mg/100 g), saponins (55.28 ± 0.02 mg/100 g), phenols (52.21 ± 0.02 mg/100 g), and tannins (51.24 ± 0.05 mg/100 g) were the most abundant compounds. Other constituents were present in the following quantities: terpenoids (40.87 ± 0.04 mg/100 g), steroids (38.79 ± 0.61 mg/100 g), reducing sugars (32.43 ± 0.02 mg/100 g), phlobatannins (32.68 ± 0.33 mg/100 g), cardiac glycosides (32.12 ± 0.04 mg/100 g), and flavonoids (25.12 ± 0.50 mg/100 g).

Table 3. Qualitative analysis of extracts of *Ocimum basilicum* plant

Phytochemicals	State
Alkaloid	++
Tannin	+
Phlobatannin	+
Saponin	++
Terpenoid	+
Cardiac glycosides	+
Steroid	+
Reducing sugar	+
Flavonoid	+
Phenol	++

Table 4. Qualitative analysis of aqueous extracts of *Momordica charantia* plant

Phytochemicals	State
Alkaloid	++
Tannin	+
Phlobatannin	+
Saponin	+
Terpenoid	+
Cardiac glycosides	+
Steroid	+
Reducing sugar	+
Flavonoid	+
Phenol	++

Table 5. Quantitative analysis of aqueous extracts of *Ocimum basilicum* plant

Phytochemicals	Quantity (mg/100 g)
Alkaloid	58.28 ± 0.01
Tannin	51.24 ± 0.05
Phlobatannin	32.68 ± 0.33
Saponin	55.28 ± 0.02
Terpenoid	40.87 ± 0.04
Cardiac glycosides	32.12 ± 0.04
Steroid	38.79 ± 0.61
Reducing sugar	32.43 ± 0.02
Flavonoid	25.12 ± 0.50
Phenol	52.21 ± 0.02

Table 6. Quantitative analysis of aqueous extracts of *Momordica charantia* plant

Phytochemicals	Quantity (mg/100g)
Alkaloid	50.47 ± 0.01
Tannin	42.39 ± 0.14
Phlobatannin	30.33 ± 0.01
Saponnin	48.29 ± 0.41
Terpenoid	36.14 ± 0.02
Cardiac Glycosides	41.42 ± 0.20
Steroid	39.76 ± 0.21
Reducing sugar	40.94 ± 0.01
Flavonoid	45.81 ± 1.00
Phenol	53.44 ± 0.10

Momordica charantia extract (Table 6) also exhibited considerable phytochemical richness. Phenols (53.44 ± 0.10 mg/100 g), flavonoids (45.81 ± 1.00 mg/100 g), and alkaloids (50.47 ± 0.01 mg/100 g) were notably high. Other components included saponins (48.29 ± 0.41 mg/100 g), reducing sugars (40.94 ± 0.01 mg/100 g), cardiac glycosides (41.42 ± 0.20 mg/100 g), tannins (42.39 ± 0.14 mg/100 g), steroids (39.76 ± 0.21 mg/100 g), terpenoids (36.14 ± 0.02 mg/100 g), and phlobatannins (30.33 ± 0.01 mg/100 g).

The QPCR analysis (Table 7) using the 2^−ΔΔCt method revealed distinct patterns in *KRAS* gene expression across the five treatment groups. Rats in the NC group (AOM only) showed significantly elevated *KRAS* expression relative to the PC group (distilled water). The RA group (200 mg/day) showed the greatest suppression, followed by RB (100 mg/day) and RC (50 mg/day). The difference between the RA group and the NC group was statistically significant ($p < 0.01$, Tukey's test).

Across the four-week period (Table 8), a dose-dependent increase in body weight was observed in the extract-treated groups (RA, RB, RC), with the RA group (200 mg/day) showing the most pronounced gain. Specifically, the RA group progressed from 114.75 ± 4.55 g in week 1 to 133.00 ± 3.08 g in week 4; conversely, the NC group (AOM only) showed a steady decline in weight from 125.25 ± 4.25 g in week 1 to 116.00 ± 2.71 g in week 4. The PC group (distilled water only) maintained a healthy weight gain trend, reaching the highest average weight by week 4 (135.25 ± 2.06 g).

Treatment description and experimental grouping (Table 9), Group PC (Positive Control): Animals received only distilled water throughout the experimental period and served as the healthy reference group. Group NC (Negative Control): Animals were administered 20 mg/kg body weight of AOM once weekly for four weeks, serving as the disease model without therapeutic intervention. Group RC (Low Dose Treatment): Animals received 20 mg/kg AOM weekly plus 50 mg/kg/day of the combined plant extract. Group RB (Medium Dose Treatment): Animals received 20 mg/kg AOM weekly plus 100 mg/kg/day of the combined plant extract. Group RA (High Dose Treatment): Animals received 20 mg/kg AOM weekly plus 200 mg/kg/day of the combined plant extract.

Table 7. Summary of *KRAS* gene expression across experimental groups

Group	Mean ΔCt ± SD	Fold Change (2^−ΔΔCt)	Direction of Modulation	p-value vs NC	Significant?
PC	4.89 ± 0.42	2.3	Upregulated	0.071	No
NC	5.94 ± 0.31	3.9	Baseline (AOM only)	–	–
RA	2.78 ± 0.33	1.2	Downregulated	0.003	Yes
RB	4.21 ± 0.37	1.8	Downregulated	0.021	Yes
RC	6.32 ± 0.55	4.6	Upregulated	0.045	Yes

Table 8. Weekly body weights of rats across all groups (g)

Week	Group RA (200 mg)	Group RB (100 mg)	Group RC (50 mg)	Group NC (AOM only)	Group PC (Distilled water)
1	114.75 ± 4.55	119.00 ± 2.16	122.75 ± 3.30	125.25 ± 4.25	128.75 ± 3.30
2	121.00 ± 2.94	120.00 ± 2.16	121.75 ± 1.71	122.00 ± 2.71	130.75 ± 1.50
3	127.00 ± 1.83	126.75 ± 3.96	123.75 ± 3.59	120.75 ± 3.30	131.25 ± 2.99
4	133.00 ± 3.08	129.25 ± 2.06	125.25 ± 1.50	116.00 ± 2.71	135.25 ± 2.06

Note: Values are presented as Mean ± Standard Deviation

Table 9. Group definitions and treatment description

Group	Treatment Description
PC (Positive control)	Rats that received distilled water only (normal control, not induced with AOM)
NC (Negative control)	Rats that received 20 mg/kg/week AOM only (cancer-induced, no treatment)
RA	Rats that received 20 mg/kg/week AOM + 200 mg/kg/day aqueous extract of *M. charantia* and *O. basilicum*
RB	Rats that received 20 mg/kg/week AOM + 100 mg/kg/day aqueous extract of *M. charantia* and *O. basilicum*
RC	Rats that received 20 mg/kg/week AOM + 50 mg/kg/day aqueous extract of *M. charantia* and *O. basilicum*

In Figure 1, the histological examination of colon tissue sections revealed marked architectural disruption of the mucosal lining. There was a visible reduction in inflammatory cell infiltration (yellow arrow), and areas containing atypically shaped malignant cells (red arrow) appeared significantly fewer. This suggests a decrease in neoplastic proliferation or the induction of apoptosis. Figure 2 sections showed mild distortion of mucosal structure with reduced inflammatory infiltrates (yellow arrow). The diminished presence of atypical malignant cells (red arrow) further suggests a decline in tumor progression and local immune activation. Moreover, in Figure 3, this sample showed less histological recovery, with multiple foci of intense inflammation (red arrows), suggestive of ongoing immune response. These may result from unresolved neoplastic cells, necrotic tissue, or a pro-tumorigenic inflammatory microenvironment. While Figure 4 histological findings were consistent with healthy colon morphology. The glandular architecture was intact, with no evidence of neoplastic or pre-neoplastic changes. Mild physiological inflammation was observed. In addition, Figure 5 sections indicated pronounced dysplasia: loss of glandular organization, nuclear pleomorphism, hyperchromasia, increased mitotic activity, and disrupted epithelial polarity features characteristic of malignant transformation.

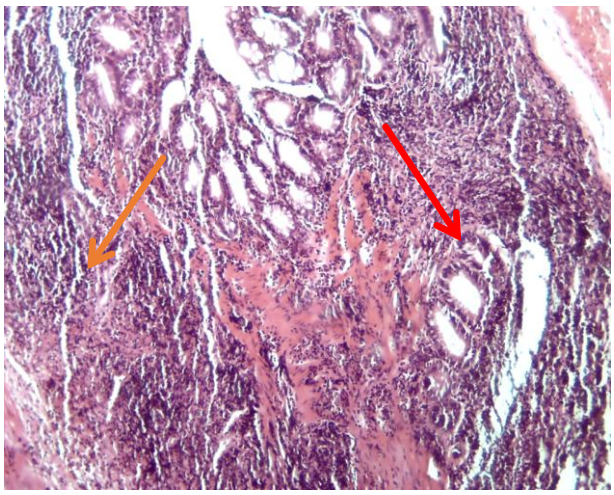

Figure 1. Histological section of colon tissue of rat from Group RA (AOM + 200 mg/day extract), H&E stain, ×400 magnification. Showing the restored crypt alignment, intact epithelial lining, and minimal inflammatory infiltration

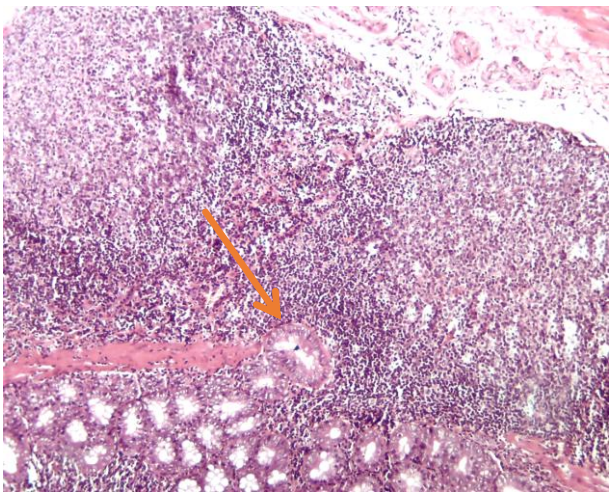

Figure 2. Histological section of colon tissue of rat from Group RB (AOM + 100 mg/day extract), H&E stain, ×400 magnification. It reveals slight distortion of the mucosal architecture, reduced inflammatory infiltrates and fewer atypical malignant cells

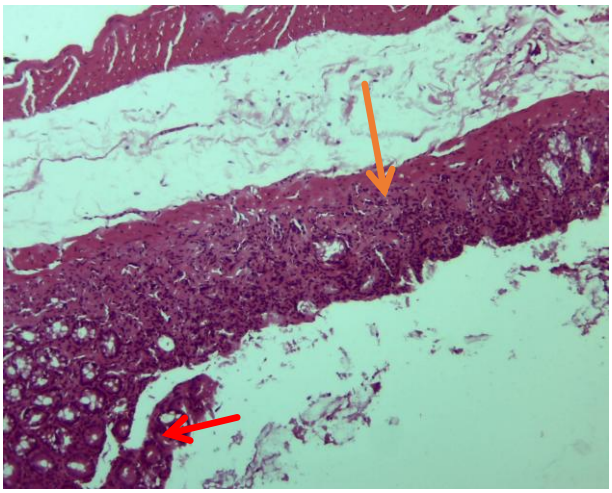

Figure 3. Histological section of the colon tissue from Group RC (AOM + 50 mg/day extract), stained with Hematoxylin and Eosin (H&E), viewed at ×400 magnification. The image shows less effective histological recovery

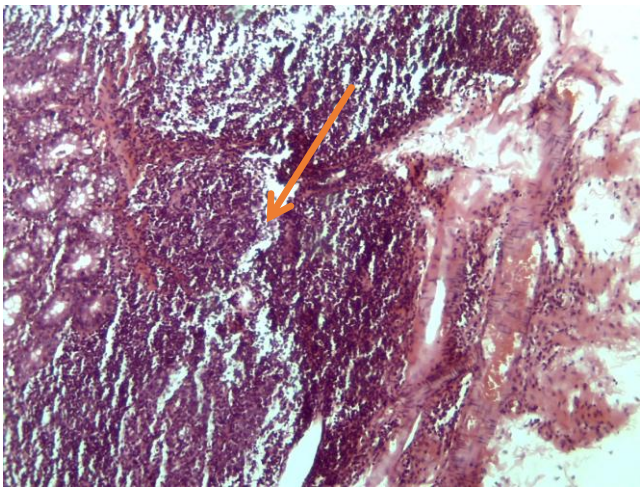

Figure 4. Histological section of the colon tissue from Group NC (AOM only), stained with Hematoxylin and Eosin (H&E), viewed at ×400 magnification. The image shows disrupted crypt architecture, mucosal erosion, and dense lymphocytic infiltration

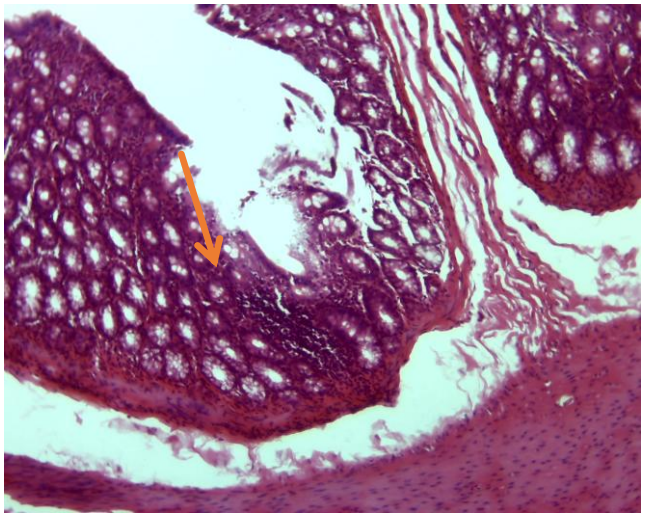

Figure 5. Histological section of colon tissue of induced colon cancer in rats from group PC (Water only) stained with Hematoxylin and Eosin (H&E), viewed at ×400 magnification. The image demonstrate preserved colonic glandular structure (no cancer or precancerous change) and mild physiological inflammation, typical of healthy tissue

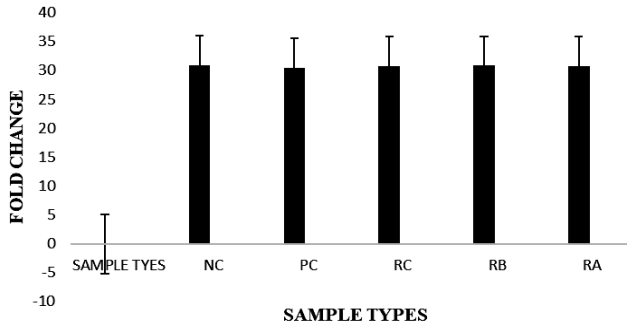

Figure 6. QPCR of *KRAS* mRNA expression in AOM induced colon cancer rats treated with different concentration of aqueous extract of *Momordica charantia* and *Ocimum basilicum* plant

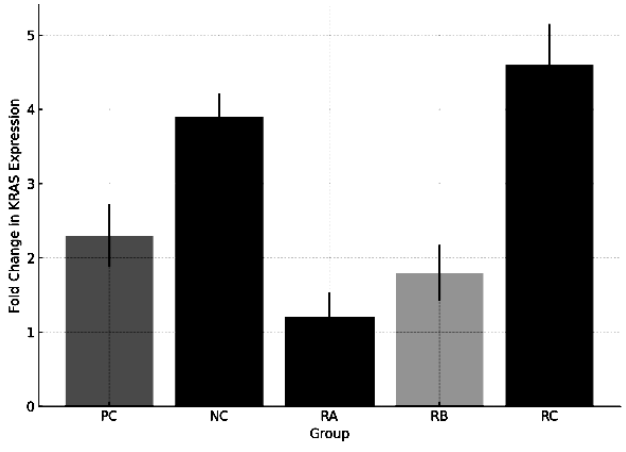

Figure 7. Relative *KRAS* gene expression levels (fold change, 2^−ΔΔCt) in colon tissue of rats across five groups

Figure 6 displays the relative expression levels of the *KRAS* oncogene across five experimental groups using the 2^−ΔΔCt method. It revealed a significant decrease in *KRAS* gene expression in Group RA compared to the AOM-only group (mean ΔCt = 2.78 vs. 5.94, p = 0.003, Cohen is d = 1.73, 95% CI [0.89, 2.57]). The large effect size suggests that the extract had a strong suppressive effect on *KRAS* activation. No significant difference was found between the PC and RB groups (p = 0.087), indicating a dose-dependent response. The highest upregulated *KRAS* expression is seen in Group RC, followed by Group PC. Group RC (low extract dose) shows fold changes above 2.0, suggesting a failure to suppress oncogenic signaling, likely due to insufficient phytochemical concentration. The PC group, which received no carcinogen or extract, unexpectedly displays moderate upregulation of *KRAS*. This may reflect baseline physiological variation or compensatory expression unrelated to AOM exposure.

Group RB (mid dose) and Group RA (high dose) showed significant downregulation of *KRAS* expression compared to both the NC and PC groups. Group RA, in particular, demonstrated *KRAS* fold changes close to 1.2, indicating effective modulation of oncogenic pathways and a potential return to near-normal expression levels. The NC group, exposed to AOM only, displayed moderate *KRAS* expression, suggesting a substantial, but not peak, activation of oncogenic pathways.

Figure 7 shows the relative *KRAS* gene expression levels (fold change, 2^−ΔΔCt) in colon tissue of rats across five groups: PC (normal control), NC (AOM only), and treatment groups RA (200 mg/kg), RB (100 mg/kg), and RC (50 mg/kg). Group RA showed the most significant downregulation of *KRAS* (p = 0.003), with expression approaching baseline. Error bars represent standard deviation (n = 8).

Discussion

Phytochemical screening of *M. charantia* and *O. basilicum* aqueous extracts confirmed the presence of several bioactive compounds, notably flavonoids, phenols, alkaloids, and saponins, which are widely documented for their antioxidant and anticancer properties. These secondary metabolites contribute synergistically to the extracts' ability to combat oxidative stress, modulate oncogenic signaling, and induce apoptosis in neoplastic cells.

Among these, flavonoids and phenolic compounds highly abundant in both plants play a pivotal role by scavenging reactive oxygen species (ROS) and stabilizing cellular redox states. These antioxidant actions are crucial in mitigating the oxidative DNA damage central to colon carcinogenesis. Flavonoids like vicenin and orientin from *O. basilicum* in colon cancer have also been shown to directly inhibit proliferation and induce apoptosis in colon cancer models (Shenoy et al. 2016), a trend echoed by the significant histological improvements in extract-treated rats in this study.

Histopathological findings revealed restoration of crypt architecture, reduced inflammatory infiltration, and

decreased nuclear atypia in treated groups compared to the AOM-only control, indicating effective suppression of tumor progression and enhancement of mucosal repair. These outcomes align with reports showing that compounds like momordicine, karavilagenin, eugenol, and methyl chavicol activate apoptotic pathways and enforce cell cycle checkpoints (Liu et al. 2019; Raina et al. 2020).

The body weight trends observed in this study confirm that *M. charantia* and *O. basilicum* extracts exhibit dose-dependent protective effects against AOM-induced systemic toxicity. These effects were reflected not only in gene expression and histology, but also in the maintenance of physiological growth and metabolism, further validating the chemopreventive potential of the combined extracts. These findings align with previous research demonstrating that flavonoid-rich plant extracts can improve appetite, enhance gut integrity, and reduce systemic inflammation, all of which contribute to weight stabilization in tumor-bearing animals (Kooti et al. 2020; Morshed et al. 2022).

This study explored the chemopreventive effect of aqueous extracts of *Momordica charantia* and *Ocimum basilicum* on AOM-induced colon cancer in rats, with particular emphasis on the expression of the *KRAS* gene, a critical proto-oncogene implicated in colorectal tumorigenesis. Our findings show a dose-dependent downregulation of *KRAS* mRNA expression, accompanied by histological evidence of mucosal restoration and decreased inflammatory infiltration, especially in the high-dose group.

The modulation of *KRAS* expression is particularly significant given its central role in driving MAPK/ERK and PI3K/AKT signaling pathways, which are frequently dysregulated in colorectal cancer (CRC). *KRAS* mutations are not only associated with tumor initiation and progression but also with resistance to EGFR-targeted therapies. Therefore, the observed suppression of *KRAS* expression, particularly in the high-dose group (RA), offers novel insight into the potential molecular mechanisms through which these plant extracts may exert anti-tumorigenic effects.

One of the noteworthy strengths of this study is the clear dose-response pattern observed in *KRAS* expression across treatment groups. While the low-dose group (RC) showed negligible changes in *KRAS* activity, the high-dose group (RA) demonstrated a significant reduction ($p < 0.01$) in *KRAS* gene expression. This finding suggests that the phytochemical synergy of the extracts is both concentration-dependent and biologically effective, supporting earlier research that linked flavonoids, phenolics, and saponins to modulation of oncogenic signaling (Ganesan and Xu 2020; Islam et al. 2023).

Moreover, the findings in this study are consistent with those of Islam et al. (2022), who reported significant antiproliferative effects of polyphenol-rich plant extracts in CRC models via suppression of RAS and PI3K/AKT pathways. Shenoy et al. (2016) similarly demonstrated that *O. basilicum* extracts induced apoptosis and inhibited proliferation in HT-29 colon cancer cells, consistent with the *KRAS* downregulation and histological restoration observed in our high-dose treatment group. Additionally, compounds such as momordicine from *M. charantia* have been reported to suppress oncogenic signaling and induce G1-phase cell cycle arrest in colon cancer lines (La Torre et al. 2020; Raina et al. 2020).

The antioxidant capacity of these extracts, conferred by flavonoids and phenolic acids, may contribute to reduced oxidative DNA damage, a key event in colon carcinogenesis. These bioactives are known to scavenge reactive oxygen species, inhibit inflammatory mediators like COX-2 and NF-κB, and modulate apoptosis-related proteins such as BAX and caspases (Ganesan and Xu 2020). Such pleiotropic effects could underlie the observed normalization of colon architecture and reduced *KRAS* gene expression.

Importantly, phytochemical screening confirmed the presence of bioactive compounds such as flavonoids, phenols, saponins, and terpenoids, which are well-documented for their antioxidant, anti-inflammatory, and antiproliferative activities. Flavonoids, in particular, have been reported to inhibit *KRAS* and downstream effectors by interfering with protein prenylation, membrane localization, or transcriptional regulation (La Torre et al. 2020). Our findings reinforce this potential and extend it to a novel botanical formulation combining *M. charantia* and *O. basilicum*.

Collectively, the findings support the chemopreventive and therapeutic potential of these extracts in colorectal cancer. By attenuating *KRAS*-driven signaling, reducing oxidative stress, and restoring histological integrity, *M. charantia* and *O. basilicum* demonstrate a multi-targeted action profile worthy of further pharmacological exploration.

In conclusion, this study demonstrated the chemopreventive potential of aqueous extracts of *Momordica charantia* and *Ocimum basilicum* in an azoxymethane (AOM)-induced colon cancer model in rats. The combined extracts downregulated oncogenic pathways—evidenced by suppressed expression of *KRAS*—and promoted mucosal recovery and reduced inflammation in a dose-dependent manner. The high-dose group (200 mg/kg/day) showed the greatest improvement across body weight, histoarchitecture, and gene expression. These results support the therapeutic relevance of the synergistic phytochemical composition of both plants, consistent with previous findings on the anticancer effects of flavonoids, phenolics, and terpenoids. However, gene expression data alone do not confirm protein-level modulation. Future studies should include protein validation via Western blot or ELISA, and explore broader targets and long-term outcomes to clarify mechanisms underlying the observed protective effects in colorectal cancer.

REFERENCES

Ahmad N, Hasan N, Ahmad Z, Zishan M, Zohrameena S. 2016. *Momordica charantia*: For traditional uses and pharmacological actions. J Drug Delivery Ther 6 (2): 40-44. DOI: 10.22270/jddt.v6i2.1202.

AOAC. 2015. Official Methods of Analysis. Association of Official Analytical Chemists, 14th edition. Washington, DC, USA.

Arthur FKN, Woode E, Terlabi EO, Larbie C. 2011. Evaluation of acute and subchlornic toxicity of *Annona muricata* (Linn.) aqueous extract in animals. Eur J Exp Biol 1 (4): 115-124.

Canon J, Rex K, Saiki AY, Mohr C, Cooke K, Bagal D, Lipford JR. 2019. The clinical *KRAS* (G12C) inhibitor AMG 510 drives anti-tumour immunity. Nature 575 (7781): 217-223. DOI: 10.1038/s41586-019-1694-1.

Eftekhar N, Moghimi A, Mohammadian Roshan N, Saadat S, Boskabady MH. 2019. Immunomodulatory and anti-inflammatory effects of hydro-ethanolic extract of *Ocimum basilicum* leaves and its effect on lung pathological changes in an ovalbumin-induced rat model of asthma. BMC Complement Altern Med 19: 349. DOI: 10.1186/s12906-019-2710-9.

Egbuna C, Akram M, Patrick-Iwuanyanwu KC, Iqbal M, Onyeike EN, Uche CZ, Hassan S. 2021. MicroRNAs as targets of dietary phytochemicals in obesity and cancer. In Dietary Phytochemicals: A Source of Novel Bioactive Compounds for the Treatment of Obesity, Cancer and Diabetes (pp. 193-203). Springer International Publishing, Cham. DOI: 10.1007/978-3-030-72999-8_10.

Ejikeme CM, Ezeonu CS, Eboatu AN. 2014. Determination of physical and phytochemicalconstituents of some tropical timbers indigenous to Niger Delta Area of Nigeria. Eur Sci J 10 (18): 247-270.

Ferlay J, Laversanne M, Ervik M, Lam F, Colombet M, Mery L, Bray F. 2021. Global Cancer Observatory: Cancer Today. Intl Agency Res Cancer.

Ganesan K, Xu B. 2020. Molecular targets of vitexin and isovitexin in cancer therapy: A critical review. Ann New York Acad Sci 1474 (1): 5-20. DOI: 10.1111/nyas.14432.

Islam MR, Akash S, Rahman MM, Nowrin FT, Akter T, Shohag S, Simal-Gandara J. 2022. Colon cancer and colorectal cancer: Prevention and treatment by potential natural products. Chemico-Biol Interact 368: 110170. DOI: 10.1016/j.cbi.2022.110170.

Kaur M, Deep G, Katiyar SK, Agarwal R. 2016. Bitter melon (*Momordica charantia*) in cancer prevention and therapy: Current evidence and future perspectives. Toxicol Appl Pharmacol 301: 37-46. DOI: 10.1016/j.taap.2016.04.010.

Khan SH, Alhumaydhi FA, Khan MA, Younus H. 2023. Therapeutic potential of polyphenols and their nanoformulations in colorectal cancer — experimental evidence and clinical perspective. Anticancer Agents Med Chem 21 (16): 2117-2135. DOI: 10.2174/1871520621666201231144007.

Kooti W, Daraei N, Pirouzi A, Rashi H, Asadi-Samani M, Ghadery H. 2020. Therapeutic and pharmacological potential of *Ocimum basilicum* L. and its main constituents: A review. Evidence-Based Complement Altern Med 2020: 1595614. DOI: 10.1155/2020/1595614.

La Torre VE, Guarniz WS, Silva-Correa C, Razco LC, Siche R. 2020. Antimicrobial activity and chemical composition of *Momordica charantia*: A Review. Pharmacognosy J 12 (1): 213-222. DOI: 10.5530/pj.2020.12.30.

Li C, Lau HC-H, Zhang X, Yu J. 2022. Mouse models for application in colorectal cancer: Understanding the pathogenesis and relevance to the human condition. Biomedicines 10 (7): 1710. DOI: 10.3390/biomedicines10071710.

Lin L, Ni B, Lin H, Zhang M, Li X, Ying M. 2021. *Momordica charantia* extract suppresses colorectal cancer via modulation of *KRAS* and apoptotic pathways. Phytomedicine 91: 153695. DOI: 10.1016/j.phymed.2021.153695.

Liu C, Sun J, Lu Y, Bo Y, Song Y. 2019. *Ocimum basilicum* extract inhibits proliferation and induces apoptosis in colorectal cancer cells. Biomed Pharmacother 112: 108600. DOI: 10.1016/j.biopha.2019.108600.

Livak KJ, Schmittgen TD. 2001. Analysis of relative gene expression data using real-time quantitative PCR and the 2^ (-ΔΔCt) method. Methods 25 (4): 402-408. DOI: 10.1006/meth.2001.1262.

Minari JB, Okelola CA, Ugochukwu NC. 2018. Analysis of *KRAS* gene from induced pancreatic cancer rats administered with *Momordica charantia* and *Ocimum basilicum* leaf extracts. J Tradit Complement Med 8 (2): 282-288.

Morshed MN, Hasan MR, Rahman MA, Islam MS, Alam MA. 2022. *Ocimum basilicum* attenuates colorectal carcinogenesis through anti-inflammatory and anti-proliferative mechanisms. J Ethnopharmacol 295: 115386. DOI: 10.1016/j.jep.2022.115386.

Raina R, Soni R, Dogra R, Kaul S, Choudhary S, Verma PK. 2020. Chemopreventive and anticancer potential of *Momordica charantia*: A mini review. J Cancer Res Ther 16 (3): 471-476. DOI: 10.4103/jcrt.JCRT_695_18.

Ros J, Vaghi C, Baraibar I, Saoudi Gonzalez N, Rodríguez-Castells M, García A, Alcaraz A, Salva F, Tabernero J, Elez E. 2024. Targeting *KRAS* G12C Mutation in Colorectal Cancer, a review: New arrows in the Quiver. Intl J Mol Sci 25 (6): 3304. DOI: 10.3390/ijms25063304.

Ryan MB, Corcoran RB. 2018. Therapeutic strategies to target RAS-mutant cancers. Nat Rev Clin Oncol 15 (11): 709-720. DOI: 10.1038/s41571-018-0107-5.

Shenoy S, Anitha T, Rajesh B. 2016. Antioxidant and antiproliferative activities of *Ocimum basilicum* extracts on colon cancer cells. Pharmacognosy J 8 (6): 579-584. DOI: 10.5530/pj.2016.6.10.

Taufik R, Pandianta A, Kusuma R, Winoto IL, Suriapranata I, Mathew G. 2020. Pilot study for azoxymethane-induced colon cancer in male wistar rats. Medicinus 8 (3): 120-132.

Vimala JR, Leema RA, Raja S. 2012. A study on the phytochemical analysis and corrosion inhibition on mild steel by *Annona muricata* L. leaves extract in 1N hydrochloric acid. Der Chemica Sinica 3 (3): 582-588.

ASIAN J NAT PROD BIOCHEM
Volume 23, Number 2, December 2025
Pages: 101-109

P-ISSN: 2775-4189
E-ISSN: 2775-4197
DOI: 10.13057/biofar/f230202

Phytochemical composition, antioxidant, and anticancer potential of *Etlingera hemisphaerica* (Zingiberaceae) from the Gayo Highlands, Indonesia

MUHAMMAD RIDHWAN[1], SAUDAH[2,♥], SALFAUQI NURMAN[3], MASYUDI[4], LIYA FITRIYANA[5], RIKA YUSNAINI[6]

[1]Department of Biology Education, Faculty of Teacher Training and Education, Universitas Serambi Mekkah. Jl. Tgk. Imum Lueng Bata, Banda Aceh 23245, Aceh, Indonesia. Tel./fax.: +62-651-22471, ♥email: saudah@serambimekkah.ac.id

[2]Master of Biology Education, Graduate School, Universitas Serambi Mekkah. Jl. Tgk. Imum Lueng Bata, Banda Aceh 23245, Aceh, Indonesia

[3]Department of Marine Angineering, Politeknik Pelayaran Malahayati. Jl. Laksamana Malahayati No.Km.19, Aceh Besar 23381, Aceh, Indonesia

[4]Faculty of Public Health, Universitas Serambi Mekkah. Jl. Tgk. Imum Lueng Bata, Banda Aceh 23245, Aceh, Indonesia

[5]Department of Agricultural Industrial Engineering, Faculty of Agricultural Technology, Universitas Serambi Mekkah. Jl. Tgk. Imum Lueng Bata, Banda Aceh 23245, Aceh, Indonesia

[6]Department of Psychology and Nursing, Faculty of Medicine, Universitas Malikussaleh. Jl. Cot Tengku Nie Reuleut, Aceh Utara 24353, Aceh, Indonesia

Manuscript received: 12 May 2025. Revision accepted: 25 August 2025.

Abstract. *Ridhwan M, Saudah, Nurman S, Masyudi, Fitriyana L, Yusnaini R. 2025. Phytochemical composition, antioxidant, and anticancer potential of* Etlingera hemisphaerica *(Zingiberaceae) from the Gayo Highlands, Indonesia. Asian J Nat Prod Biochem 23: 101-109.* The increasing global incidence of cancer underscores the urgent need for sefar and more effective alternative therapies. *Etlingera hemisphaerica* (Blume) R.M.Sm. (Zingiberaceae), an andemic medicinal plant from the Gayo Highlands of Indonesia, has traditional uses but remains underexplored for its pharmacological potential. This study investigated the phytochemical composition, antioxidant capacity, and anticancer of *E. hemisphaerica* leaf extracts using methanol, ethyl acetate, and aquadest. Total phenolic and flavonoid contents were determined spectrophotometrically. Antioxidant activity was assessed using the DPPH (2,2-diphenyl-1-picrylhydrazyl) assay, and anticancer activity was evaluated via the MTT assay against the MCF-7 human breast cancer cell line (ATCC HTB-22), with IC_{50} values calculated through linear regression analysis. Qualitative screening revealed the presence of major phytochemicals including flavonoids, phenolics, tannins, terpenoids, saponins, and steroids. Quantitative analysis showed that the methanol extract contained the highest total phenolic content (506.4 ± 15.41 mg GAE/g), while the ethyl acetate extract had the highest flavonoid content (471.5 ± 20.55 mg QE/g). Antioxidant activity was evaluated using the DPPH (2,2-diphenyl-1-picrylhydrazyl) assay, with the methanol extract exhibiting the strongest radical scavenging capacity IC_{50} (0.40 ppm). Cytotoxic effects were determined by MTT assay against MCF-7 human breast cancer cells (ATCC HTB-22), where the methanol extract showed the most potent activity (IC_{50} = 0.446 ppm; 43.47% inhibition at 200 ppm), outperforming ethyl acetate (IC_{50} (10.45 ppm) and aquadest IC_{50} (4.12 ppm) extracts. These results suggest that *E. hemisphaerica*, particularly in methanol extract, is a promising natural source of antioxidant and anticancer agents. Further bioassay-guided fractionation and in vivo studies are warranted to explore its therapeutic potential.

Keywords: Cancer MCF-7, *Etlingera hemisphaerica*, Gayo Highland, herb medicine, Zingiberaceae

INTRODUCTION

Cancer is one of the leading causes of death globally (Yuan et al. 2022). Despite the availability of anticancer therapies, the incidence of cancer continues to rise steadily. According to the World Health Organization (WHO) and global cancer statistics (GLOBOCAN), the global cancer burden is projected to reach 28.4 million cases by 2040, a 47% increase from 2020 (Sung et al. 2021). Conventional cancer treatments such as surgery, radiotherapy, chemotherapy, and immunotherapy are commonly used but often associated with limitations, including complications, drug resistance, and significant side effects (Mali 2023). Consequently, there is a growing interest in developing alternative or complementary therapies derived from natural sources.

Natural products, especially those derived from plants, have long been used in medical practice. Plants are rich in bioactive compounds and have shown promise as sources of anticancer agents. These include vitamins, minerals, phosphates, and various secondary metabolites such as phenolics, flavonoids, alkaloids, and polyphenols, all of which have demonstrated antioxidant, anti-inflammatory, and chemopreventive properties (Block et al. 2015; Lee et al. 2017; Lichota and Gwozdzinski 2018; Jiang 2019).

Spices are widely used as flavor enhancers and aromatic ingredients in food, as well as traditional remedies for chronic diseases. They contain tannins, alkaloids, flavonoids, and polyphenols with potent biological activities. Clove, cinnamon, and ginger species, in particular, are excellent sources of antioxidants due to their high phenolic content (Jiang et al. 2019). The pharmacological effects of these spices include antitumor, antioxidant, and anti-inflammatory properties (Chin 2016). Moreover, the antioxidant activity of edible and medicinal plant extracts has been proven to counteract reactive oxygen species (ROS)-mediated damage in various human cancers (Sammar et al. 2019).

The Zingiberaceae family, commonly known as the ginger family, is one of the key spice producing families with

numerous species used in traditional medicine for cancer prevention. The genus *Etlingera* Giseke, belonging to this family, comprises more than 100 species distributed throughout Southeast Asia, many of which are used in ethnomedicine (Adegoke and Ojo 2017; Saudah et al. 2022). Pharmacologically, studies have demonstrated that *Etlingera* species exhibit antioxidant (Anzian et al. 2017), antibacterial (Shahid-Ud-Daula et al. 2019; Ernilasari et al. 2021), anti-inflammatory (Sahidin et al. 2019), antifungal (Ghasemzadeh et al. 2015), cytotoxic and antiproliferative activities (Mankhong et al. 2019; Shahid Ud-Daula and Mohammad 2019), as well as insect-repellent (particularly against *Aedes aegypti* (Linnaeus, 1762)) (Siregar et al. 2020), anti-aging and antiviral effects (Ruyani et al. 2019).

The Gayo Highlands of Central Aceh, Indonesia, situated at elevations of 1,000-3,000 meters above sea level (masl), form part of the biodiverse Leuser Ecosystem (Cane et al. 2023). Ethnobotanical surveys in this region have documented the traditional use of *Etlingera* species, particularly *Etlingera elatior* (Jack) R.M.Sm. and *Etlingera hemisphaerica* (Blume) R.M.Sm. (Saudah et al. 2021). While *E. elatior* is relatively well studied, *E. hemisphaerica* remains scientifically underexplored. It is a morphologically distinct, highland-adapted species, traditionally used by the Gayo ethnic community for postpartum care, anti-fatigue remedies, and general health support (Saudah et al. 2022; Riyanti et al. 2022). Given that altitude can influence secondary metabolite production and antioxidant activity in plants (Setyawati et al. 2021; Adhikari et al. 2022), the unique ecological niche of *E. hemisphaerica* may contribute to a distinct phytochemical profile.

Although both species share similarities in leaf morphology they differ significantly in flower structure (Lim 2014; Handayani et al. 2020). Taxonomically, *E. hemisphaerica* is a distinct species native to highland environments and traditionally used by the Gayo ethnic community for postpartum care and general health support (Riyanti et al. 2022). Its unique ecological niche in the high-altitude Gayo Highlands is believed to influence its phytochemical composition. Studies have shown that elevation can significantly affect the production of secondary metabolites and antioxidant potential in plants (Setyawati et al. 2021; Adhikari et al. 2022). The high-altitude environment of the Gayo Highlands, characterized by increased UV exposure and temperature variation, may enhance the synthesis of bioactive compounds in *E. hemisphaerica*.

Despite its ethnopharmacological relevance, *E. hemisphaerica* remains scientifically underexplored. No previous studies have reported its phytochemical profile or evaluated its pharmacological activity, particularly with regard to antioxidant and anticancer properties. Given its traditional use, ecological uniqueness, and taxonomic distinction, *E. hemisphaerica* from the Gayo Highlands may serve as a promising candidate for further development in cancer therapeutics. Therefore, this study aims to evaluate the phytochemical composition, antioxidant capacity, and cytotoxic activity of *E. hemisphaerica* leaf extracts collected from the Gayo Highlands, Indonesia. The findings are expected to contribute to the scientific validation of traditional knowledge and support the exploration of novel therapeutic agents from highland tropical biodiversity.

MATERIALS AND METHODS

Study area

Leaves of *E. hemisphaerica* were collected from the Gayo Highlands, Aceh Province, Indonesia, at elevations between 1,000 and 1,500 meters above sea level (Figure 1). The region is characterized by a cool climate and fertile volcanic soil, which are known to support high levels of phytochemical accumulation in local flora (Cane et al. 2023; Lestari et al. 2023). Plant identification was confirmed using the Plants of the World Online database (https://powo.science.kew.org/) (POWO 2023). The collected leaves were washed, air-dried at room temperature for seven days, and then ground into a fine powder using a mechanical grinder (Figure 2).

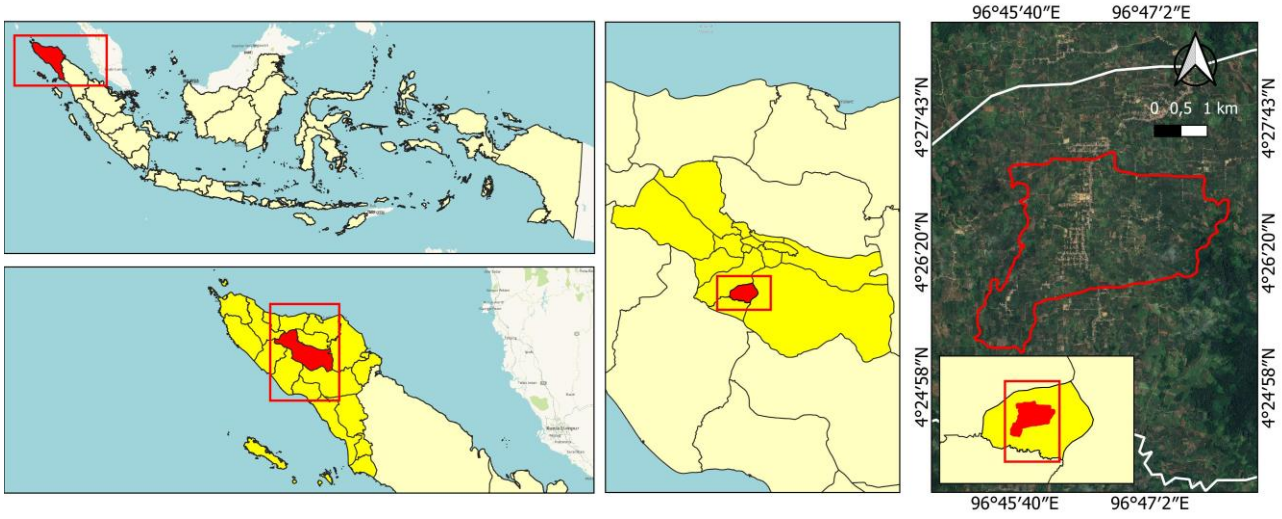

Figure 1. Map of the research location in Gayo Highlands, Central Aceh District, Aceh Province, Indonesia

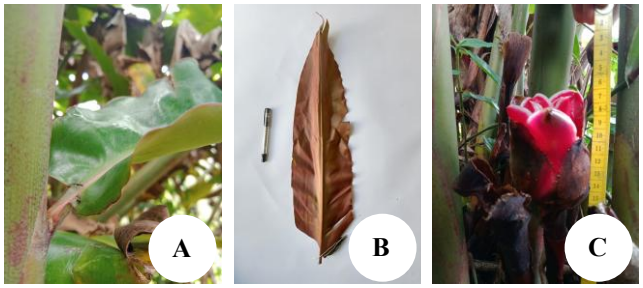

Figure 2. Morphology of *Etlingera hemisphaerica*. A. Stem, B. Leaf, C. Flower

Chemicals and equipments used

The following analytical-grade chemicals and reagents were used in this study: Quercetin, Vitamin C (ascorbic acid), gallic acid, 2,2-diphenyl-1-picrylhydrazyl (DPPH) (Sigma-Aldrich), methanol, ethyl acetate (Brataco), and distilled water. Other reagents included sodium carbonate, aluminum chloride, sodium nitrite, Folin-Ciocalteu reagent, and sodium carboxymethyl cellulose. For cell culture and cytotoxicity assays, human dermal fibroblast cell line, MCF-7 human breast cancer cell line (ATCC HTB-22), Dulbecco's Modified Eagle's Medium (DMEM), fetal bovine serum (FBS), trypsin-EDTA, penicillin-streptomycin, phosphate-buffered saline (PBS), and 3-(4,5-dimethylthiazol-2-yl)-2,5-diphenyltetrazolium bromide (MTT) were obtained from Gibco (Thermo Fisher Scientific) or equivalent suppliers.

Equipment

The equipment used in the study included a rotary evaporator (Büchi), water bath (Memmert), UV-Visible spectrophotometer (Shimadzu UV-1800), ELISA reader (Bio-Rad), and standard laboratory glassware such as volumetric flasks, pipettes, and measuring cylinders.

Procedures

Extraction and maceration of Etlingera hemisphaerica *leaf samples*

Fresh leaves *E. hemisphaerica* were collected from the Gayo Highlands, Aceh Province, Indonesia. The leaves were thoroughly washed with distilled water to remove debris and soil, air-dried in a shaded, well ventilated area at ambient temperature (25-30°C) for 7 days, and than ground into a fine powder using an electric grinder. A total of 1000 g of dried leaf powder was used for extraction. The powdered sample was divided equally into three parts (approximately 333 g each) and macerated with three different solvents: methanol, ethyl acetate, and distilled water (aquadest). Each portion was immersed in 1,000 mL of the respective solvent in a clean, dry maceration flask. The maceration was carried out at room temperature (± 27°C) for 72 hours with occasional shaking to maximize extraction efficiency. After 72 hours, the mixtures were filtered using Whatman No. 1 filter paper to separate the extract solution from the plant residues. This process was repeated twice to ensure exhaustive extraction. The filtrates were collected, pooled, and concentrated under reduced pressure using a rotary evaporator at 40°C for methanol and ethyl acetate extracts. The aqueous extract was concentrated using a freeze dryer. The resulting crude extracts of *E. hemisphaerica* from methanol, ethyl acetate, and aqueous were stored in sealed glass containers at 4°C until further analysis. The percentage yield of each extract was calculated based on the weight of the dried extract relative to the original plant material (Fithrotunnisa et al. 2020).

Phytochemical screening procedures

Alkaloid test

A total of 100 mg of plant extract was dissolved in 10 mL of methanol and filtered. Then, 2 mL of the filtrate was acidified with 1 mL of 1% hydrochloric acid (HCl), followed by the addition of 2-3 drops of Dragendorff's reagent. The presence of alkaloids was indicated by the formation of a reddish-brown precipitate (Tiwari et al. 2011). The formation of an orange to reddish-brown precipitate indicated the presence of alkaloids. For the Mayer's test, another 2 mL of the same filtrate was mixed with 1 mL of 1% HCl and treated with 2-3 drops of Mayer's reagent. The presence of a cream or yellowish-white precipitate confirmed the presence of alkaloid compounds (Rahimah et al. 2019).

Triterpenoid and steroid test

Fifty milligrams (50 mg) of the plant extract were dissolved in 5 mL chloroform and filtered or the Liebermann Burchard test, 2 mL of the filtrate was treated with 1-2 mL of acetic anhydride and carefully layered with 2-3 drops of concentrated sulfuric acid (H_2SO_4). The gradual appearance of a red to blue, followed by green color indicated the presence of sterols. In a separate test, 2 mL of chloroform extract was mixed with a few drops of concentrated H_2SO_4 and gently shaken. A reddish to yellow coloration in the acid layer indicated the presence of steroids, while a brownish-red coloration confirmed the presence of triterpenoids (Gadouche et al. 2023).

Saponin test

The extract (approximately 1 g or equivalent extract volume) was diluted with 20 mL of distilled water and heated to boil for 2-3 minutes, then cooled to room temperature. The mixture was then vigorously shaken for 30 seconds. The formation of stable, persistent foam (lasting more than 10 minutes) indicated the presence of saponins (Noviyanty et al. 2020).

Flavonoid test

A measured amount of the extract (approx. 100 mg) was heated with 10 mL of ethyl acetate over a boiling water bath for 3 minutes and filtered. The filtrate was then mixed with 1 mL of 1% ammonia solution and gently shaken. The development of a yellow coloration in the ammonia layer indicated the presence of flavonoids (Kancherla et al. 2019).

Determination of phenolic content (TPC)

The total phenolic content (TPC) of the plant was determined using the Folin-Ciocalteu colorimetric method as described by Ghasemzadeh et al. (2014), with slight modifications. Gallic acid (GA) was used as the reference

standard, prepared in distilled water at concentrations ranging from 0.01 to 0.19 mg/mL to construct a calibration curve. A 0.10 mL aliquot of each gallic acid standard solution or plant extract (5.0 mg/mL) was pipetted into a 10.0 mL volumetric flask. Subsequently, 0.5 mL of 10% (w/v) Folin-Ciocalteu reagent was added, followed by a 3-minute incubation at room temperature. Then, 4.0 mL of 7.5% (w/v) sodium carbonate solution was added. The solution was diluted to the mark with distilled water, thoroughly mixed, and incubated at 40°C in a water bath for 30 minutes. Absorbance was measured at 765 nm using a UV-Vis spectrophotometer (Shimadzu UV-1800). The TPC was calculated from the standard curve and expressed as milligrams of gallic acid equivalent per gram of dried extract (mg GAE/g), using the formula:

$$\text{TFC (mg GAE/g)} = \frac{\text{C x V}}{\text{M}}$$

Where: C: concentration of gallic acid (mg/mL) obtained from the calibration curve, V: volume of extract used (mL), M: weight of dried extract (g). Results were expressed as milligrams of gallic acid equivalent per gram of dried extract (mg GAE/g).

Determination of flavonoid content

The total flavonoid content (TFC) was measured using a colorimetric method based on the formation of a flavonoid aluminum complex, as described by Ayele et al. (2022). Quercetin was used as the reference standard, prepared in methanol at concentrations ranging from 0.01 to 0.10 mg/mL to construct the calibration curve. For the reaction, 0.5 mL of standard or plant extract (5.0 mg/mL) was transferred into a 10.0 mL volumetric flask. Then, 1.0 mL of 20% aluminum chloride ($AlCl_3$) solution and 0.3 mL of 5% sodium nitrite ($NaNO_2$) solution were added. The volume was adjusted with distilled water to 10.0 mL. After standing for 5 minutes at room temperature, the absorbance was read at 430 nm. The TFC was calculated using the following formula:

$$\text{TPC (mg QE/g)} = \frac{\text{C x V}}{\text{M}}$$

Where: C: concentration of quercetin (mg/mL) from the calibration curve, V: volume of extract used in the assay (mL), M: mass of dried extract used (g). Results were expressed as milligrams of quercetin equivalent per gram of dried extract (mg QE/g), representing the total flavonoid concentration (Ayele et al. 2022).

DPPH antioxidant activity

The antioxidant activity of *E. hemisphaerica* leaf extract was evaluated using the DPPH (2,2-diphenyl-1-picrylhydrazyl) radical scavenging assay, based on the method described by Bello et al. (2024) and Sari et al. (2024), with minor modifications. DPPH is a stable free radical that changes color from violet (DPPH•) to yellow (DPPH-H) upon reduction by an antioxidant. This color change corresponds to a decrease in absorbance at 517 nm and is inversely proportional to the antioxidant capacity of the sample. A 0.004% DPPH solution was freshly prepared in methanol. Extract solutions were prepared in methanol at concentrations of 0, 20, 40, 50, 70, 90, and 100 µg/mL. For each reaction, 200 µL of extract solution was mixed with 800 µL of DPPH solution. The mixture was vortexed and incubated in the dark at 25 ± 2°C for 30 minutes. A negative control was prepared using 200 µL of methanol and 800 µL of DPPH solution. Ascorbic acid, prepared at the same concentration range, was used as the positive control. The absorbance of each sample was measured at 517 nm using a UV-Vis spectrophotometer (Shimadzu UV-1800), and the radical scavenging activity was calculated as follows:

$$\text{Inhibition (\%)} = \frac{\text{A}_{\text{control}} - \text{A}_{\text{sample}}}{\text{A}_{\text{control}}} x100$$

Where: A_control: absorbance of the control reaction (DPPH + methanol), A_sample: absorbance of the test sample (DPPH + extract). The IC_{50} value, defined as the concentration required to inhibit 50% of DPPH radicals, was calculated from the dose-response curve using linear regression analysis.

Anticancer activity using the MTT assay

The cytotoxic potential of *E. hemisphaerica* extract was assessed against MCF-7 human breast cancer cells (ATCC HTB-22) using the MTT assay, following the protocol of Williams et al. (2017) with slight modifications. MCF-7 cells were cultured in RPMI-1640 medium supplemented with 5% fetal bovine serum (FBS), 100 U/mL penicillin, and 100 µg/mL streptomycin. Cells were maintained at 37°C in a humidified incubator with 5% CO_2. Cells were seeded in a 96-well plate at a density of 5,000 cells per well in 100 µL of complete medium and incubated for 24 hours to allow attachment. Afterward, cells were treated with various concentrations of the extract (e.g., 10-640 µg/mL) and incubated for 48 hours. On day three, 10 µL of MTT solution (5 mg/mL in PBS) was added to each well, followed by a 4-hour incubation at 37°C. After the formation of formazan crystals, the medium was carefully removed, and 100 µL of ethanol was added to each well to dissolve the crystals. Absorbance was measured at 595 nm using a microplate reader (Bio-Rad) Williams et al. (2017). MTT solution (5 mg/mL) was added to each well at a final concentration of 10 µL and incubated for 4 hours at 37°C. After incubation, formazan crystals formed by viable cells were dissolved using ethanol. The absorbance was measured at 595 nm using a microplate reader. The percentage of inhibition is calculated using the formula:

$$\%Inhibition \frac{abs\ control - abs\ sample}{abs\ control} x\ 100\%$$

Where: abs_control is the absorbance of untreated cells, and abs_sample is the absorbance of treated cells. The IC_{50} value, representing the concentration required to inhibit 50% of cell viability, was determined via linear regression and used to evaluate the antiproliferative potential of the extract.

RESULTS AND DISCUSSION

Phytochemical screening of *Etlingera hemisphearica* leaves

Phytochemical screening of *E. hemisphearica* leaf extract using three different solvents methanol, n-hexane, and ethyl acetate the presence of various secondary metabolites, including flavonoids, phenolics, steroids, tannins, saponins, and alkaloids (Table 1). The methanol extract, representing a polar solvent, was rich in flavonoids, phenolics, saponins, and steroids. The ethyl acetate extract, a semi-polar solvent, contained flavonoids, steroids, saponins, and alkaloids. Meanwhile, the non-polar n-hexane extract primarily exhibited the presence of steroids, with minimal detection of polar compounds. These findings suggest that solvent polarity influences the efficiency of secondary metabolite extraction, with methanol being the most effective in isolating bioactive polar compounds known for their pharmacological potential. The presence of these compounds supports the traditional medicinal use of *E. hemisphaerica* and highlights its potential as a source of antioxidant and anticancer agents.

Total phenolic and flavonoid content (TPC)

The total phenolic content (TPC) and total flavonoid content (TFC) of *E. hemisphaerica* leaf extract were analyzed using a UV-vis spectrophotometer. TPC was determined using the Folin-Ciocalteu reagent, with gallic acid as the standard, and absorbance measured at 745 nm. The results are expressed in milligrams of gallic acid equivalents per gram of extract (mg GAE/g). TFC was measured using quercetin as the standard and expressed in milligrams of quercetin equivalents per gram of extract (mg QE/g). The type of solvent significantly influenced the amount of bioactive compounds extracted. The methanol extract exhibited the highest TPC value at 506.4 ± 15.41 mg GAE/g, indicating high solubility of phenolic compounds in polar solvents. Conversely, the highest TFC was found in the ethyl acetate extract, with a value of 471.5 ± 20.55 mg QE/g, suggesting better solubility of flavonoids in semi-polar solvents. Aquadest yielded the lowest values for both phenolics and flavonoids, confirming its lower efficiency in extracting these classes of compounds. These findings emphasize the critical role of solvent polarity in the efficiency of phytochemical extraction.

Antioxidant activity using the DPPH method

The antioxidant activity of *E. hemisphaerica* leaf extracts was evaluated using the 2,2-diphenyl-1-picrylhydrazyl (DPPH) radical scavenging assay. The results were expressed as IC_{50} values (mean ± SD, n = 3), representing the concentration of extract required to inhibit 50% of DPPH radical activity. A lower IC_{50} values corresponds to stronger antioxidant potential. As shown in Table 3 and, all extracts exhibited concentration-dependent antioxidant activity. Among the three solvent extracts tested, the methanol extract demonstrated the strongest antioxidant activity, with an IC_{50} value of 0.40 ± 0.03 ppm, significantly ($p < 0.05$) lower than those of the other extracts and the standard. The aqueous extract showed moderate activity with an IC_{50} of 1.07 ± 0.05 ppm, followed by the ethyl acetate extract at 1.97 ± 0.06 ppm. Interestingly, all extracts outperformed ascorbic acid as a positive control, which had an IC_{50} of 6.74 ± 0.12 ppm. These results indicate that solvent polarity significantly affects the extraction of antioxidant compounds. The superior performance of the methanol extract may be attributed to its higher content of phenolic and flavonoid compounds, as previously reported in phytochemical studies. The significant differences among the treatments were confirmed via one-way ANOVA followed by Tukey's post-hoc test ($p < 0.05$).

Table 1. Qualitative analysis of secondary metabolites in leaf extracts of *Etlingera hemisphaerica* from the Gayo Highlands using different solvents

Secondary metabolites	Methanol Extract	Ethyl Acetate Extract	Aquadest Extract
Flavonoids	+++	++	+
Terpenoids	+	+	+
Steroids	++	+	+
Tannin	+	-	+
Saponin	++	+	+
Phenolic	+++	+	+
Alkaloids	+	+	+

Note: (-): Not detected, (+): Weakly present, (++): Moderately present, (+++): Strongly present

Table 2. Total phenolic and flavonoid content of *Etingera hemisphaerica* leaf extract

Solvent	Total bioactive content	
	TPC (mg GAE/g)	TFC (mg QE/g)
Methanol	506.4 ± 15.41c	320.4 ± 11.72c
Ethyl acetate	226.1 ± 12.80d	471.5 ± 20.55e
Aquadest	± 3.50d	114.2± 4.68c

Note: Superscript letters (c, d, e) indicate statistically significant differences ($p < 0.05$) based on post hoc analysis

Table 3. IC_{50} values of antioxidant activity of *Etlingera hemisphaerica* leaf extracts

Solvent	IC_{50} (ppm)
Methanol	0.40 ± 0.03^{a}
Ethyl acetate	1.97 ± 0.06^{b}
Aquadest	1.07 ± 0.05^{c}
Ascorbic acid	6.74 ± 0.12^{d}

Note: Different superscript letters indicate significant differences among groups at $p < 0.05$ (Tukey HSD)

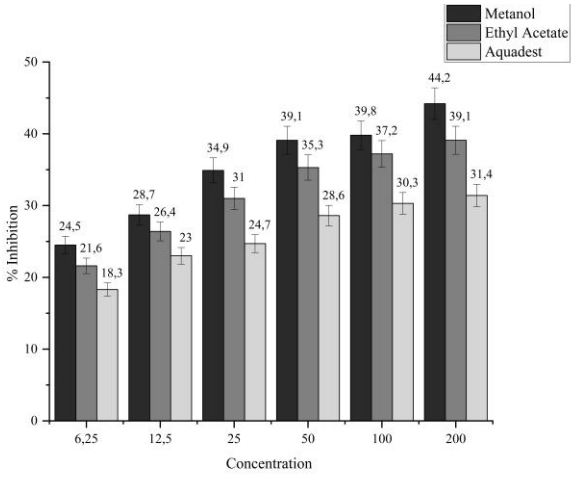

Figure 3. Percentage of MCF-7 breast cancer cell inhibition by *Etlingera hemisphaerica* leaf extracts

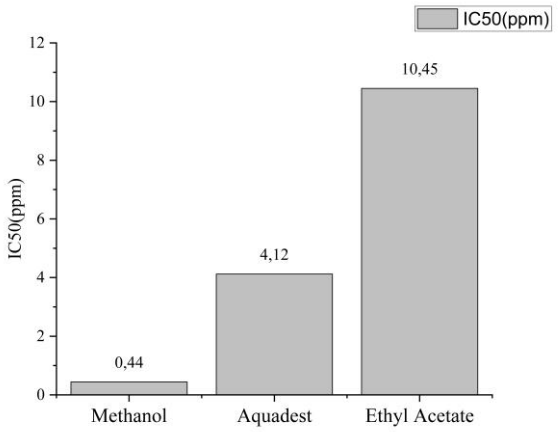

Figure 4. IC_{50} values of *Etlingera hemisphaerica* leaf extracts against MCF-7 breast cancer cells

MTT assay test of *Etlingera hemisphaerica* leaf extract

The cytotoxic activity of *E. hemisphaerica* leaf extracts against MCF-7 breast cancer cells was evaluated using the MTT assay. The percentage of cell inhibition at various extract concentrations (6.25-200 ppm) is shown in Figure 3. The results demonstrate a concentration-dependent inhibitory effect for all extracts tested. At the highest concentration of 200 ppm, the methanol extract exhibited the most potent cytotoxic activity, inhibiting 43.47% of MCF-7 cell viability. As the concentration decreased, the inhibition percentage also declined, reaching 23.21% at 6.25 ppm. This pattern indicates a clear dose-response relationship. The ethyl acetate extract also showed cytotoxic effects, although to a lesser extent than the methanol extract. At 200 ppm, the inhibition was 37.53%, decreasing to 17.59% at the lowest concentration. The aquadest extract displayed the weakest activity, with a maximum inhibition of 30.12% at 200 ppm and 18.21% at 6.25 ppm. These findings suggest that methanol is the most effective solvent for extracting bioactive compounds with anticancer potential from *E. hemisphaerica*. The superior cytotoxicity of the methanol extract correlates with its higher content of flavonoids and phenolics, as previously shown in the phytochemical and antioxidant assays. These compounds are known to exert anticancer activity by inducing apoptosis and inhibiting cancer cell proliferation.

The IC_{50} value of *E. hemisphaerica* leaf extracts against MCF-7 breast cancer cell were determined to assess their cytotoxic potency. The methanol extract exhibited the strongest anticancer activity with an IC_{50} value of 0.446 ppm, indicating that only a very low concentration was required to inhibit 50% of cancer cell viability (Figure 4). This suggests a high cytotoxic potential, likely attributed to the elevated levels of flavonoids and phenolics present in the methanol extract, as previously confirmed in the phytochemical and antioxidant analyses. The ethyl acetate extract showed a markedly weaker effect, with an IC_{50} value of 10.45 ppm, indicating lower anticancer efficacy. In comparison, the aquadest extract displayed moderate cytotoxicity, with an IC_{50} of 4.12 ppm, which was less effective than methanol but more active than ethyl acetate. These findings demonstrate that solvent polarity significantly influences the extraction of cytotoxic compounds, with methanol proving to be the most efficient. The strong inverse correlation between IC_{50} values and phenolic/flavonoid content further supports the role of these compounds in mediating anticancer activity.

Discussion

The phytochemical screening of *E. hemisphaerica* leaf extract from the Gayo Highlands revealed the presence of major classes of bioactive secondary metabolites, including flavonoids, phenolics, terpenoids, steroids, tannins, and saponins (Table 1). These classes of compounds are known to play central roles in mediating various pharmacological effects, particularly antioxidant and anticancer activities. The qualitative phytochemical profile observed aligns with prior reports on other *Etlingera* species such as *E. elatior*, *Etlingera pavieana* (Pierre ex Gagnep.) R.M.Sm., and *Etlingera alba* (Blume) A.D.Poulsen, which exhibit comparable metabolite compositions and traditional medicinal relevance (Iawsipo et al. 2018; Al-Mansoub et al. 2021; Padmanabhan et al. 2024). This also corroborates the findings of Riyanti et al. (2022), confirming the traditional use of the species based on its rich phytochemical content.

Quantitative analyses demonstrated that the methanol extract possessed the highest total phenolic content (506.4 ± 15.41 mg GAE/g), while the ethyl acetate extract had the highest total flavonoid content (471.5 ± 20.55 mg QE/g). These results reflect the solvent-dependent solubility of different phytoconstituents, with methanol being more effective for polar phenolic compounds and ethyl acetate for moderately polar flavonoids. This observation is in agreement with findings from *E. elatior* and *Curcuma longa* L., which highlight solvent polarity as a key factor influencing extraction efficiency (Widyasari et al. 2014; Fithrotunnisa et al. 2020).

Flavonoids and compounds are prominent contributors to antioxidant defense due to their capacity to scavenge free radicals, chelate metal ions, and enhance the activity of

endogenous antioxidant enzymes such as catalase and superoxide dismutase. Their electron donating and hydrogen-transfer capabilities make them effective in neutralizing reactive oxygen species (ROS), thereby mitigating oxidative stress a known contributor to cancer, cardiovascular disease, and neurodegenerative disorders (Perez-Vizcaino and Fraga 2018; Kopustinskiene et al. 2020; Rahmiyani et al. 2023). Additionally, flavonoids exhibit anti-inflammatory, antimicrobial, and antiproliferative properties through modulation of NF-κB signaling, inhibition of angiogenesis, and induction of mitochondrial-mediated apoptosis (Sak 2014; Nabavi et al. 2020). Phenolic compounds, synthesized via the shikimate pathway, phenylpropanoid pathways, are similarly associated with cell cycle arrest and tumor-suppressive effects (Maheshwari and Sharma 2023).

The methanol extract displayed the highest antioxidant capacity with an IC_{50} of 0.40 ppm, which was markedly more potent than ethyl acetate (1.97 ppm), aqueous extract (1.07 ppm), and the standard antioxidant ascorbic acid (6.74 ppm). This exceptional activity is likely attributed to the high concentration of phenolics and flavonoids in the methanol extract. Similar solvent-dependent antioxidant trends have been reported in *E. elatior*, *Zingiber officinale* Roscoe, and *C. longa*, further reinforcing the critical role of solvent polarity and phytochemical abundance in antioxidant efficacy (Ghasemzadeh et al. 2015; Chin 2016; Anzian et al. 2017).

In terms of cytotoxic potential, the methanol extract exhibited the most potent inhibition of MCF-7 human breast cancer cells, with an IC_{50} of 0.446 ppm. This strong cytotoxicity at low concentrations suggests a significant presence of antiproliferative constituents. Comparative studies with *E. elatior* and *E. pavieana* have shown similar activity against various cancer cell lines, attributed primarily to flavonoids (quercetin, kaempferol) and diarylheptanoids that induce apoptosis and ROS-mediated DNA damage (Iawsipo et al. 2018; Zhao et al. 2019). Flavonoids are known to activate intrinsic apoptotic pathways via mitochondrial membrane disruption, upregulation of pro-apoptotic proteins, and inhibition of anti-apoptotic proteins (e.g., Bcl-2), culminating in caspase activation and cancer cell death (Nabavi et al. 2020).

The potent cytotoxic effect of the methanol extract may also be attributed to terpenoids and steroids, which have been reported to disrupt cellular homeostasis through membrane destabilization, modulation of cell cycle regulatory proteins, and interference with angiogenesis (Jiang 2019). Such synergistic interactions among phytochemicals likely enhance the therapeutic potential of the extract.

Compared to other Zingiberaceae species, *E. hemisphaerica* appears to demonstrate superior or comparable bioactivity. For example, *C. longa* typically exhibits DPPH IC_{50} values between 2-5 ppm and MCF-7 IC_{50} values ranging from 10-20 ppm (Maheshwari and Sharma 2023), whereas the IC_{50} values of *E. hemisphaerica* are substantially lower, suggesting stronger bioefficacy. The observed activities also support the ethnomedical relevance of *E. hemisphaerica*, indicating that its traditional usage may have a scientific basis grounded in phytochemistry. Moreover, the results provide a comparative framework with related *Etlingera* species, strengthening the claim that this genus represents a rich source of antioxidant and anticancer agents.

In summary, the bioactivities of *E. hemisphaerica* leaf extracts particularly those obtained with methanol are closely linked to their phytochemical composition, especially the high phenolic and flavonoid content. These compounds likely act through multiple cellular mechanisms, including oxidative stress modulation, apoptosis induction, and inhibition of cancer cell proliferation. Given the remarkably low IC_{50} values observed, *E. hemisphaerica* holds strong potential for development as a natural antioxidant and anticancer agent. However, further studies are required to isolate and characterize the active compounds, confirm efficacy in in vivo systems, and assess toxicity and safety for therapeutic use.

ACKNOWLEDGEMENTS

This research was funded by the Research for Beginner Lecturers program (Project Number 055/LPPM-USM/VII/2024), supported by the Ministry of Research, Technology, and Higher Education of of the Republic of Indonesia. The authors would like to express their sincere gratitude for this support, which made the completion of this study possible.

REFERENCES

Adegoke GO, Ojo OA. 2017. Phytochemical, antioxidant and antimicrobial activities in the leaf, stem and fruit fractions of *Basella alba* and *Basella rubra*. Science 5 (5): 73-79.

Adhikari P, Joshi K, Singh M, Pandey A. 2022. Influence of altitude on secondary metabolites, antioxidants, and antimicrobial activities of Himalayan yew (*Taxus wallichiana*). Plant Biosyst - An Intl J Dealing All Asp Plant Biol 156 (1): 187-195. DOI: 10.1080/11263504.2020.1845845.

Al-Mansoub MA, Asif M, Revadigar V, Hammad MA, Chear NJ, Hamdan MR, Majid AM, Asmawi MZ, Murugaiyah V. 2021. Chemical composition, antiproliferative and antioxidant attributes of ethanolic extract of resinous sediment from *Etlingera elatior* (Jack.) inflorescence. Braz J Pharm Sci 57: e18954. DOI: 10.1590/s2175-97902020000418954.

Anzian Ab, Rashidah S, Nazamid S, Sapawi CWNSbCW, Hussin ASbM. 2017. Chemical composition and antioxidant activity of torch ginger (*Etlingera elatior*) flower extract. Food Appl Biosci J 5 (1): 32-49. DOI: 10.14456/fabj.2017.4.

Ayele DT, Akele ML, Melese AT. 2022. Analysis of total phenolic contents, flavonoids, antioxid ant and antibacterial activities of *Croton macrostachyus* root extracts. BMC Chem 16 (1): 30. DOI: 10.1186/s13065-022-00822-0.

Bello AA, Katta A, Obaydo RH, Jazmati A. 2024. Phytochemical analysis and antioxidant efficacy of *Chrysojasminum fruticans* (L.) Banfi in Syrian flora. Heliyon 10 (17): e37322. DOI: 10.1016/j.heliyon.2024.e37322.

Block KI, Gyllenhaal C, Lowe L, Amedei A, Amin ARMR, Amin A, Aquilano K, Arbiser J, Arreola A, Arzumanyan A, Ashraf SS, Azmi AS, Benencia F, Bhakta D, Bilsland A, et al. 2015. Designing a broad-spectrum integrative approach for cancer prevention and treatment. Semin Cancer Biol 35 Suppl (Suppl): S276-S304. DOI: 10.1016/j.semcancer.2015.09.007.

Cane HPCA, Musman M, Yahya M, Saidi N, Darusman D, Nanda M, Rizki DR, Puspita K. 2023. Phytochemical screening and antibacterial activity of ethnomedicinal plants from Gayo Lues Highland, Indonesia. J Pharm Pharmacogn Res 11 (1): 117-128. DOI: 10.56499/jppres22.1526_11.1.117.

Chin KY. 2016. The spice for joint inflammation: Anti-inflammatory role of curcumin in treating osteoarthritis. Drug Des Devel Ther 10: 3029-3042. DOI: 10.2147/DDDT.S117432.

Ernilasari, Walil K, Fitmawati, Roslim DI, Zumaidar, Saudah, Rayhannisa. 2021. Antibacterial activity of leaves, flowers, and fruits extract of *Etlingera elatior* from Nagan Raya District, Indonesia against *Escherichia coli* and *Staphylococcus aureus*. Biodiversitas 22 (10): 4457-4464. DOI: 10.13057/biodiv/d221039.

Fithrotunnisa Q, Arsianti A, Kurniawan G, Qorina F, Tejaputri NA, Azizah NN. 2020. In vitro cytotoxicity of *Hibiscus sabdariffa* Linn extracts on A549 lung cancer cell line. Pharmacogn J 12 (1): 14-19. DOI: 10.5530/pj.2020.12.3.

Gadouche L, Alsoufi ASM, Pacholska D, Skotarek A, Pączkowski C, Szakiel A. 2023. Triterpenoid and steroid content of lipophilic extracts of selected medicinal plants of the Mediterranean Region. Molecules 28 (2): 697. DOI: 10.3390/molecules28020697.

Ghasemzadeh A, Jaafar HZ, Rahmat A, Ashkani S. 2015. Secondary metabolites constituents and antioxidant, anticancer and antibacterial activities of *Etlingera elatior* (Jack) R.M.Sm grown in different locations of Malaysia. BMC Complement Altern Med 15: 335. DOI: 10.1186/s12906-015-0838-6.

Ghasemzadeh A, Nasiri A, Jaafar HZ, Baghdadi A, Ahmad I. 2014. Changes in phytochemical synthesis, chalcone synthase activity and pharmaceutical qualities of sabah snake grass (*Clinacanthus nutans* L.) in relation to plant age. Molecules 19 (11): 17632-17648. DOI: 10.3390/molecules191117632.

Handayani ND, Esquibet M, Montarry J, Lestari P, Couvreur M, Dikin A, Helder J, Grenier E, Bert W. 2020. Distribution, DNA barcoding and genetic diversity of potato cyst nematodes in Indonesia. Eur J Plant Pathol 158: 363-380. DOI: 10.1007/s10658-020-02078-7.

Iawsipo P, Srisook E, Ponglikitmongkol M, Somwang T, Singaed O. 2018. Cytotoxic effects of *Etlingera pavieana* rhizome on various cancer cells and identification of a potential anti-tumor component. J Food Biochem 42 (4): e12540. DOI: 10.1111/jfbc.12540.

Jiang Q, Zhao Y, Zhang X, Yang X, Chen Y, Chu Z, Ye Q, Li X, Yin Z, You J. 2019. Surface passivation of perovskite film for efficient solar cells. Nat Photonics 13: 460-466. DOI: 10.1038/s41566-019-0398-2.

Jiang TA. 2019. Health benefits of culinary herbs and spices. Journal of AOAC International 102 (2): 395-411. DOI: 10.5740/jaoacint.18-0418.

Kancherla N, Dhakshinamoothi A, Chitra K, Komaram RB. 2019. Preliminary analysis of phytoconstituents and evaluation of anthelminthic property of *Cayratia auriculata* (*in vitro*). Maedica (Bucur) 14 (4): 350-356. DOI: 10.26574/maedica.2019.14.4.350.

Kopustinskiene DM, Jakstas V, Savickas A, Bernatoniene J. 2020. Flavonoids as anticancer agents. Nutrients 12 (2): 457. DOI: 10.3390/nu12020457.

Lee J, Shin A, Oh JH, Kim J. 2017. Colors of vegetables and fruits and the risks of colorectal cancer. World J Gastroenterol 23 (14): 2527-2538. DOI: 10.3748/wjg.v23.i14.2527.

Lestari W, Hasballah K, Listiawan MY, Sofia S. 2023. Antioxidant and phytometabolite profiles of ethanolic extract from the cascara pulp of *Coffea arabica* collected from Gayo Highland: A study for potential anti-photoaging agent. F1000Res 12: 12. DOI: 10.12688/f1000research.126762.2.

Lichota A, Gwozdzinski K. 2018. Anticancer activity of natural compounds from plant and marine environment. Intl J Mol Sci 19 (11): 3533. DOI: 10.3390/ijms19113533.

Lim TK. 2014. *Etlingera hemisphaerica*. In: Edible Medicinal and Non Medicinal Plants. Springer, Dordrecht. DOI: 10.1007/978-94-017-8748-2_74.

Maheshwari N, Sharma MC. 2023. Anticancer properties of some selected plant phenolic compounds: Future leads for therapeutic development. J Herb Med 42: 100801. DOI: 10.1016/j.hermed.2023.100801.

Mali SB. 2023. Cancer treatment: Role of natural products. Time to have a serious rethink. Oral Oncol Rep 6: 100040. DOI: 10.1016/j.oor.2023.100040.

Mankhong S, Iawsipo P, Srisook E, Srisook K. 2019. 4-methoxycinnamyl p-coumarate isolated from *Etlingera pavieana* rhizomes inhibits inflammatory response via suppression of NF-κB, Akt and AP-1 signaling in LPS-stimulated RAW 264.7 macrophages. Phytomedicine 54: 89-97. DOI: 10.1016/j.phymed.2018.09.193.

Nabavi SM, Šamec D, Tomczyk M, Milella L, Russo D, Habtemariam S, Suntar I, Rastrelli L, Daglia M, Xiao J, Giampieri F, Battino M, Sobarzo-Sanchez E, Nabavi SF, Yousefi B, Jeandet P, Xu S, Shirooie S. 2020. Flavonoid biosynthetic pathways in plants: Versatile targets for metabolic engineering. Biotechnol Adv 38: 107316. DOI: 10.1016/j.biotechadv.2018.11.005.

Noviyanty YN, Herlina H, Fazihkun C. 2020. Identification and determination of saponin levels from bidurrot extract (*Calotropis gigantea* L) using gravimetry method. J Pharm Sci 3 (2): 100-105.

Padmanabhan V, Kumar SS, Giridhar P. 2024. Phytochemicals and UHPLC-QTOF-HRMS characterisation of bioactives of butterfly pea (*Clitoria ternatea* L.) seeds and their antioxidant potentials. Food Chem 433: 137373. DOI: 10.1016/j.foodchem.2023.137373.

Perez-Vizcaino F, Fraga CG. 2018. Research trends in flavonoids and health. Arch Biochem Biophys 646: 107-112. DOI: 10.1016/j.abb.2018.03.022.

POWO. 2023. Plants of the World Online. Plant of the World. Royal Botanic Gardens, Kew. http://www.plantsoftheworldonline.org.

Rahimah SB, Djunaedi DD, Soeroto AY, Bisri T. 2019. The phytochemical screening, total phenolic contents and antioxidant activities *in vitro* of white oyster mushroom (*Pleurotus Ostreatus*) preparations. Open Access Maced J Med Sci 7 (15): 2404-2412. DOI: 10.3889/oamjms.2019.741.

Rahmiyani I, Rolita Pasa AN, Amin S, Yuliana A. 2023. Formulation of mouthwash honje laka (*Etlingera hemisphaerica* (Blume) R.M.Sm.) flower extract against *Streptococcus mutans*. FITOFARMAKA: Jurnal Ilmiah Farmasi 13 (1): 50-60. DOI: 10.33751/jf.v13i1.6830.

Riyanti S, Windyaswari AS, Syam AK, Karlina Y, Anjelista D, Faramayuda F, Aulia N, Ratnawati J. 2022. Phytochemical content and antioxidant activity of forest honje leaf (*Etlingera hemisphaerica* (Blume) R.M. Sm). IOP Conf Ser Earth Environ Sci 1104 (1): 012022. DOI: 10.1088/1755-1315/1104/1/012022.

Ruyani A, Putri RZE, Jundara P, Gresinta E, Ansori I, Sundaryono A. 2019. Protective effect of leaf ethanolic extract *Etlingera hemisphaerica* Blume against mercuric chloride toxicity in blood of mice. J Diet Suppl 16 (1): 51-65. DOI: 10.1080/19390211.2018.1429516.

Sammar M, Abu-Farich B, Rayan I, Falah M, Rayan A. Correlation between cytotoxicity in cancer cells and free radical-scavenging activity: In-vitro evaluation of 57 medicinal and edible plant extracts. 2019. Oncol Lett 18 (6): 6563-6571. DOI: 10.3892/ol.2019.11054.

Sahidin S, Syefira S, Wahyuni W, Fristiohady A, Imran I. 2019. Potensi antibakteri ekstrak metanol dan senyawa aromatik dari buah wualae (*Etlingera elatior*). Jurnal Kimia Valensi 5 (1): 1-7. DOI: 10.15408/jkv.v5i1.8658

Sak K. 2014. Cytotoxicity of dietary flavonoids on different human cancer types. Pharmacognosy Rev 8 (16): 122. DOI: 10.4103/0973-7847.134247.

Saudah, Fitmawati, Dewi IR, Zumaidar, Darusman, Ernilasari. 2021. Ethnobotany *Etlingera elatior* (Jack) R.M. Smith (Cikala) in Ethnic Gayo. Proceedings of the 3rd KOBI Congress, International and National Conferences (KOBICINC 2020) 14 (Kobicinc 2020): 205-209. DOI: 10.2991/absr.k.210621.034.

Saudah, Zumaidar, Darusman, Fitmawati, Roslim DI, Ernilasari. 2022. Ethnobotanical knowledge of *Etlingera elatior* for medicinal and food uses among ethnic groups in Aceh Province, Indonesia. Biodiversitas 23 (8): 4361-70. DOI: 10.13057/biodiv/d230862.

Shahid Ud-Daula AFM, Mohammad AB. 2019. Genus *Etlingera* - A review on chemical composition and antimicrobial activity of essential oils. J Med Plants Res 13 (7): 135-56. DOI: 10.5897/jmpr2019.6740.

Shahid-Ud-Daula AFM, Kuyah MAA, Kamariah AS, Lim LBL, and Ahmad N. 2019. Phytochemical and pharmacological evaluation of methanolic extracts of *Etlingera fimbriobracteata* (Zingerberaceae). South Afr J Bot 121: 45-53. DOI: 10.1016/j.sajb.2018.10.013.

Siregar AZ, Pradana MG, Rahmi D. 2020. Effect of kecombrang (*Etlingera elatior*) as larvacide to control *Aedes aegypti* (Diptera: Culicidae). In International Conference and the 10th Congress of the Entomological Society of Indonesia (ICCESI 2019) Effect: 35-40. DOI: 10.2991/absr.k.200513.006.

Setyawati A, Komariah, Pujiaasmanto B, Fatawi A, Batubara I. 2021. Secondary metabolites of turmeric and ginger on various altitudes and soil characteristics. IOP Conf Ser Earth Environ Sci 724 (1): 012020. DOI: 10.1088/1755-1315/724/1/012020.

Sung H, Ferlay J, Siegel RL, Laversanne M, Soerjomataram I, Jemal A. Global Cancer Statistics. 2020. GLOBOCAN estimates of incidence and mortality worldwide for 36 Cancers in 185 Countries. CA Cancer J Clin 2021 71 (3): 209-49. DOI: 10.3322/caac.21660.

Tiwari P, Kumar B, Kaur M, Kaur G, Kaur H. 2011. Phytochemical Screening and Extraction: A Review. Intl Pharm Sci 1 (1): 98-106. DOI: 10.33084/bjop.v3i1.1245.

Widyasari P, Budianta T, Kusuma F, Wijaya L. 2014. Difference of solvent polarity to phytochemical content and antioxidant activity of *Pluchea indicia* less leaves extracts. Intl J Pharmacognosy Phytochem Res 6 (4): 850-855.

Yuan M, Zhang G, Bai W, Han X, Li C, Bian S. 2022. The role of bioactive compounds in natural products extracted from plants in cancer treatment and their mechanisms related to anticancer effects. Oxid Med Cell Longev 22 : 1-19. DOI: 10.1155/2022/1429869.

Zhao L, Yuan X, Wang J, Feng Y, Ji F, Li Z, Bian J. 2019. A review on flavones targeting serine/threonine protein kinases for potential anticancer drugs. Bioorg Med Chem 27(5): 677-685. DOI: 10.1016/j.bmc.2019.01.027.

ASIAN J NAT PROD BIOCHEM
Volume 23, Number 2, December 2025
Pages: 110-121

P-ISSN: 2775-4189
E-ISSN: 2775-4197
DOI: 10.13057/biofar/f230103

Polyisoprenoid-based chemotaxonomy and cluster analysis of mangrove reproductive tissues from North Sumatra, Indonesia

MOHAMMAD BASYUNI[1,2,♥], WAHYUNI PULUNGAN[1], SHOFIYAH SABILAH AL MUSTANIROH[2], SHIGEYUKI BABA[3]

[1]Department of Forestry, Faculty of Forestry, Universitas Sumatera Utara. Jl. Lingkar USU, Deli Serdang 20353, North Sumatera, Indonesia. Tel.: +62-61-8220605, ♥email: m.basyuni@usu.ac.id
[2]Center of Excellence for Mangrove, Universitas Sumatera Utara. Jl. Dr. T. Mansur No. 9, Kampus, Medan 20155, North Sumatera, Indonesia
[3]International Society for Mangrove Ecosystems, University of the Ryukyus. Nishihara, Okinawa 903-0129, Japan

Manuscript received: 8 July 2025. Revision accepted: 9 October 2025.

Abstract. *Basyuni M, Pulungan W, Al Mustaniroh SS, Baba S. 2025. Polyisoprenoid-based chemotaxonomy and cluster analysis of mangrove reproductive tissues from North Sumatra, Indonesia. Asian J Nat Prod Biochem 23: 110-121.* This study investigates the chemotaxonomic significance of polyisoprenoids—specifically polyprenols and dolichols—in the reproductive organs (flowers and fruits) of fourteen mangrove species from North Sumatra, Indonesia. Employing Two-Dimensional Thin-Layer Chromatography (2D-TLC) as a high-resolution analytical tool and Unweighted Pair Group Method with Arithmetic mean (UPGMA) clustering as a classification approach, we profiled the polyisoprenoid compounds in flowers. We classified them into three types based on their relative abundance. Type I, with a predominance of dolichols over polyprenols (more than ninefold), was observed in *Barringtonia asiatica*, *Lumnitzera racemosa*, *Ricinus communis*, and *Scyphiphora hydrophyllacea*. Type II, with the occurrence of both polyprenols and dolichols, was observed in *Acanthus ilicifolius*, *Excoecaria agallocha*, *Hibiscus tiliaceus*, *Melastoma candidum*, and *Sonneratia alba*. Type III, with a predominance of polyprenols over dolichols, was observed in *Avicennia officinalis*, *Bruguiera sexangula*, *Rhizophora apiculata*, and *Rhizophora mucronata.* However, in the fruits, a type-I distribution was observed in nine species. In comparison, five species, *Acanthus illicifolius*, *A. officinalis*, *H. tiliaceus*, *Lumnitzera littorea*, and *M. candidum*, corresponded to a type II distribution and were not type III. Quantitative analyses revealed that dolichols were dominant in 64% of the fruit tissues, while floral tissues showed more diversity. Hierarchical cluster analysis using /UPGMA grouped species based on polyisoprenoid similarity, demonstrating their value as chemotaxonomic markers. These findings provide a significant foundation for mangrove conservation strategies by linking biochemical markers to species resilience in the coastal ecosystem, inspiring potential new approaches to conservation.

Keyword: 2D-TLC, chemotaxonomy, generative tissues, mangrove, polyisoprenoid

Abbreviations: 2D-TLC: Two-Dimensional Thin Layer Chromatography, Dol: Dolichols, HPTLC: High Performance Thin Layer Chromatography, Pol: Polyprenols, Poly: Polyisoprenoids, TL: Total Lipids, UPGMA: Unweighted-Pair Group Method with Arithmetic mean

INTRODUCTION

Mangroves are among the most productive and ecologically significant coastal ecosystems, supporting biodiversity, shoreline stability, and climate regulation, particularly in tropical and subtropical regions (Friess et al. 2020; Kasihiw et al. 2024). Accurate identification of mangrove species is critical for conservation planning, especially in the face of habitat loss and climate stress. The integration of chemical profiling, such as polyisoprenoid analysis, with ecological data could enhance biodiversity monitoring and reveal species-specific adaptation strategies (Umoh 2020; Upadhyay et al. 2025). This is particularly important in Southeast Asia, a major hotspot for mangrove diversity and degradation pressure (Friess et al. 2020).

In addition to their ecological roles, mangrove plants are increasingly recognized as rich sources of phytochemical compounds, including secondary metabolites with potential pharmacological applications (Bibi et al. 2019; Upadhyay et al. 2025). Among these are polyisoprenoids, a class of long-chain isoprene compounds including polyprenols and dolichols, which are linear polymers of five-carbon isoprene units found across all domains of life (Swiezewska and Danikiewicz 2005; Surmacz and Swiezewska 2011; Basyuni et al. 2017a).

One of the abundant secondary metabolites in mangrove plants is polyisoprenoid alcohol. Polyisoprenoid alcohols are linear polymers of five-carbon chain units that are present in almost all living cells. Long-chain polyisoprenoids are present in various plant tissues (Swiezewska and Danikiewicz 2005). Polyisoprenoid alcohol (dolichol and polyprenol) is found in all living organisms, from bacteria to mammals/animals (Surmacz and Swiezewska 2011). Polyisoprenoids are found in cells and tissues in a variety of different forms. Polyisoprenoids are present in plants with different chain lengths, including increasing age (tissue aging) (Swiezewska and Danikiewicz 2005; Basyuni et al. 2017b), salinity stress (Basyuni et al. 2021), tissue differences (Tateyama et al. 1999; Surmacz and Swiezewska 2011), light (Bajda et al. 2005; Swiezewska and Danikiewicz 2005), and temperature (Salvador-Castell et al. 2020). Polyisoprenoids are present as free alcohols or esterified with acetate or fatty acids (Gelder et al. 2021).

Chemotaxonomy, which involves using chemical constituents for taxonomic classification, has become a valuable complementary tool alongside morphological and molecular methods (Basyuni et al. 2017a). This approach is especially important in mangrove research, where traditional identification techniques may fail due to convergent traits among unrelated taxa. Polyisoprenoids, including polyprenols and dolichols, are long-chain isoprenoid alcohols that play essential roles in cellular processes such as glycoprotein synthesis and maintaining membrane integrity (Basyuni et al. 2021).

In plants, polyisoprenoids are involved in various biological functions, particularly in response to environmental stressors such as salinity, light, and tissue aging (Swiezewska and Danikiewicz 2005; Basyuni et al. 2017a). The biosynthesis and accumulation of polyisoprenoids can vary with tissue type and developmental stage (Tateyama et al. 1999; Surmacz and Swiezewska 2011; Rizkiany et al. 2021). However, beyond their biochemical function, their distribution among plant taxa shows potential as chemotaxonomic markers, especially in complex and poorly resolved genera like *Rhizophora* and *Bruguiera* (Bandaranayake 2002). Recent studies have emphasized the need to explore secondary metabolites, including polyisoprenoids, for better species delimitation and ecological function interpretation within mangrove ecosystems (Upadhyay et al. 2025; Mali et al. 2023).

Despite their widespread presence, little is known about how these compounds are distributed in mangrove reproductive structures. Therefore, this study aims to investigate the occurrence and chemotaxonomic significance of polyisoprenoid profiles in the generative tissues—flowers and fruits—of fourteen mangrove species in North Sumatra, Indonesia. By employing Two-Dimensional Thin-Layer Chromatography (2D-TLC) and hierarchical cluster analysis, we evaluated the variation in polyprenol and dolichol contents to explore their potential roles in species differentiation and adaptation, as well as the further roles of polyisoprenoids.

MATERIALS AND METHODS

Plant materials

Reproductive organs (flowers and fruits) from 14 carefully selected mangrove species were collected from Lubuk Kertang and Pulau Sembilan, North Sumatra, Indonesia, during the peak fruiting season. The selection of these species was based on their abundance, reproductive activity, and ecological distribution, ensuring a comprehensive study. The harvested flowers and fruits were harvested from healthy, mature plants and immediately preserved in cool, dark conditions for laboratory analysis. Fourteen mangrove species were selected based on their abundance, reproductive activity, and ecological distribution. Flowers and fruits were harvested during the peak reproductive season (May-August) as shown in Figure 1, with three individual plants per species being sampled, and tissues were analyzed separately. Habitat characteristics, such as tidal exposure and salinity, were recorded at the time of collection. All samples were transported on ice and stored at -20°C until further analysis to minimize metabolic degradation.

Extraction

Polyisoprenoid compounds were extracted via a modified protocol from Swiezewska and Danikiewicz (2005) and Basyuni et al. (2017a). Fresh plant tissue (approximately 2 g) was homogenized and subjected to lipid extraction with chloroform-methanol (2:1, v/v). The extract was partitioned and washed with aqueous solutions to isolate the lipid fraction, which was then saponified and purified as previously reported (Basyuni et al. 2021).

Polyprenol and dolichol profiles were analyzed via 2D-TLC. Silica gel plates were developed in two solvent systems to resolve polyisoprenoid compounds. Identification was based on chromatography with authentic standards and confirmed by visualization via iodine vapor staining. The enhanced chromatograph was imaged and alphanumerically scanned with an Epson L360 series printer.

Two-Dimensional Thin Layer Chromatography (2D-TLC) analysis

Polyisoprenoid profiles were analyzed via 2D-TLC on silica gel RP-18 HPTLC plates (Merck). The plates were first developed in toluene:ethyl acetate (9:1 v/v), then in acetone to separate polyprenols and dolichols on the basis of polarity and to resolve compound families.

Visualization was achieved via the use of iodine vapor. Polyprenols and dolichols were identified on the basis of their Rf values relative to those of authentic standards and by their characteristic yellow–brown coloration upon iodine exposure. The polyprenols and dolichols that were traced on RP-18 HPTLC plates were measured with dolichol and polyprenol specifications according to previously reported criteria (Basyuni et al. 2017b). Chromatograms were visualized using iodine vapor and documented via an Epson L360 scanner. Quantitative measurements were performed by densitometry.

Quantification and cluster analysis

Quantification of polyisoprenoids was performed by densitometry, using a standard solution prepared with dolichol or polyprenol as internal standards for two-dimensional TLC. A standard curve was generated by correlating iodine-stained band intensities with concentrations of dolichol on a reverse-phase C18 plate.

Figure 1. Generative organs were collected from mangrove trees

The polyisoprenoid types were classified into three categories on the basis of the predominance of the compound class: Type-I (dolichol dominant), Type-II (both present), and Type-III (polyprenol dominant). Cluster analysis was performed on subsets of flower and fruit data. In this analysis, 62 variables, each representing polyprenols and dolichols from the flowers and fruits of 14 species, were log-transformed (base 10) as previously described (Basyuni et al. 2017a, b). From these data, dendrograms representing the flower and fruit data were drawn by clustering analysis via the Unweighted-Pair Group Method with Arithmetic mean (UPGMA) and Multivariate Statistical Package (MVSP) 3.22 (Kovach Computing Service). The choice of Euclidean distance as the measure to quantify dissimilarity in polyisoprenoid abundance profiles was significant, as it is a widely accepted measure in cluster analysis.

RESULTS AND DISCUSSION

Polyisoprenoid profiles

The analysis of polyisoprenoid content in the reproductive organs of 14 mangrove species revealed distinct patterns, allowing for classification into three chemotypes. Table 1 presents the relative abundance or presence of polyprenols and dolichols in the flowers of 14 mangrove species, which are categorized into three distinct types. These findings were based on the relative dominance of dolichols and polyprenols.

Type I dolichol-dominant were found in the flowers of *Barringtonia asiatica* (L.) Kurz., *Lumnitzera racemosa* Willd., *Ricinus communis* L., and *Scyphiphora hydrophyllacea* C.F.Gaertn.. These species exhibited a greater than ninefold greater abundance of dolichols than of polyprenols. This profile suggests a strong shift toward dolichol biosynthesis, possibly associated with tissue aging, specific physiological roles in floral development, or species-specific genetic control (Surmacz and Swiezewska 2011; Tholl 2015; Rizkiany et al. 2021).

Type II (mixed profile) included *Acanthus ilicifolius* L., *Excoecaria agallocha* L., *Hibiscus tiliaceus* L., *Melastoma candidum* D. Don, and *Sonneratia alba* Sm., which presented relatively balanced levels of both polyprenols and dolichols. This balanced occurrence could indicate a dual role of both compounds in cellular processes, such as stress tolerance or active membrane remodeling in flowers (Basyuni et al. 2017a). Type III (polyprenol-dominant) were identified in *Avicennia officinalis* L., *Bruguiera sexangula* (Lour.) Poir., *Rhizophora apiculata* Blume, and *Rhizophora mucronata* Lam., where polyprenols outnumbered dolichols.

Interestingly, in the fruit tissues, 64% of the species exhibited a slight dominance of dolichols over polyprenols, although the diversity was less pronounced than that in flowers. This result indicates a shift in polyisoprenoid metabolism compared with that in floral tissues (Rizkiany et al. 2021).

Figure 2 displays 2D-TLC profiles of polyisoprenoid extracts from mangrove flowers. The chromatograms reveal distinct banding patterns, allowing the differentiation of polyprenol- and dolichol-rich species. The polyisoprenoid profile derived from: *Acanthus illicifolius* L. flowers, *A. officinalis* flowers, *B. asiatica* flowers, *B. sexangula* flowers, *E. agallocha* flowers, *H. tiliaceus* flowers.

Figure S1 displays the diversity of polyisoprenoid alcohols extracted from mangrove fruits. The 2D-TLC spots are marked with carbon chain lengths (C60 to C140), differentiating polyprenols (typically shorter chains) and dolichols (longer chains with a saturated alpha isoprene unit). *Excoecaria agallocha* shows a notably wide range (up to C140), indicating high polyisoprenoid complexity (Figure 2.E). Both polyprenols and dolichols are present in several species, suggesting diverse biosynthetic capabilities.

Figure S2 presents a similar polyisoprenoid profile from: *Lumnitzera littorea* (Jack) Voigt flowers, *L. racemosa* flowers, *M. candidum* flowers, *R. communis* flowers, depicting comparative intensities and mobility differences, which reflect tissue-specific polyisoprenoid accumulation.

Figure S3 summarizes the chemical diversity across tissues and species, reinforcing the findings from Table 1, specifically dolichols and polyprenols, which are known to play critical roles in membrane fluidity, protein glycosylation, and antioxidant defense. Dolichols are key intermediates in N-linked glycoprotein biosynthesis and are essential for protein folding and stress signal transduction in plants (Banerjee et al. 2017). In mangroves, which are exposed to high salinity and oxidative stress, the accumulation of dolichols could serve as a protective adaptation, helping to stabilize membrane-associated processes during reproduction (Basyuni et al. 2017a).

Figure S1 shows the two-dimensional TLC separation of polyisoprenoids from six mangrove fruit species. The results revealed diverse carbon chain lengths, especially in *E. agallocha*, which presented the richest dolichol profile among the groups. This diversity could reflect ecological adaptations to saline environments or functional roles in stress tolerance.

Figure 3 highlights differences in polyisoprenoid profiles between mangrove, coastal, and nonmangrove (mangrove associates) species. *Lumnitzera* fruits are high-molecular-weight dolichols typical of mangrove species. In contrast, *M. candidum* and *R. communis* present a more limited polyisoprenoid composition, suggesting a possible link between environmental stress and isoprenoid diversity (Basyuni et al. 2021).

Figure 4 presents polyisoprenoid profiles from Rhizophoraceae and related mangroves. The Rhizophora species maintain consistent dolichol chain lengths, whereas *S. alba* produces a wider spectrum, including shorter-chain dolichols. These biochemical patterns could reflect their physiological roles in saline environments and reproductive tissue development. *Rhizophora apiculata* and *R. mucronata* present mid- to long-chain dolichols (C85-C105), which are consistent with their structural or stress-protective functions. *Scyphiphora hydrophyllacea* displays dolichols from C70 to C95. *Sonneratia alba* is unique in that it contains both short- and long-chain dolichols (C50 to C90), indicating a complex isoprenoid biosynthesis pathway.

Table 1. Carbon-chain lengths and type of polyprenol and dolichol occurring in 14 Indonesian mangrove generative organ*

Species	Tissue	Polyprenol	Dolichol	Type
A. illicifolius	flower	80 85 90 95	80 85 90 95 100	II
A. officinalis	flower	60 65		III
B. asiatica	flower		65 70 75 80 85 90 95 100 105 110 115 120 125 130 135 140	I
B. sexangula	flower	40 45 50 55 60 65		III
E. agallocha	flower	80 85 90 95	80 85 90 95	II
H. tiliaceus	flower	55 60 65 70 75 80 85	55 60 65 70 75 80 85 90 95 100 105 110 115 120 125 130 135 140	II
L. littorea	flower	70 75 80 85 90 95 100 105 110 115 120	70 75 80 85 90 95 100 105 110 115 120	II
L. racemosa	flower		65 70 75 80 85 90 95	I
M. candidum	flower	75 80 85 90	70 75 80 85 90	II
R. communis	flower		75 80 85 90 95 100 105 110 115 120	I
R. apiculata	flower	45 50 55 60 65 70		III
R. mucronata	flower	45 50 55 60 65		III
S. hydrophyllacea	flower		65 70 75 80 85 90 95 100 105 110 115 120	I
S. alba	flower	70 75 80 85 90 95 100 105	65 70 75 80 85 90 95 100 105 110 115 120 125	II
A. illicifolius	fruit	75 80 85	75 80 85 90	II
A. officinalis	fruit	70 75 80 85 90 95 100 105 110 115 120 125 130 135 140	95 100 105 110 115	II
B. asiatica	fruit		75 80 85 90 95 100 105	I
B. sexangula	fruit		90 95 100 105 110 115 120	I
E. agallocha	fruit		70 75 80 85	I
H. tiliaceus	fruit	60 65 70 75 80	60 65 70 75 80 85 90 95 100 105 110	II
L. littorea	fruit	75 80 85 90 95 100 105 110 115 120	70 75 80 85 90 95 100 105 110 115 120 125 130 135 140	II
L. racemosa	fruit		45 50 55 60 65 70 75 80 85	I
M. candidum	fruit	70 75 80 85 90 95	70 75 80 85 90 95 100	II
R. communis	fruit		80 85 90	I
R. apiculata	fruit		85 90 95 100	I
R. mucronata	fruit		90 95 100 105	I
S. hydrophyllacea	fruit		70 75 80 85 90 95	I
S. alba	fruit		50 55 60 65 70 75 80 85 90	I

Note: *The numbers refer to the carbon-chain length of the polyisoprenoid alcohols

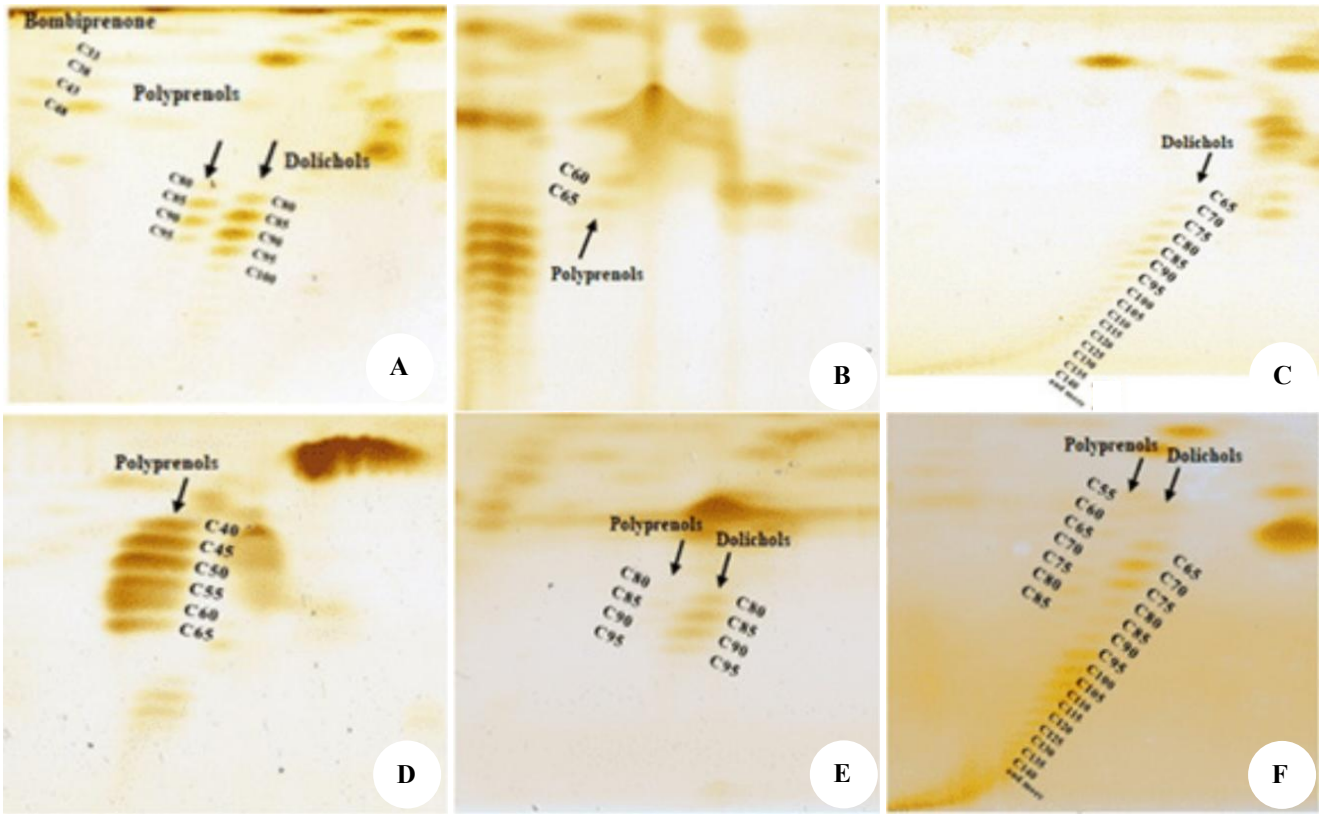

Figure 2. 2D-TLC chromatograms profile of hexane extracts of polyisoprenoid from: A. *Acanthus illicifolius* flowers, B. *Avicennia officinalis* flowers, C. *Barringtonia asiatica* flowers, D. *Bruguiera sexangula* flowers, E. *Excoecaria agallocha* flowers, F. *Hibiscus tiliaceus* flowers. The number shows the carbon chain length of polyisoprenoid alcohols

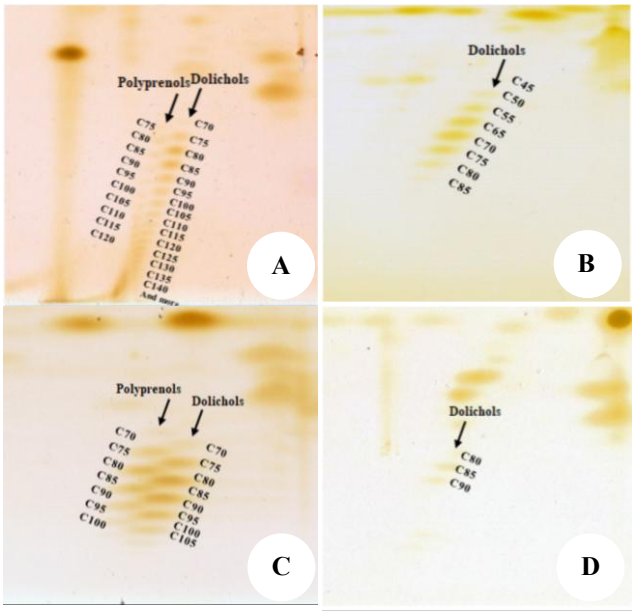

Figure 3. 2D-TLC chromatograms of hexane extracts of polyisoprenoid from: A. *Lumnitzera littorea* fruit, B. *Lumnitzera racemosa* fruit, C. *Melastoma candidum* fruit, D. *Ricinus communis* fruit. The number shows the carbon chain length of polyisoprenoid alcohols

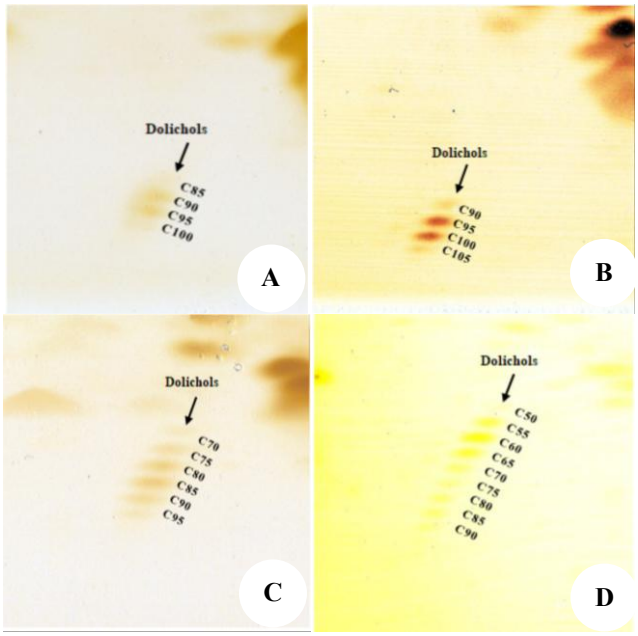

Figure 4. 2D-TLC chromatograms of hexane extracts of polyisoprenoid from: A. *Rhizophora apiculata* fruit, B. *Rhizophora mucronata* fruit, C. *Sciphiphora hydrophyllacea* fruit, D. *Sonneratia alba* fruit. The number shows the carbon chain length of polyisoprenoid alcohols

The dominance of dolichols in Type I species could suggest a greater investment in protein glycosylation machinery during floral development, potentially to maintain reproductive viability under harsh environmental conditions (Basyuni et al. 2017b). Conversely, the prevalence of polyprenols in Type III species could reflect a greater role in modulating membrane properties and interacting with other lipid-based signaling pathways, especially during pollen or seed development.

The intermediate profile observed in Type II species suggests a transitional metabolic state or a dual-functional need for both glycosylation and membrane stability. This balance might be critical for species that inhabit ecotones—zones where salinity, inundation, and light availability fluctuate more dramatically.

Previous studies have demonstrated that polyisoprenoid chain length and type vary across species, organs, and even developmental stages (Tateyama et al. 1999; Basyuni et al. 2021). For example, in the study by Basyuni et al. (2017a, b), longer-chain dolichols were more abundant in roots. In comparison, flowers and leaves presented a broader range of both dolichol and polyprenol types. These observations align with the tissue-specific distributions observed in the present study and support the theory that polyisoprenoid diversity is under adaptive selection in mangrove systems.

The interspecific variation observed in polyisoprenoid content and composition may indicate genetic and ecological differences among mangrove taxa. These biochemical markers could complement traditional morphological classification and provide reliable tools for distinguishing species and assessing populations, especially where hybridization and phenotypic plasticity make field identification challenging (Nakamura 2019; Mali et al. 2023; Upadhyay et al. 2025).

Quantitative analysis of polyisoprenoids

Table 2 presents the quantitative distribution of Total Lipids (TL), polyisoprenoids (Poly), polyprenols (Pol), and dolichols (Dol) in the generative organs (flower and fruit) of 14 mangrove species from North Sumatra. Values were given in mg/g Dry Weight (dw), including standard deviations for total lipids. The percentage contribution of polyprenols and dolichols to both total lipid and total polyisoprenoids was also shown. Two main types of polyisoprenoid alcohols have been described with respect to the OH-terminal (α-) isoprene unit. These include dolichols (α-saturated, Figure 5, Structure 1) and polyprenols (α-unsaturated, Figure 5, Structure 2).

The highest total lipid content was recorded in the flower of *S. hydrophyllacea* (774±30 mg/g dw). Flowers generally exhibited higher lipid content than fruits across species (Table 2). The highest total polyisoprenoid content was found in the flower of *H. tiliaceus* (103.0 mg/g dw), followed by *S. alba* (94.2 mg/g dw) and *L. littorea* (72.8 mg/g dw). In most samples, polyisoprenoids were dominated by either polyprenols or dolichols, but rarely both. The % contribution of dolichols to total polyisoprenoids was highest in *S. alba* flower (85.2%) and *H. tiliaceus* flower (82.7%). In contrast, several species showed 100% contribution from either polyprenols or dolichols.

Table 2 presents the relative abundance or presence of polyprenols and dolichols in the fruits of the same mangrove species. These findings are significant as they suggest that polyisoprenoid biosynthesis is regulated at the organ-specific level, possibly in relation to developmental function and the stress response (Basyuni et al. 2017a). This distribution also implies that fruits tend to have more dolichols, suggesting a potential developmental or protective role during fruit formation or seed maturation (Basyuni et al. 2021). These are linear isoprenoid alcohols that play important biological roles in membrane structure and glycoprotein biosynthesis. Their relative proportions can reflect metabolic, taxonomic, or ecological differences among species. This result therefore provides insight into species-specific and organ-specific variation in lipid metabolism, potentially reflecting different physiological roles of polyisoprenoids in mangrove reproduction tissue and stress adaptation (Basyuni et al. 2017a).

Chemotaxonomic relevance

The cluster analysis effectively grouped mangrove species on the basis of similarities in their polyisoprenoid profiles from generative tissues (Figures 6, 7). Species sharing similar polyisoprenoid patterns—such as those high in dolichols or polyprenols—were placed in proximity within the dendrogram, revealing distinct chemotaxonomic relationships (Yu et al. 2023). This dendrogram illustrates the hierarchical clustering of the fourteen mangrove species on the basis of the composition and abundance of polyprenols and dolichols in their flower tissues. Clustering was performed using UPGMA and Euclidean distance as the similarity metric. Three distinct clusters are observed, representing the predominance of dolichol (Type I), mixed profile (Type II), and polyprenol (Type III) types across species. This clustering highlights the taxonomic potential of polyisoprenoid signatures in differentiating mangrove species at the reproductive organ level.

Dolichols and polyprenols were selected due to their critical roles in membrane integrity, protein glycosylation, and stress response. Their varying chain lengths and relative abundance provide chemotaxonomic insight not offered by other minor isoprenoid derivatives (Menezes et al. 2021). While other compounds, such as sterols and terpenoids, may be present, the consistent detectability, functional importance, and reproducibility of polyisoprenoids make them suitable chemotaxonomic markers.

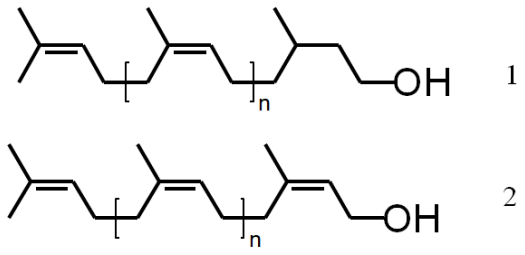

Figure 5. Structure of dolichol (1) and polyprenol (2)

Table 2. Quantitative analysis of polyprenols and dolichols in the generative organs of North Sumatran mangroves in Indonesia

Species	T	TL	Poly	Pol	Dol	% in TL			% in Poly	
		(mg/g dw)	(mg/g dw)	(mg/g)	(mg/g)	Poly	Pol	Dol	Pol	Dol
Acanthus illicifolius L.	Flower	118±17	20.4	9.0	11.3	17.2	7.6	9.6	44.3	55.7
Avicennia officinalis L.	Flower	622±29	28.2	28.2	nd	4.5	4.5	nd	100.0	nd
Barringtonia asiatica (L.) Kurz	Flower	690.1±30	41.9	nd	41.9	6.1	nd	6.1	nd	100.0
Bruguiera sexangula (Lour.) Poir.	Flower	603±60	25.9	25.9	nd	4.3	4.3	nd	100.0	nd
Excoecaria agallocha L.	Flower	603±69	52.8	26.0	26.8	8.8	4.3	4.5	49.2	50.8
Hibiscus tiliaceus L.	Flower	558±20	103.0	17.8	85.2	18.4	3.2	15.3	17.3	82.7
Lumnitzera littorea (Jack) Voigt	Flower	611±40	72.8	21.7	51.1	11.9	3.6	8.4	29.9	70.1
Lumnitzera racemosa Willd.	Flower	657+50	27.4	nd	27.4	4.2	nd	4.2	nd	100.0
Melastoma candidum D. Don	Flower	610±25	34.3	9.0	25.3	5.6	1.5	4.2	26.2	73.8
Ricinus communis L.	Flower	708±30	14.5	nd	14.5	2.0	nd	2.0	nd	100.0
Rhizophora apiculata Blume	Flower	648±7	35.5	35.5	nd	5.5	5.5	nd	100.0	nd
Rhizophora mucronata Lam.	Flower	618±25	17.9	17.9	nd	2.9	2.9	nd	100.0	nd
Scyphiphora hydrophyllacea C.F.Gaertn.	Flower	774±30	28.11	nd	28.11	3.6	nd	3.6	nd	100.0
Sonneratia alba Sm.	Flower	609±40	94.2	13.9	80.3	15.5	2.3	13.2	14.8	85.2
Acanthus illicifolius	Fruit	630±30	29	5.9	23.1	4.6	0.9	3.7	20.3	79.7
Avicennia officinalis L.	Fruit	548±63	32.8	22.4	10.4	6.0	4.1	1.9	68.3	31.7
Barringtonia asiatica (L.) Kurz	Fruit	568±7	21.8	nd	21.8	3.8	nd	3.8	nd	100.0
Bruguiera sexangula (Lour.) Poir.	Fruit	539±46	18.71	nd	18.71	3.5	nd	3.5	nd	100.0
Excoecaria agallocha L.	Fruit	596±55	29.2	nd	29.2	4.9	nd	4.9	nd	100.0
Hibiscus tiliaceus L.	Fruit	535±24	24.9	11.8	13.1	4.7	2.2	2.5	47.4	52.6
Lumnitzera littorea (Jack) Voigt	Fruit	563±28	91.43	18.09	73.34	16.2	3.2	13.0	19.8	80.2
Lumnitzera racemosa Willd.	Fruit	585±60	31.3	nd	31.3	5.3	nd	5.3	nd	100.0
Melastoma candidum D. Don	Fruit	582±39	35.1	13.7	21.4	6.0	2.4	3.7	39.0	61.0
Ricinus communis L.	Fruit	657±40	13	nd	13	2.0	nd	2.0	nd	100.0
Rhizophora apiculata Blume	Fruit	566±49	16.6	nd	16.6	2.9	nd	2.9	nd	100.0
Rhizophora mucronata Lam.	Fruit	543±3	23.4	nd	23.4	4.3	nd	4.3	nd	100.0
Scyphiphora hydrophyllacea C.F.Gaertn.	Fruit	584±6	24.7	nd	24.7	4.2	nd	4.2	nd	100.0
Sonneratia alba Sm.	Fruit	478±21	21.8	nd	21.8	4.6	nd	4.6	nd	100.0

Note: nd: Not detected, total lipids expressed as a fraction of a crude lipid estimated gravimetrically and represented as the mean ± SD (n=3). T: Tissue, TL: Total Lipids, Poly: Polyisoprenoid, Pol: Polyphenol, Dol: Dolichol

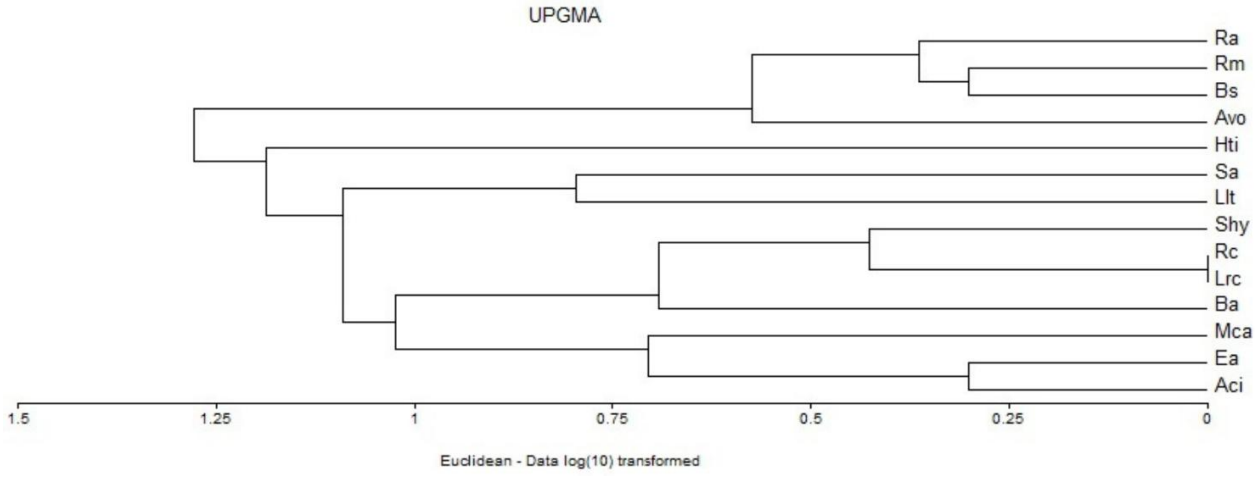

Figure 6. Hierarchical cluster analysis (UPGMA) of polyisoprenoid profiles in mangrove flowers. Ra: *Rhizophora apiculata*, Rm: *Rhizophora mucronata*, Bs: *Brguiera sexangula*, Avo: *Avicennia officinalis*, Hti: *Hibiscus tiliaceus*, Sa: *Sonneratia alba*, Llt: *Lumnitzera* littorea, Shy: *Scyphiphora hydrophyllacea*, Rc: *Ricinus communis*, Lrc: *Lumnitzera racemosa*, Ba: *Barrington asiatica*, Mca: *Melastoma candidum*, Ea: *Excoecaria aggallocha*, Aci: *Acanthus ilicifolius*

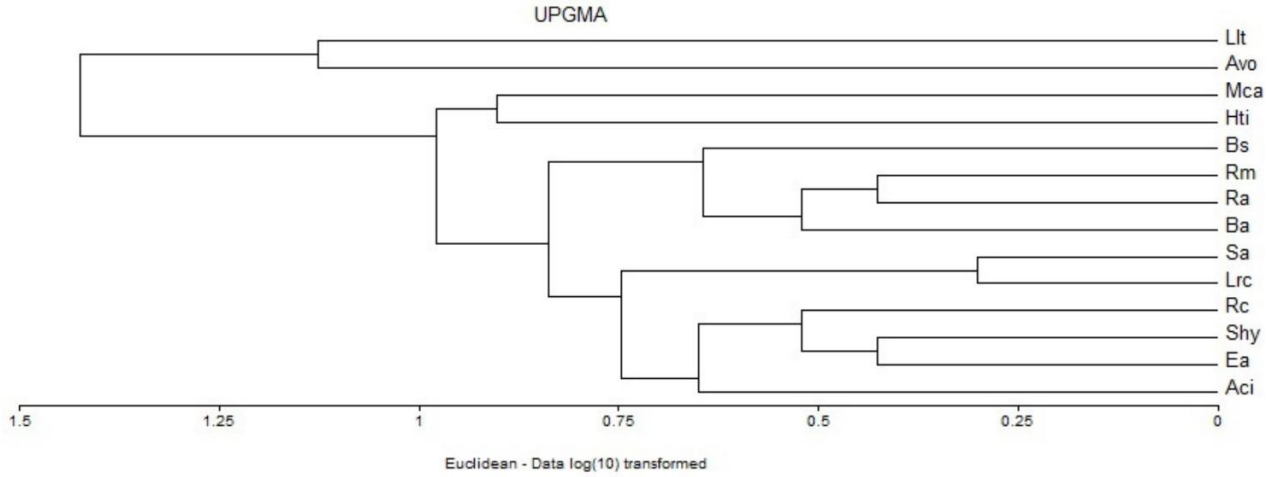

Figure 7. Hierarchical cluster analysis (UPGMA) of polyisoprenoid profiles in mangrove fruits. Llt: *Lumnitzera* littorea, Avo: *Avicennia officinalis*, Mca: *Melastoma candidum*, Hti: *Hibiscus tiliaceus*, Bs: *Brguiera sexangula*, Rm: *Rhizophora mucronata*, Ra: *Rhizophora apiculata*, Ba: *Barrington asiatica*, Sa: *Sonneratia alba*, Lrc: *Lumnitzera racemosa*, Rc: *Ricinus communis*, Shy: *Scyphiphora hydrophyllacea*, Ea: *Excoecaria aggallocha*, Aci: *Acanthus ilicifolius*

These findings indicate that polyisoprenoid composition is not only tissue-specific but also species-dependent, serving as a robust biochemical criterion for mangrove classification. Cluster analysis on the basis of polyisoprenoid composition successfully grouped species with taxonomic proximity, confirming the chemotaxonomic potential of these metabolites. These findings support previous work by Basyuni et al. (2017a), where polyisoprenoid profiles were used to cluster 14 North Sumatran mangrove species into meaningful genus-based groups.

Moreover, the discovery of polyprenyl acetones—novel derivatives identified in *Sonneratia caseolaris* (L.) Engl. and *Xylocarpus granatum* J.Koenig (Basyuni et al. 2017b)—opens new perspectives on the chemical diversity within mangrove taxa. Although not the focus of this study, such findings suggest that the scope of polyisoprenoid-based taxonomy can be extended beyond polyprenol and dolichol profiling.

These patterns are consistent with previous work by Basyuni et al. (2017a), where clustering on the basis of isoprenoid concentration distinguished species more effectively than morphology alone. Chemotaxonomic classification using polyisoprenoids is a promising tool for resolving taxonomic ambiguity among mangrove species, particularly in hybrid zones or areas with overlapping morphological traits (Umoh 2020; Basyuni et al. 2021; Mali et al. 2023).

The observation of distinct chain length distributions (e.g., C70-C120 for dolichols and C60-C140 for polyprenols) among species adds another layer of specificity. In Okinawa mangroves, *L. racemosa* presented a bimodal distribution of long-chain polyprenols, which could be replicated in our study for specific flower tissues (Basyuni et al. 2017b). These features further increase the taxonomic utility of polyisoprenoid profiling. This finding supports the use of polyisoprenoid signatures as chemotaxonomic markers, aligning with prior work in medicinal and woody plants where isoprenoid profiling has revealed meaningful evolutionary patterns.

The clustering patterns derived from polyisoprenoid profiles generally correspond to known phylogenetic relationships, reinforcing the taxonomic relevance of this approach. Moreover, the alignment of chemotypes with ecological zones indicates a connection between isoprenoid metabolism and environmental adaptation. For instance, species from high-salinity or frequently inundated zones exhibited higher dolichol accumulation, supporting their role in osmotic stress mitigation and ecological resilience (Alongi 2015).

By incorporating ecological and botanical insights, this study positions chemotaxonomy as a valuable tool for biodiversity assessment and monitoring, and plant taxonomy. As mangrove habitats face growing pressures from sea-level rise, land conversion, and climate change, biochemical approaches play a crucial role in tracking species dynamics, stress responses, and conservation outcomes, complementing morphological and molecular data (Friess et al. 2020).

Adaptive physiology

Mangroves thrive under conditions of fluctuating salinity, tidal inundation, and oxidative stress. Polyisoprenoid diversity may reflect evolved biochemical strategies to ensure reproductive resilience. For example, dolichol accumulation during flower development may stabilize protein glycosylation under osmotic stress, whereas polyprenol-rich flowers may support flexible physiological responses (Basyuni et al. 2018, 2021).

Furthermore, the tissue-specific distribution of polyisoprenoids observed in this study mirrors the PCA-derived gene expression variability in *Eucommia ulmoides* Oliv., where fruit tissues were enriched in MEP-linked gene expression, and stems showed MVA dominance (Lipko et al. 2023). This regulation suggests that mangroves, such as *E. ulmoides*, exhibit spatial and developmental

coordination of isoprenoid pathway activity. The presence of long-chain polyprenyl alcohols in photosynthetically active tissues such as leaves and flowers also suggests their involvement in photosynthetic membrane maintenance, redox signaling, or stress adaptation, which are essential for survival in saline, sun-exposed intertidal zones (Surmacz and Swiezewska 2011; Basyuni et al. 2017a).

In contrast, polyprenol-rich species might utilize more dynamic, stress-responsive pathways. For example, their role in modulating lipid bilayers, possibly through interactions with sterols and phospholipids, may provide reproductive organs greater flexibility under osmotic or thermal stress (Swiezewska and Danikiewicz 2005; Surmacz and Swiezewska 2011).

Furthermore, a recent study by Zhao et al. (2024) in *E. ulmoides* highlighted the tissue-specific coexpression of isoprenoid biosynthesis genes, supporting the idea that differential pathway activation could underlie the observed polyisoprenoid patterns in mangroves. These findings suggest a molecular basis for the developmental and ecological regulation of isoprenoid biosynthesis in plants, which is likely parallel in mangrove species.

Finally, the presence of novel isoprenoid derivatives, such as polyprenyl acetones found in *X. granatum* and *S. caseolaris* (Basyuni et al. 2017b), suggests that mangrove polyisoprenoid metabolism is not only diverse but also chemically innovative. These compounds may play additional functional roles in defense, signaling, or reproduction, thereby opening avenues for future biochemical and pharmacological studies (Bibi et al. 2019; Upadhyay et al. 2025).

Limitations and future work

This study has several limitations, as it focused solely on generative tissues (flowers and fruits) of mangroves. Other organs, such as leaves, stems, and roots, which are known to exhibit different isoprenoid profiles, have not been analyzed by Basyuni et al. (2017a, b, 2018, 2021), which may limit the comprehensive understanding of whole-plant chemotaxonomic variation. Furthermore, the work did not integrate genetic or transcriptomic data (e.g., isoprenoid pathway gene expression), which could provide a molecular basis for the observed chemical patterns and strengthen the link between phenotype chemotaxonomy and genotype in mangrove taxonomy. Although this study relied primarily on 2D-TLC, future work should incorporate spectroscopic techniques such as UV-Vis and FTIR to confirm compound identity and structure, particularly for distinguishing structurally similar isoprenoid alcohols. Given the ecological and conservation importance of mangrove forests, the findings of this study contribute to a broader framework of integrative biodiversity monitoring. By combining remote sensing, ecological surveys, and biochemical profiling, including polyisoprenoids, future conservation strategies can more precisely identify priority areas for protection and restoration (Friess et al. 2020; Umoh 2020).

Conclusion, this study revealed significant variation in the polyisoprenoid profiles—specifically dolichols and polyprenols—across the reproductive tissues of fourteen mangrove species from North Sumatra, Indonesia. The classification into three chemotypes (dolichol-dominant, polyprenol-dominant, and mixed) reflects both species-specific and tissue-specific metabolic regulation. Flowers tended to exhibit greater diversity in isoprenoid composition than fruits did, suggesting a dynamic biochemical adjustment during reproductive development. The biochemical signatures identified herein contribute to mangrove biodiversity assessment, help species delimitation, and may support conservation programs by providing molecular insight where morphological traits overlap or are environmentally plastic. This study establishes polyisoprenoids as reliable chemotaxonomic markers for mangroves, helping conservation efforts in biodiverse areas. The findings also demonstrate that polyisoprenoid profiles are useful chemotaxonomic markers, with clustering patterns generally aligning with known phylogenetic relationships. The occurrence of distinct chain length distributions and compound dominance indicates ecological adaptation, possibly linked to reproductive success under saline, oxidative, and tidal stress conditions. This expands the scope of polyisoprenoid studies to include mangrove reproductive tissues. These findings support the hypothesis that these compounds play essential physiological and evolutionary roles. Future work should focus on integrating genomic data to unravel the genetic basis of polyisoprenoid diversity.

ACKNOWLEDGEMENTS

This research is financed by the Center of Excellence for Mangrove, Universitas Sumatera Utara, Medan, Indonesia, through grants from the Ministry of Education, Culture, Research, and Technology 2024.

REFERENCES

Alongi DM. 2015. The impact of climate change on mangrove forests. Curr Clim Change Rep 1: 30-39. DOI: 10.1007/s40641-015-0002-x.

Bajda A, Chojnacki T, Hertel J, Swiezewska E, Wójcik J, Kaczkowska A, Marczewski A, Bojarczuk T, Karolewski P, Oleksyn J. 2005. Light conditions alter the accumulation of long-chain polyprenols in leaves of trees and shrubs throughout the vegetation season. Acta Biochim Pol 52 (1): 233-241. DOI: 10.18388/abp.2005_3514.

Bandaranayake WM. 2002. Bioactivities, bioactive compounds and chemical constituents of mangrove plants. Wetlands Ecol Manag 10 (6): 421-452. DOI: 10.1023/A:1021397624349.

Banerjee DK, Zhang Z, Baksi K, Serrano-Negrón JE. 2017. Dolichol phosphate mannose synthase: A glycosyltransferase with unity in molecular diversities. Glycoconj J 34 (4): 467-479. DOI: 10.1007/s10719-017-9777-4.

Basyuni M, Hayati R, Nuryawan A, Siregar ES, Sumaiyah S, Kajita T. 2021. Polyisoprenoid profiling of mangrove litters–based zonations and salinity groups in North Sumatra, Indonesia. Intl J Adv Sci Eng Inf Technol 11(5): 2062-2070. DOI: 10.18517/ijaseit.11.5.13941.

Basyuni M, Sagami H, Baba S, Oku H. 2017b. Distribution, occurrence, and cluster analysis of new polyprenyl acetones and other polyisoprenoids from North Sumatran mangroves. Dendrobiology 78: 18-31. DOI: 10.12657/denbio.078.003.

Basyuni M, Sagami H, Baba S, Putri LAP, Wati R, Oku H. 2017a. Salinity alters the polyisoprenoid alcohol content and composition of both salt-secreting and non-salt-secreting mangrove seedlings. Hayati J Biosci 24 (4): 206-214. DOI: 10.1016/j.hjb.2017.11.006.

Basyuni M, Wati, R, Prabuanisa AN, Kusuma IKTW, Hamiudin, Guntur, Sagami H. 2018. Changes to the polyisoprenoid composition in aging

leaves of mangrove plants. AIP Conf Proc 1: 030007. DOI: 10.1063/1.5062731

Bibi SN, Fawzi MM, Gokhan Z, Rajesh J, Nadeem N, Kannan R RR, Albuquerque RDDG, Pandian SK. 2019. Ethnopharmacology, phytochemistry, and global distribution of mangroves—A comprehensive review. Mar Drugs 17 (4): 231. DOI: 10.3390/md17040231.

Friess DA, Yando ES, Alemu JB, Wong LW, Soto SD, Bhatia N. 2020. Ecosystem services and disservices of mangrove forests and salt marshes. In: Hawkins SJ, Allcock AL, Bates AE, Firth LB, Smith IP, Swearer SE, Evans AJ, Todd PA, Russell BD, McQuaid CD (Eds.). Oceanography and Marine Biology: An Annual Review. Taylor & Francis, United Kingdom. DOI: 10.1201/9780429351495-3.

Gelder KV, Virta LKA, Easlick J, Prudhomme N, McAlister JA, Geddes-McAlister J, Akhtar TA. 2021. A central role for polyprenol reductase in plant dolichol biosynthesis. Plant Sci 303: 110773.

Kasihiw P, Bawole R, Marwa J, Murdjoko A, Wihyawari A, Heipon Y, Cabuy RL, Benu NMH, Hematang F, Leftungun NY. 2024. Mangrove distribution to support biodiversity management in Teluk Bintuni District, West Papua, Indonesia. Biodiversitas 25: 644-653. DOI: 10.13057/biodiv/d250223.

Lipko A, Pączkowski C, Perez-Fons L, Fraser PD, Kania M, Hoffman-Sommer M, Danikiewicz W, Rohmer M, Poznanski J, Swiezewska E. 2023. Divergent contribution of the MVA and MEP pathways to the formation of polyprenols and dolichols in *Arabidopsis*. Biochem J 480 (8): 495-520. DOI: 10.1042/BCJ20220578.

Mali S, Yadav R, Gauttam V, Sawale J. 2023. An updated review on taxonomy and chemotaxonomy. Toxicol Intl 30 (1): 121-129. DOI: 10.18311/ti/2023/v30i1/32123.

Menezes RPB, Sessions Z, Muratov E, Scotti L, Scotti MT. 2021. Secondary metabolites extracted from Annonaceae and chemotaxonomy study of terpenoids. J Braz Chem Soc 32: 2061-2070. DOI: 10.21577/0103-5053.20210097.

Nakamura H. 2019. Plant-derived triterpenoid biomarkers and their applications in paleoenvironmental reconstructions: Chemotaxonomy, geological alteration, and vegetation reconstruction. Res Org Geochem 35 (2): 11-35. DOI: 10.20612/rog.35.2_11.

Rizkiany MC, Amelia R, Bimantara Y, Sagami H, Basyuni M. 2021. Polyisoprenoid compounds from tropical fruit trees in Universitas Sumatera Utara campus. Sci Technol Indones 6 (4): 267-272. DOI: 10.26554/sti.2021.6.4.267-272.

Salvador-Castell M, Brooks NJ, Peters J, Oger P. 2020. Induction of nonlamellar phases in archaeal lipids at high temperature and high hydrostatic pressure by apolar polyisoprenoids. Biochim Biophys Acta Biomembr 1862 (2): 183130. DOI: 10.1016/j.bbamem.2019.183130.

Surmacz L, Swiezewska E. 2011. Polyisoprenoids – secondary metabolites or physiologically important superlipids? Biochem Biophys Res Commun 407 (4): 627-632. DOI: 10.1016/j.bbrc.2011.03.059.

Swiezewska E, Danikiewicz W. 2005. Polyisoprenoids: Structure, biosynthesis and function. Prog Lipid Res 44 (4): 235-258. DOI: 10.1016/j.plipres.2005.05.002.

Tateyama S, Wititsuwannakul R, Wititsuwannakul D, Sagami H, Ogura K. 1999. Dolichols of rubber plant, ginkgo, and pine. Phytochemistry 51 (1): 11-15. DOI: 10.1016/S0031-9422(98)00581-0.

Tholl D. 2015. Biosynthesis and biological functions of terpenoids in plants. Adv Biochem Eng Biotechnol 148: 63-106. DOI: 10.1007/10_2014_295.

Umoh OT. 2020. Chemotaxonomy: The role of phytochemicals in chemotaxonomic delineation of taxa. Asian Plant Res J 5 (1): 43-52. DOI: 10.9734/aprj/2020/v5i130100.

Upadhyay R, Saini R, Shukla PK, Tiwari KN. 2025. Role of secondary metabolites in plant defense mechanisms: A molecular and biotechnological insight. Phytochem Rev 24 (1): 953-983. DOI: 10.1007/s11101-024-09976-2.

Yu J, Su X, Shi Z, Li Y, Wang C, Zhu S, Wang Y. 2023. Comparative metabolomic reveals chemotaxonomic markers of resin fossils for identification of botanical origins. Int J Coal Geol 270: 104230. DOI: 10.1016/j.coal.2023.104230

Zhao D, Long S, Song L, Zhu Y, Wang R, Zhao D. 2024. Comparative study of rubber biosynthesis pathways in *Eucommia ulmoides* and *Hevea brasiliensis*. Biosci Methods 15 (6): 289-301. DOI: 10.5376/bm.2024.15.0029.

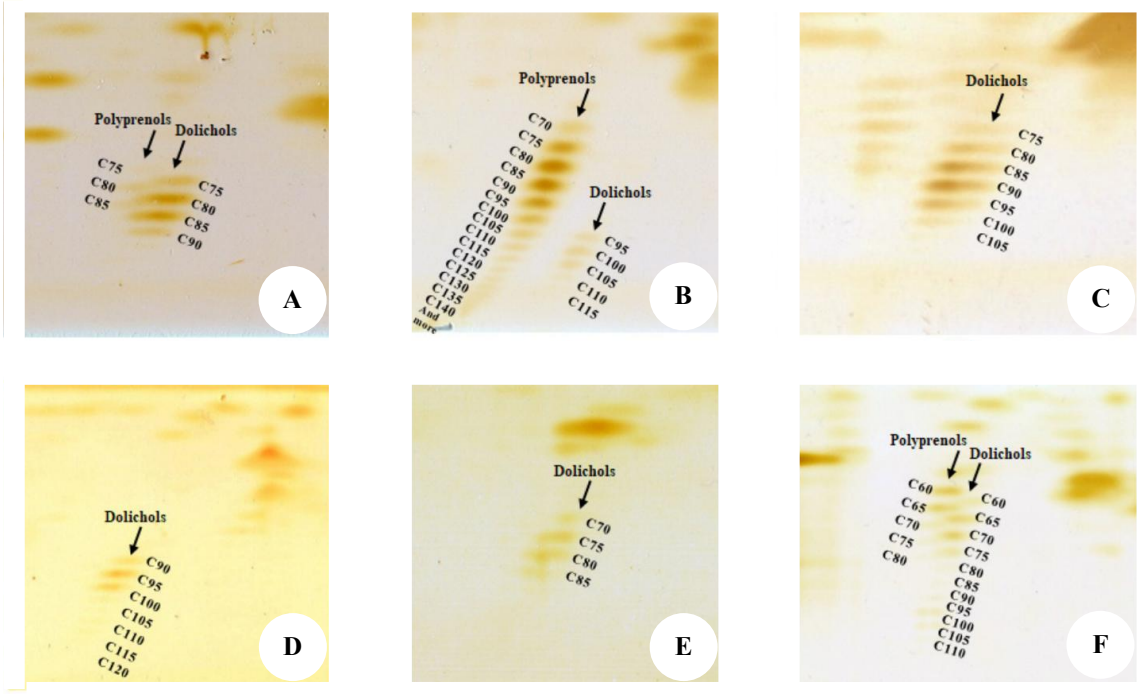

Figure S1. 2D-TLC chromatograms profile of hexane extracts of polyisoprenoid from: A. *Acanthus illicifolius* fruit, B. *Avicennia officinalis* fruit, C. *Barringtonia asiatica* fruit, D. *Bruguiera sexangula* fruit, E. *Excoecaria agallocha* fruit, F. *Hibiscus tilliaceus* fruit. The number shows the carbon chain length of polyisoprenoid alcohols

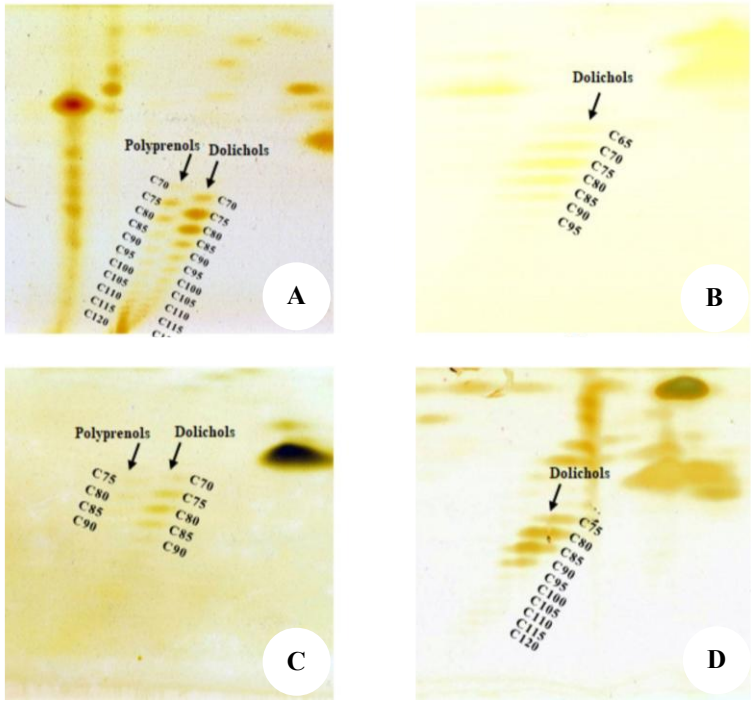

Figure S2. 2D-TLC chromatograms profile of hexane extracts of polyisoprenoid from: A. *Lumnitzera littorea* flowers, B. *Lumnitzera racemosa* flowers, C. *Melastoma candidum* flowers, D. *Ricinus communis* flowers. The number shows the carbon chain length of polyisoprenoid alcohols

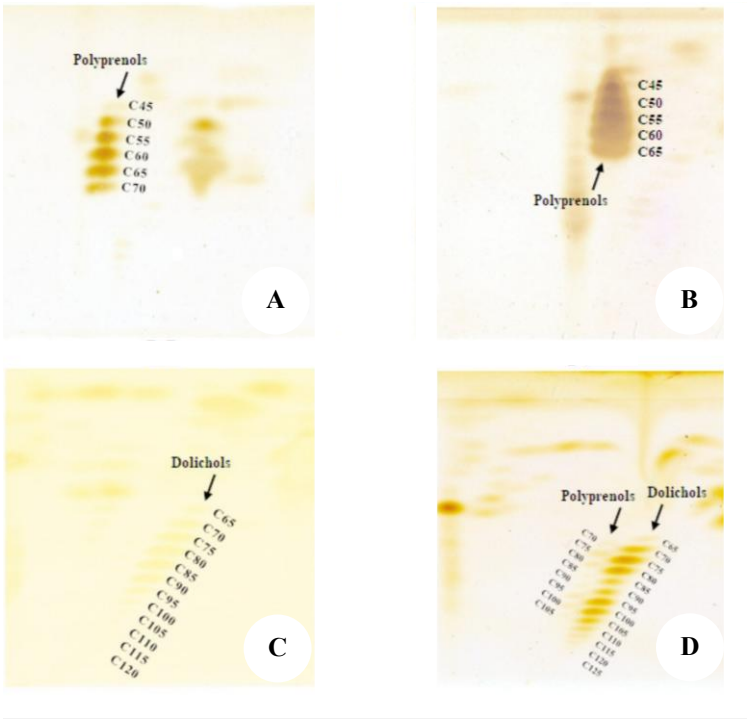

Figure S3. 2D-TLC chromatograms of hexane extracts of polyisoprenoid from: A. *Rhizophora apiculat*a flower, B. *Rhizophora mucronata* flower, C. *Sciphiphora hydrophyllacea* flower, D. *Sonneratia alba* flower. The number shows the carbon chain length of polyisoprenoid alcohols

ASIAN J NAT PROD BIOCHEM
Volume 23, Number 2, December 2025
Pages: 122-130

P-ISSN: 2775-4189
E-ISSN: 2775-4197
DOI: 10.13057/biofar/f230204

Inhibition of α-amylase and α-glucosidase by raw and boiled garlic extracts for postprandial hyperglycemia management

MD JAHANGIR ALAM♥, NISHAT SALSABIL SUMAIYA RAHMAN
Department of Genetic Engineering and Biotechnology, Shahjalal University of Science and Technology. Sylhet-314, Bangladesh.
Tel.: +88-01911-93-90-40, ♥email: jalambioru@yahoo.com; jahangir-btc@sust.edu

Manuscript received: 27 August 2025. Revision accepted: 25 October 2025.

Abstract. *Alam MJ, Rahman NSS. 2025. Inhibition of α-amylase and α-glucosidase by raw and boiled garlic extracts for postprandial hyperglycemia management. Asian J Nat Prod Biochem 23: 122-130.* Diabetes Mellitus (DM) is a severe metabolic disorder that causes hyperglycemia due to impaired insulin function. Inhibition of carbohydrate-hydrolyzing enzymes, such as α-amylase and α-glucosidase, can reduce postprandial blood glucose levels. This study investigated the ability of garlic extracts (*Allium sativum*) to inhibit these important enzymes in Type 2 Diabetes Mellitus (T2DM). Raw and boiled Deshi and Indian garlic extracts were prepared and assessed for their ability to inhibit α-amylase and α-glucosidase activities using standard in vitro enzyme inhibition assays. The types of enzyme inhibition were analyzed through Lineweaver-Burk plots. Deshi raw garlic extract at 20 mg/mL inhibited the α-amylase enzyme by 52.49%, with an IC_{50} value of 17.62 mg/mL, while Deshi boiled garlic extract exhibited the lowest inhibition at the lowest concentration. Similarly, Deshi raw garlic extract showed the highest inhibition of α-glucosidase at the maximum concentration tested, whereas Indian boiled garlic extract demonstrated the lowest inhibition at the minimum tested concentration. Notably, raw and boiled garlic extracts inhibited α-amylase and α-glucosidase activities by 70% at concentrations comparable to acarbose, a commercial antidiabetic medication and the mode of inhibition for both enzymes by the both types of garlic extracts were evaluated as competitive inhibition. The findings demonstrate that both raw and boiled garlic extracts exhibit inhibitory action against α-glucosidase and α-amylase, indicating their potential for managing postprandial hyperglycemia. These results support the development of garlic-based nutraceuticals or dietary interventions for the management of T2DM.

Keywords: Acarbose, *Allium sativum*, antidiabetic activity, enzyme inhibition activity, nutraceuticals

INTRODUCTION

Traditional medicine has long turned to nature, with medicinal plants being central to the discovery and development of modern drugs. These plants are valued for their broad pharmacological benefits and low side effects. Historically, plant extracts have been essential in treating various diseases for their antidiabetic, antioxidant, antimalarial, antibacterial, antiviral, antifungal, antithrombogenic, and enzyme-inhibitory properties (e.g., amylase, lipase, invertase) (D'Britto et al. 2012).

Diabetes Mellitus (DM) is a metabolic disorder resulting from inadequate insulin production and/or secretion by the pancreas (Balamurugan et al. 2014; Zafar et al. 2022). Additionally, insulin resistance in body cells can lead to increased blood glucose levels (Khatun et al. 2015). According to the World Health Organization (WHO), over 347 million people worldwide have diabetes, a number projected to rise to 549 million by 2030 (Rowley et al. 2017; Thakre et al. 2017). Diabetes symptoms include weight loss, polyuria, polyphagia, polydipsia, fatigue, slow wound healing, and pruritus (Thakre et al. 2017). Chronic diabetes can cause severe complications like diabetic retinopathy, cardiovascular disease, stroke, poor circulation (resulting in amputations), and renal failure (Sathishkumar et al. 2015).

Carbohydrates are the primary source of energy for the body. Digestive enzymes including α-glucosidase, α-amylase, and invertase break down starch and other dietary carbohydrates into monosaccharides, primarily glucose (Behl and Kotwani 2017; Paul et al. 2021). This enzymatic process can cause rapid blood glucose spikes, complicating T2DM management. Inhibitors of α-glucosidase and α-amylase can help lower blood glucose after carbohydrate-rich meals, supporting glycemic control.

Current antidiabetic treatments include thiazolidinediones, insulin analogs, α-glucosidase inhibitors, sulfonylureas, and meglitinides (Gellad et al. 2013). Acarbose reduces both α-glucosidase and α-amylase activity, whereas voglibose and miglitol specifically reduce α-glucosidase activity. Despite their effectiveness in managing diabetes, these medications are associated with significant side effects (Thakre et al. 2017). About 80% of people with diabetes live in low- to middle-income countries (IDF 2015), where medication costs hinder effective management. As a result, researchers are exploring potent enzyme inhibitors from natural sources like bacteria, plants, and marine algae (Fatmawati et al. 2011; Konishi et al. 2012; Orhan et al. 2013; Panwar et al. 2015). While few plant extracts have shown activity against all the major digestive enzymes related to DM, the majority have shown inhibitory actions against either α-amylase or α-glucosidase (Debnath et al. 2020; Sani et al. 2020, 2024; Mahmud et al. 2023; Sarker et al. 2024). Traditionally known medicinal plants have been explored for their hypoglycemic potential, and the bioactive

compounds isolated from these plants appear highly promising (Rahmani 2015). Since α-amylase hydrolyzes complex carbohydrates into glucose—contributing to postprandial hyperglycemia—inhibiting this enzyme remains a key strategy in the development of improved antidiabetic drugs (Subramanian et al. 2008).

Garlic (*Allium sativum* L.), a widely cultivated member of the family *Alliaceae*, is commonly used as a culinary spice (Vazquez-Armenta et al. 2016). Traditionally, garlic has been used to treat ailments like diabetes, colds, and heart disease. Garlic oil extracts possess antidiabetic and antioxidant properties (Mnayer et al. 2014; Phan et al. 2019). Additionally, ethanolic extracts of *A. sativum* have demonstrated α-amylase inhibitory activity (Nickavar and Yousefian 2009). Raw garlic improves insulin sensitivity, and lowers blood sugar more effectively than cooked garlic. Raw or minimally process garlic significantly lowers fasting blood glucose and HbA1c levels in people with metabolic syndrome or type 2 diabetes (Zhao et al. 2024). Organosulfur content varies among garlic types, affecting their enzyme inhibition capacity (Lu et al. 2023; Wu et al. 2023).

Boiling garlic can alter its ability to inhibit carbohydrate-hydrolyzing enzymes (α-amylase and α-glucosidase), potentially impacting glycemic control. This study aimed to investigate how raw and boiled garlic, especially Deshi and Indian varieties, influence health benefits, and therapeutic potential, given their local prevalence and distinct bioactivity. However, in most comparison studies investigating enzyme inhibition have been conducted using *in vivo* models, particularly in diabetic rats. In contrast, the present study utilized an *in vitro* enzyme inhibition assay to more accurately assess the inhibitory potential of raw and boiled garlic (*A. sativum*) extracts on key digestive enzymes- α-glucosidase and α-amylase- associated with diabetes. This approach may offer a novel therapeutic strategy for diabetes management and also provides insight into the mode of enzyme inhibition.

MATERIALS AND METHODS

Collection and preparation of samples

This study utilized two types of garlic (*A. sativum*): Deshi and Indian varieties, both procured from local markets in Sylhet, Bangladesh. All bulbs were purchased in triplicate from different markets and only visually uniform, healthy, and undamaged bulbs were selected. Samples were processed under identical lab conditions immediately after purchase. Upon collection, the outer layers of the garlic bulbs were manually removed. The cloves were then separated and thoroughly cleaned with tap water, followed by two to three washes with distilled water to eliminate dirt and other impurities. The cleaned cloves were wiped with tissue paper to remove any residual water and allowed to air dry at room temperature. Consequently, the dried cloves were divided into two groups. One group was immersed in boiling water (100±1°C) for 10 minutes, while the other was set aside as raw. The boiled samples were then air-dried. Both raw and boiled samples from the Deshi and Indian varieties (*A. sativum*) were stored separately in four labeled containers for later use.

Chemicals/reagents

α-Glucosidase and α-amylase were purchased from The Merck Group, Darmstadt, Germany. Analytical-grade reagents, solvents, and chemicals were used in this investigation. Acarbose, a commercially available antidiabetic medication marketed under the brand name Sugatrol® (The Pacific Pharmaceuticals Ltd.), utilized as the experimental positive control.

Preparation of garlic extracts

Extracts from all samples (raw and boiled (Simmered in water at 100±1°C for 10 minutes), Deshi and Indian garlic) were prepared using a previously published method with minor modifications (Yibchok-Anun et al. 2006). Briefly, the samples were ground using a mortar and pestle with ice-cold acid-ethanol. After filtration, the homogenates were centrifuged at 8,000 rpm for 10 minutes. The pH of the resulting supernatants was adjusted to 3.0, followed by incubation at 4°C for 24 hours. After incubation, the mixtures were centrifuged again at 6,000 rpm for 10 minutes. The resulting pellet was washed with 80% acetone and allowed to air dry. Ice-cold acid-ethanol was chosen to facilitate the extraction of sulfur-containing compounds, while acetone was used for its ability to purify the extract by removing non-polar impurities. Finally, the air-dried pellet was dissolved in a 10 mM Tris–HCl buffer (pH 8.0). All extracts were stored at -20°C until further use.

α-Amylase inhibition assay

The α-amylase inhibition activity of the extracts was carried out by a previously reported method with slight modifications, employing 3,5-dinitrosalicylic acid (DNSA) (Poovitha and Parani 2016). Briefly, the extracts or acarbose at different doses (200-2000 µg/mL) were mixed with α-amylase (1 IU/mL) in test tubes. 20 mM sodium phosphate buffer (pH 6.9) was added in each reaction mixture, and the mixture was then pre-incubated for ten minutes at 25°C. Starch solution (as the substrate) was then added to initiate the reaction, followed by another 10-minute incubation at 25°C in a thermostatic water bath.

To stop the reaction, 3,5-dinitrosalicylic acid was added, and the mixture was placed in a thermostatic water bath at 100°C. After boiling, the solution was cooled to room temperature and diluted with distilled water at a 1:5 ratio. The inhibitory activity of α-amylase was determined by measuring the Optical Density (OD) at 540 nm using a spectrophotometer (Shimadzu, Japan). Following formula was used to figure out the percentage of inhibition of α-amylase.

Inhibition of α-amylase (%) = [(Enzyme Activity of Control - Enzyme Activity of Test) / Enzyme Activity of Control] x 100.

α-glucosidase inhibition assay

The extracts' α-glucosidase inhibition assay was carried out by a previously reported method with minor modifications, employing *p*-nitrophenyl-α-D-glucopyranoside

(pNPG) as the substrate (Poovitha and Parani 2016). Briefly, α-glucosidase (1 IU/mL) was mixed with the extracts or acarbose at various concentrations (200-2000 µg/mL) in test tubes and pre-incubated for 20 minutes at 37°C in a thermostatic water bath. Subsequently, 10 mM *p*-nitrophenyl-α-D-glucopyranoside was added to each tube, and the mixture was incubated in a thermostatic water bath again at 37°C for 30 minutes. The reaction was terminated by adding sodium carbonate, and the absorbance was measured at 405 nm using a spectrophotometer (Shimadzu, Japan). The formula below use used to calculate the percentage of α-glucosidase inhibition.

Inhibition of α-glucosidase (%) = [(Enzyme Activity of Control – Enzyme Activity of Test) / Enzyme Activity of Control] × 100.

Analysis of the mode of enzyme inhibition

The mechanism of α-amylase and α-glucosidase inhibition was analyzed following a previously reported method (Poovitha and Parani 2016). The enzyme solution (1 IU/mL) was incubated for 10 minutes at 25°C in a thermostatic water bath with either the acarbose (10 mg/mL), extracts (10 mg/mL), or phosphate buffer (pH 6.9) in order to perform the α-amylase assay. Reaction was initiated using the same procedure as described in 'α-amylase inhibition assay' section. The assay for α-glucosidase was conducted in a similar manner. Acarbose (10 mg/mL), extracts (10 mg/mL), or phosphate buffer (pH 6.9) were incubated in a thermostatic water bath with the enzyme solution (1 IU/mL) for 10 minutes at 37°C. Reaction was performed as described in the 'α-glucosidase inhibition assay' section. To determine the mode of inhibition, a double reciprocal plot (1/V vs. 1/[S]) was constructed using the reaction velocity (V) and substrate concentration ([S], ranging from 0.5-25 mh/mL). The type of enzyme inhibition was identified by analyzing the Lineweaver–Burk plot based on Michaelis–Menten kinetics.

Statistical analysis

All experiments were performed in triplicate (n=3) for each concentration to ensure both physiological consistency and statistical accuracy. Results are expressed as the mean ± Standard Deviation (SD), offering a reliable indication of central tendency and variation, thereby reinforcing the validity and reproducibility of the findings. Linear regression analysis, performed using Excel-generated plots, was used to calculate the IC_{50} values (the concentration required to inhibit 50% of enzyme activity) for both α-amylase and α-glucosidase.

RESULTS AND DISCUSSION

α-amylase inhibition activity of Deshi and Indian raw and boiled garlic extracts

This study evaluated the potential antidiabetic effects of Deshi and Indian garlic extracts by measuring their α-amylase inhibitory activity and comparing the results to those of the conventional antidiabetic drug, acarbose. To further understand the strength of α-amylase inhibition, IC_{50} values were also determined.

α-amylase inhibition by Deshi raw and boiled garlic extracts

The α-amylase inhibitory activity of raw and boiled Deshi garlic extracts was evaluated at various concentrations. Among the raw garlic extracts, the highest inhibition was observed at 20 mg/mL, with an inhibition rate of 52.49±3.17% and an IC_{50} value of 17.62 mg/mL (Figure 1, Table 1). The lowest inhibition was recorded at 2 mg/mL, showing 11.23±0.45% activity. For the boiled garlic extracts, the maximum inhibition was also observed at 20 mg/mL, yielding 29.36±0.987% inhibition in an IC_{50} value of 34.05 mg/mL. The lowest inhibition in this group was 5.54±1.34% at 2 mg/mL. Acarbose, used as a positive control, demonstrated the highest α-amylase inhibition (70.77±2.58%) at 20 mg/mL in an IC_{50} value of 9.03 mg/mL. The lowest inhibition by acarbose was 19.22±0.764% at 2 mg/mL (Figure 1, Table 1).

α-amylase inhibition by Indian raw and boiled garlic extracts

The α-amylase inhibitory potential of raw and boiled Indian garlic extracts was assessed across a range of concentrations. Among the raw garlic extracts, the highest inhibition was observed at 20 mg/mL, with an inhibition rate of 46.59±1.12% and an IC_{50} value of 22.00 mg/mL (Figure 2; Table 1). The lowest inhibition for the same extract was recorded at 2 mg/mL, showing 10.53±1.06% activity. In the case of boiled Indian garlic, the maximum inhibition was also found at 20 mg/mL, with a value of 31.55±0.89% and an IC_{50} of 32.96 mg/mL. The lowest inhibitory activity for this extract was 6.66±1.67% at 2 mg/mL (Figure 2; Table 1).

α-glucosidase inhibition activity of Deshi and Indian raw and boiled garlic extracts

The α-glucosidase inhibition activity of Deshi and Indian garlic extracts was evaluated and compared with that of acarbose. IC_{50} values for each extract were also determined to better understand their inhibitory effects.

α-glucosidase inhibition by raw and boiled Deshi garlic extracts

The percentage of α-glucosidase inhibition was measured using both raw and boiled Deshi garlic extracts. Among the raw garlic extracts, the highest inhibition (46.73±0.90%) was observed at 20 mg/mL, with an IC_{50} value of 21.77 mg/mL (Figure 3, Table 2). The lowest inhibition (8.81±3.54%) was seen at 2 mg/mL. For the boiled garlic extracts, the highest inhibition at 20 mg/mL was 24.45 mg/mL, corresponding to the IC_{50} value. As a positive control, acarbose was tested at the same concentrations. At 20 mg/mL, acarbose exhibited the highest α-glucosidase inhibition of 68.86±1.82%, with an IC_{50} value of 10.22 mg/mL.

The α-glucosidase inhibitory activity of raw and boiled Indian garlic extracts was evaluated at various concentrations. The raw garlic extract at 20 mg/mL exhibited the highest inhibition of 42.15%, with an IC_{50} value of 25.70 mg/mL (Figure 4, Table 2). The lowest

inhibition for the raw extract was 9.77% at 2 mg/mL. Among the boiled garlic extracts, the maximum inhibition of 37.51% was also observed at 20 mg/mL, with IC_{50} value of 26.21 mg/mL. The lowest inhibitory activity in this group was 4.67% at 2 mg/mL (Figure 4, Table 2).

Enzyme kinetics and mode of inhibition

To determine the type of enzyme inhibition exerted by the garlic extracts, enzyme kinetics studies were conducted using Lineweaver–Burk plots. The effects of both raw and boiled Deshi and Indian garlic extracts on α-amylase and α-glucosidase activities were analyzed and compared with the control.

Mode of α-amylase inhibition by raw and boiled Deshi garlic extracts

Using the Lineweaver–Burk plot, the K_m values were determined for the raw and boiled Deshi garlic extracts as well as for the control (phosphate buffer). While V_{max} remained constant, the K_m values for the buffer and raw garlic extract were 19.43 and 34.97, respectively (Figure 5). Similarly, V_{max} remained unchanged for both samples, while the K_m values for the buffer and boiled garlic extract were 19.43 and 27.04, respectively. This increase in K_m with no change in V_{max} indicates that both raw and boiled Deshi garlic extracts inhibit α-amylase through a competitive inhibition mechanism.

Mode of inhibition of α-amylase assessed by raw and boiled Indian garlic extract

The K_m values for raw and boiled Indian garlic extracts, along with the control (phosphate buffer), were determined using Lineweaver–Burk plots. While the V_{max} values remained constant across all samples, the K_m values for the buffer and raw Indian garlic extract were 31.86 and 19.43, respectively (Figure 6). In a separate experiment, V_{max} again remained unchanged, while the K_m values for the buffer and boiled Indian garlic extract were 19.43 and 29.29, respectively. The observed increase in K_m with a constant V_{max} indicates that both raw and boiled Indian garlic extracts act as competitive inhibitors of α-amylase.

Mode of inhibition of α-glucosidase assessed by Deshi raw and boiled garlic extract

The K_m values for both raw and boiled Deshi garlic extracts, along with the control (phosphate buffer), were determined using Lineweaver–Burk plots. For the buffer and raw Deshi garlic extract, the K_m values were 16.92 and 30.06, respectively, while V_{max} remained constant for both (Figure 7). Similarly, for the buffer and boiled Indian garlic extract, the K_m values were 25.75 and 16.92, respectively, with V_{max} again remaining unchanged. The increase in K_m coupled with an unchanged V_{max} in the presence of both raw and boiled Indian garlic extracts indicates that the inhibition follows a competitive mechanism.

Table 1. IC_{50} values of α-amylase inhibition activity under the treatment of different varieties of garlic extracts. Among the extracts, Deshi raw garlic extract demonstrated the highest efficacy, reaching about half the activity of the positive control, acarbose

Type of extracts	IC_{50} (mg/mL)
Deshi Raw Garlic	17.62
Deshi Boiled garlic	34.05
Indian Raw garlic	22.0004
Indian Boiled Garlic	32.96
Acarbose	9.03

Table 2. IC_{50} values of α-glucosidase inhibition activity under the treatment of different varieties of garlic extracts. All the extracts demonstrated inhibition levels ranging from approximately half to two-thirds of that shown by the standard inhibitor, acarbose

Type of extracts	IC_{50} (mg/mL)
Deshi Raw Garlic	21.76
Deshi Boiled garlic	24.45
Indian Raw garlic	25.70
Indian Boiled Garlic	26.21
Acarbose	10.22

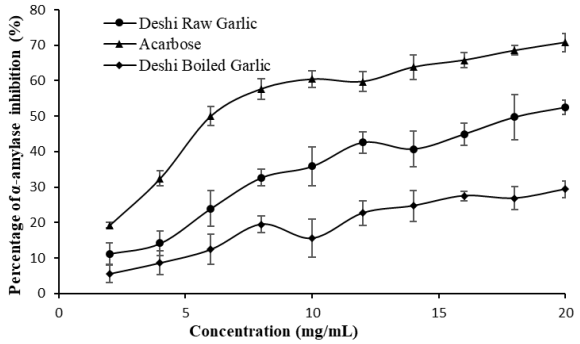

Figure 1. α-Amylase inhibition by Deshi raw and boiled garlic extracts. The extract concentrations ranged from 2-20 mg/mL. The inhibition of α-amylase by Deshi raw garlic extract was greater than that of the Deshi boiled garlic extract and approximately two-thirds that of the positive control, acarbose

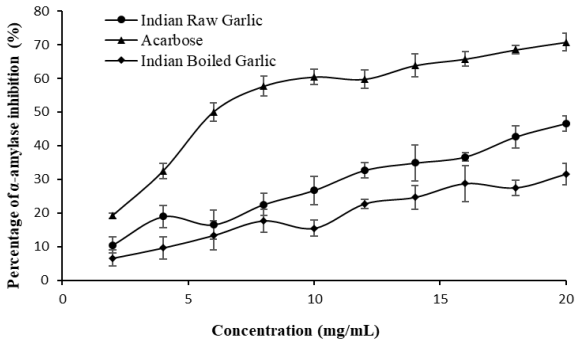

Figure 2. α-Amylase inhibition by Indian raw and boiled garlic extracts. The experimental concentrations of the extracts ranged from 2 to 20 mg/mL. The inhibition occurred in a concentration-dependent manner. At a concentration of 20 mg/mL, Indian raw garlic extract inhibited α-amylase more effectively than the Indian boiled garlic extract, with inhibition reaching approximately two-thirds of that observed with the positive control, acarbose

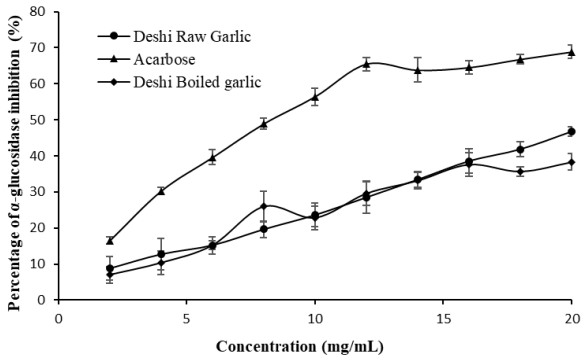

Figure 3. Concentration-dependent α-glucosidase inhibition by Deshi raw and boiled garlic extracts. Both Deshi raw and boiled garlic extracts exhibited comparable levels of α-glucosidase inhibition, whereas the positive control, acarbose, demonstrated nearly twice the inhibitory activity.α-glucosidase inhibition by raw and boiled Indian garlic extracts

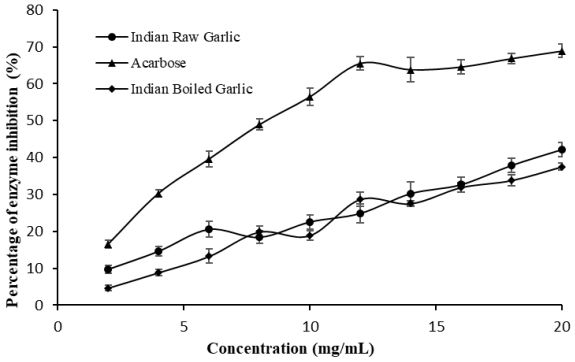

Figure 4. Concentration-dependent α-glucosidase inhibition by Indian raw and boiled garlic extracts. Indian raw and boiled garlic extracts exhibited comparable α-glucosidase inhibitory effects, achieving approximately two-thirds of the inhibition observed with the standard reference inhibitor, acarbose

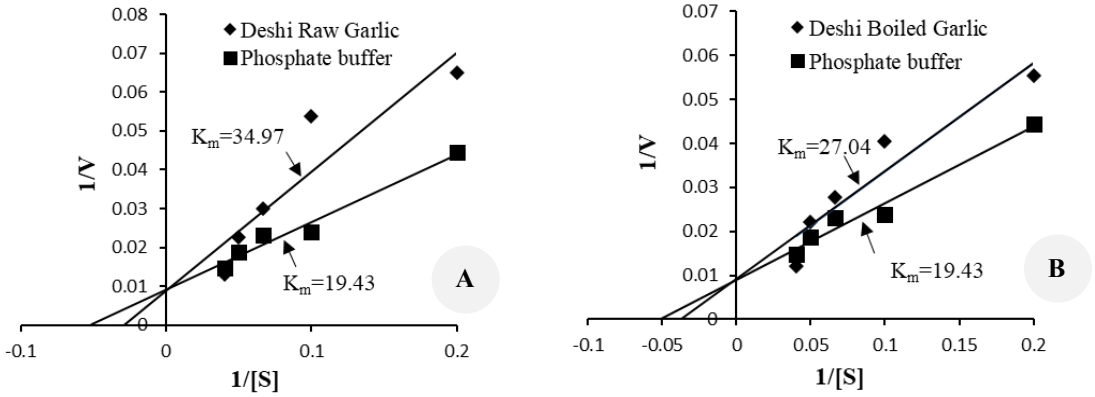

Figure 5. Lineweaver–Burk plot for the analysis of mode of α-amylase inhibition by A. Deshi raw and B. Deshi boiled garlic extracts. At a constant substrate concentration ([S]), the observed increase in K_m values of α-amylase in the presence of both Deshi raw and boiled garlic extracts suggests a pattern consistent with competitive inhibition. This indicates that compounds within the extracts may be competing with the substrate for binding to the enzyme's active site

Mode of inhibition of α-glucosidase assessed by Indian raw and boiled garlic extract

Using Lineweaver–Burk plots, the K_m values for both Indian raw and boiled garlic extracts, as well as the control (phosphate buffer), were determined. The K_m values for the Deshi raw garlic extract and buffer solution were 28.75 and 16.92, respectively, while V_{max} remained constant (Figure 8). Similarly, the K_m values for the Indian boiled garlic extract and buffer solution were 23.12 and 16.92, respectively, with V_{max} also unchanged for both samples. Since V_{max} remained constant and K_m increased in the presence of both Indian raw and boiled garlic extracts, the inhibition was classified as competitive in both cases.

Discussion

DM is a major global health issue, with its prevalence rising steadily in both developed and developing nations. In Bangladesh alone, around 10 million people are currently living with either type I or type II diabetes. DM is a long-term metabolic disorder that affects carbohydrate metabolism. One effective way to manage this condition, particularly type II diabetes, is through the use of glycosidic enzyme inhibitors. These compounds inhibit key digestive enzymes such as α-amylase, α-glucosidase, and invertase, which play important roles in carbohydrate breakdown (Kim et al. 2004). As oral hypoglycemic agents, these inhibitors help regulate blood sugar levels by slowing the digestion and absorption of carbohydrates (Iwakura et al. 2003). This results in delayed glucose uptake and a lower rise in blood glucose after meals (Iwakura et al. 2003). α-Amylase initiates the breakdown of starch into smaller sugar units by hydrolyzing complex polysaccharides into oligosaccharides and disaccharides. These are subsequently broken down by α-glucosidase into monosaccharides. The resulting simple sugars are then absorbed through the small intestine into the hepatic portal vein, contributing to increased postprandial blood glucose levels (Teng and Chen 2017).

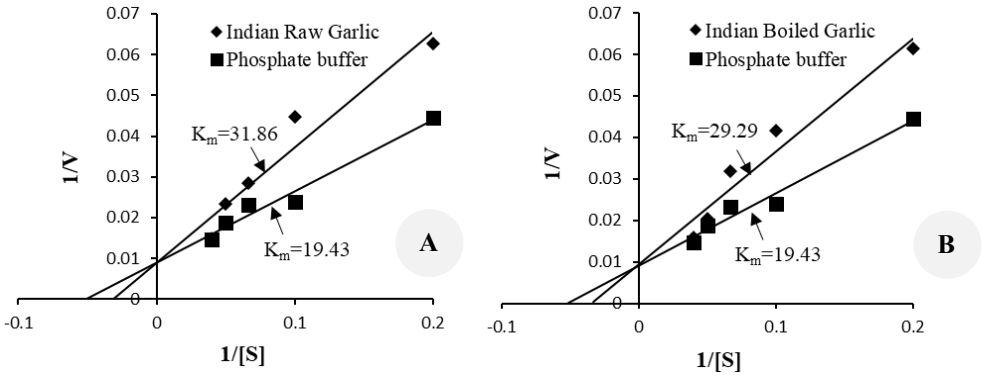

Figure 6. Lineweaver–Burk plot for the analysis of mode of α-amylase inhibition by A. Indian raw and B. Indian boiled garlic extracts. At a constant substrate concentration ([S]), the observed increase in the K_m values of α-amylase in the presence of both raw and boiled garlic extracts indicates a pattern consistent with competitive inhibition. This suggests that constituents in the extracts may be interfering with substrate binding by competing for the enzyme's active site

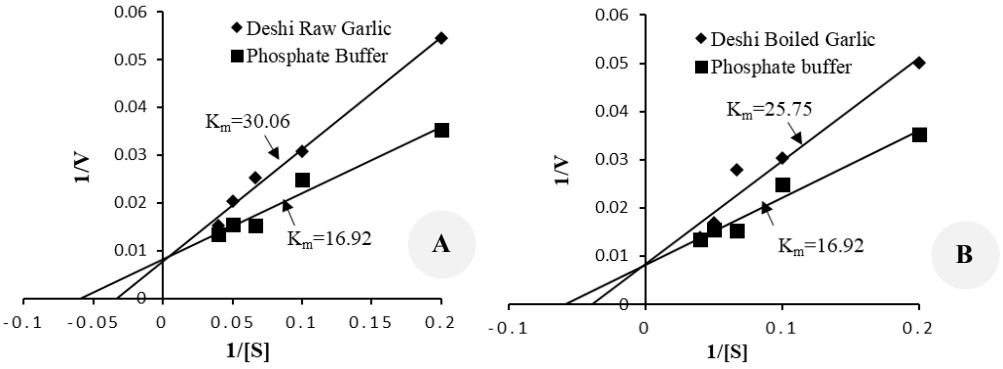

Figure 7. Lineweaver–Burk plot for the analysis of mode of α-glucosidase inhibition by A. Deshi raw and B. Deshi boiled garlic extracts. The elevated K_m values of α-glucosidase observed in the presence of both Deshi raw and boiled garlic extracts, under constant substrate concentration ([S]), indicate a decreased affinity between the enzyme and its substrate—an effect characteristic of competitive inhibition. This suggests that bioactive compounds in the garlic extracts are likely competing with the substrate for binding at the enzyme's active site

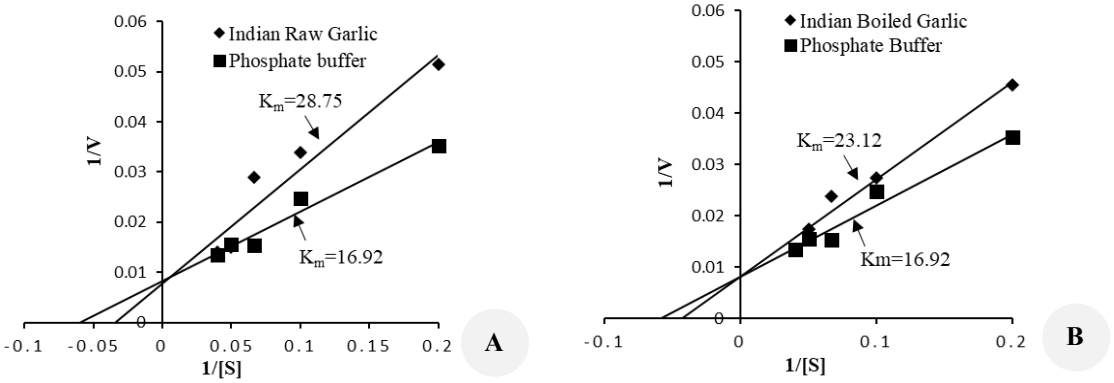

Figure 8. Lineweaver–Burk plot for the analysis of mode of α-glucosidase inhibition by A. Indian raw and B. Indian boiled garlic extracts. The plots were constructed by assessing enzyme activity across a range of substrate concentrations ([S]) while varying the concentrations of garlic extracts. In both cases, the Lineweaver–Burk analysis revealed an increase in the apparent Michaelis constant (K_m) at a constant substrate concentration, which is characteristic of competitive inhibition. This suggests that bioactive compounds present in both Indian raw and boiled garlic extracts compete with the substrate for binding at the active site of the α-glucosidase enzyme

Synthetic medications such as sulfonylureas, α-glucosidase inhibitors, insulin analogues, meglitinides, and thiazolidinediones are commonly used to manage diabetes. However, prolonged use of these drugs may lead to adverse effects, including liver dysfunction, diarrhea, skin irritation or itching, weight gain, fatigue or dizziness, increased risk of anemia, swelling in the legs or ankles, and even potential cancer risks. Additionally, the high cost of these medications presents a significant challenge, especially in low- and middle-income countries, which bear more than 80% of the global diabetes burden. As an alternative, plant-based enzyme inhibitors have attracted growing interest due to their affordability, fewer side effects, and promising antidiabetic properties. More than 400 plant species have been identified globally for their ability to lower blood glucose levels. Among them, garlic (*A. sativum*) stands out for its bioactive compounds with known hypoglycemic effects. Using medicinal plant extracts to inhibit enzymes like α-amylase and α-glucosidase offers a potential natural strategy for managing diabetes while minimizing the side effects associated with synthetic drugs (Kim et al. 2004).

Acarbose, miglitol, and voglibose are enzyme inhibitors currently used in the management of DM. Acarbose functions by inhibiting both α-amylase and α-glucosidase, whereas miglitol and voglibose selectively inhibit α-glucosidase only (Yibchok-Anun et al. 2006). Although these inhibitors have demonstrated effectiveness in controlling postprandial blood glucose levels, their use is often limited due to gastrointestinal side effects, making them less suitable for long-term therapy. Additionally, the high cost of these drugs poses a financial challenge—particularly in low- and middle-income countries, where approximately 80% of the global diabetic population resides. As a result, significant research efforts have been directed toward identifying alternative α-amylase and α-glucosidase inhibitors from natural sources such as plants, bacteria, marine algae, and fungi.

In this study, the antidiabetic potential of two garlic (*A. sativum*) varieties—Deshi and Indian—was evaluated in both raw and boiled forms through α-amylase and α-glucosidase inhibition assays, along with enzyme kinetic analyses. Previous research has demonstrated that garlic extracts possess significant antidiabetic effects, particularly in diabetic rat models (Mahmoud and Abdalla 2011; Masjedi et al. 2013; Jiang et al. 2024). Our results showed that the raw Deshi garlic extract exhibited the highest α-amylase inhibition, achieving 52.49% inhibition at a concentration of 20 mg/mL, with an IC_{50} value of 17.62 mg/mL. This inhibitory effect was comparable to that of acarbose, a standard antidiabetic drug, which showed 70.77% inhibition with an IC_{50} of 9.03 mg/mL at the same concentration. On the other hand, the boiled Deshi garlic extract demonstrated the lowest inhibition, with only 5.54% inhibition at 2 mg/mL. A similar trend was observed in the α-glucosidase inhibition assay, where raw garlic extracts consistently outperformed their boiled counterparts.

Previous studies have reported that aqueous garlic extracts possess significant in vitro inhibitory activity against α-amylase and α-glucosidase (Teng and Chen 2017). In our study, we utilized acetone extracts of both raw and boiled garlic varieties to assess their antidiabetic potential. Consistent with the findings from the α-amylase inhibition assay, the raw Deshi garlic extract exhibited the highest α-glucosidase inhibition, achieving 46.73% inhibition at 20 mg/mL, with an IC_{50} value of 21.77 mg/mL.

While the Deshi boiled garlic extract showed the lowest inhibition against α-amylase in our earlier results, a different pattern emerged in the α-glucosidase assay. Here, the Indian boiled garlic extract recorded the lowest inhibition, with only 4.67% inhibition at 2 mg/mL and an IC_{50} value of 26.21 mg/mL. Overall, raw Deshi garlic extracts demonstrated the strongest inhibitory activity against both α-amylase and α-glucosidase, highlighting their potential as a natural antidiabetic agent.

Although varying concentrations of different garlic extracts exhibited differing degrees of enzyme inhibition, acarbose—used as the positive control in this study—showed consistent inhibitory activity against both enzymes. Specifically, acarbose demonstrated 70.77% inhibition of α-amylase and 68.86% inhibition of α-glucosidase. These results highlight the effectiveness of acarbose as a reference inhibitor. However, the garlic extracts showed around two-third inhibition of α-amylase and α-glucosidase in comparison to positive control, acarbose, underscores their potential as natural alternatives or complementary agents to conventional antidiabetic drugs. To gain further insight into the mechanism of enzyme inhibition, Lineweaver-Burk plots were analyzed. Both raw and boiled garlic extracts were tested as potential inhibitors, using 20 mM phosphate buffer as the control. The resulting Lineweaver-Burk plots were used to determine the mode of inhibition, distinguishing between competitive and non-competitive inhibition patterns.

The mode of α-amylase inhibition by different garlic extracts (Deshi and Indian, in both raw and boiled forms) was determined through Lineweaver-Burk plot analysis. The K_m values for Deshi raw, Deshi boiled, Indian raw, and Indian boiled garlic extracts were found to be 34.97, 27.04, 31.86, and 29.29, respectively. In comparison, the control (20 mM sodium phosphate buffer) showed a K_m value of 19.43. Similarly, the inhibitory mode of α-glucosidase was assessed using Lineweaver-Burk plots. The K_m values for Deshi raw, Deshi boiled, Indian raw, and Indian boiled garlic extracts were 30.06, 25.75, 28.75, and 23.12, respectively, while the control exhibited a K_m value of 16.92.

In both enzyme assays, the presence of garlic extracts led to an increase in K_m values without significant changes in V_{max}, indicating a competitive mode of inhibition for both α-amylase and α-glucosidase. In both cases, the inhibition type was initially assessed as "competitive inhibition." However, further experiments involving multiple substrate concentrations and varying inhibitor levels are needed to definitively confirm the nature of the inhibition.

Raw garlic's inhibitory effects on carbohydrate-digesting enzymes are likely mediated by sulfur-containing compounds such as allicin and its derivatives, which may

interact with thiol groups in enzyme active sites, disrupting substrate binding (Wu et al. 2023). A study demonstrated that melanoidins from black garlic non-competitively inhibit α-amylase and α-glucosidase, with stronger activity linked to fluorescent groups (Wu et al. 2023). In silico docking has shown compounds like methionol and caffeic acid to have higher binding affinity to α-glucosidase than standard drugs like miglitol, indicating potential competitive inhibition (Sadeghi et al. 2021). Fermentation has also been shown to enhance garlic's inhibitory activity, with variability observed based on garlic origin (Ye et al. 2023). Additionally, thermal processing alters garlic's biochemical profile by deactivating alliinase and reducing allicin content, though other bioactive sulfur or melanoidin compounds may form (Lu et al. 2023). Reviews highlight that garlic's pharmacological properties are highly dependent on variety, cultivation, and processing methods, which influence the composition and activity of its sulfur compounds (Batiha et al. 2020). While raw or standardized garlic extracts may serve as adjuncts in managing postprandial hyperglycemia in T2DM, significant limitations remain—particularly in translating in vitro effects to in vivo outcomes due to variability in bioavailability, metabolism, and efficacy (Batiha et al. 2020; Sadeghi et al. 2021; Lu et al. 2023).

These findings suggest that garlic extracts, particularly in their raw form, exhibit significant inhibitory activity against key digestive enzymes, α-amylase and α-glucosidase, which play crucial roles in carbohydrate metabolism. The observed dual inhibition of both enzymes highlights the potential of garlic extracts to regulate blood sugar by slowing carbohydrate digestion and glucose absorption. This combined effect supports garlic's therapeutic potential in managing diabetes and controlling postprandial blood glucose spikes. However, in this study, we were unable to identify the specific active compound(s) in garlic responsible for competing with the enzyme substrates at the active site. Further investigation is needed to characterize these inhibitory components. This underscores the potential of garlic extracts as natural therapeutic agents for managing postprandial hyperglycemia, particularly in individuals with Type 2 Diabetes Mellitus (T2DM).

In conclusion, the findings of this study demonstrate that both Deshi and Indian garlic extracts, especially in their raw forms, exhibit significant in vitro inhibitory activity against α-amylase and α-glucosidase—key enzymes involved in carbohydrate digestion. These inhibitory effects, identified as competitive in nature, highlight garlic's potential as a functional food or nutraceutical for managing postprandial hyperglycemia and T2DM. These findings are based on observed data and require further experimental validation, such as molecular docking and/or compositional profiling, to confirm the underlying mechanism, while future investigations should aim to isolate and characterize the active bioactive compounds, assess their in vivo efficacy, and develop optimized formulations for potential clinical applications.

ACKNOWLEDGEMENTS

This work was technically supported by the Department of Genetic Engineering and Biotechnology, Shahjalal University of Science and Technology (SUST), Sylhet-3114, Bangladesh. The research work was performed by the financial assistance of SUST Research Center (LS/2022/1/17), Shahjalal University of Science and Technology, Sylhet-3114, Bangladesh.

REFERENCES

Balamurugan K, Nishanthini A, Mohan VR. 2014. Antidiabetic and antihyperlipidaemic activity of ethanol extract of *Melastoma malabathricum* Linn. leaf in alloxan induced diabetic rats. Asian Pac J Trop Biomed 4 (1): S442-S488. DOI: 10.12980/APJTB.4.2014C122.

Batiha GE, Beshbishy AM, Wasef LG, Elewa YHA, Al-Sagan AA, El-Hack MEA, Taha AE, Abd-Elhakim YM, Devkota HP. 2020. Chemical constituents and pharmacological activities of garlic (*Allium sativum* L.): A review. Nutrients 12 (3): 872. DOI: 10.3390/nu12030872.

Behl T, Kotwani A. 2017. Proposed mechanisms of *Terminalia catappa* in hyperglycaemia and associated diabetic complications. J Pharm Pharmacol 69 (2):123-134. doi: 10.1111/jphp.12676. Epub 2016 Dec 20. PMID: 28000229.

D'Britto V, Devi PP, Prasad BLV, Dhawan A, Mantri VG, Prabhune A. 2012. Medicinal plant extracts used for blood sugar and obesity therapy shows excellent inhibition of invertase activity: Synthesis of nanoparticles using this extract and its cytotoxic and genotoxic effects. J Life Sci Pharm Res 2: 61-74. DOI: 10.5555/20123374791.

Debnath A, Salim M, Miah MF, Karim MR, Alam MJ. 2020. Evaluation of invertase inhibition activities and cytotoxicity of ethanol and acetone extracts of *Swietenia macrophyllia* leaves, *Syzygium cumini* and *Trigonella foenum-graecum* seeds. Tradit Integr Med 5 (2): 59-69. DOI: 10.18502/tim.v5i2.3626.

Fatmawati S., Shimizu K., Kondo R. 2011. Ganoderol B: A potent α-glucosidase inhibitor isolated from the fruiting body of *Ganoderma lucidum*. Phytomedicine 18: 1053-1055. DOI: 10.1016/j.phymed.2011.03.011.

Gellad WF, Donohue JM, Zhao X, Mor MK, Thorpe CT, Smith J, Good CB, Fine MJ. and Morden ME. 2013. Brand-name prescription drug use among diabetes patients in the VA and medicare part D: A national comparison. Ann Intern Med 159: 105-114. DOI: 10.7326/0003-4819-159-2-201307160-00664.

International Diabetes Federation (IDF). 2015. Diabetes Atlas: http://www.idf.org/ diabetesatlas/.

Iwakura K, Ito H, Ikushima M, Kawano S, Okamura A, Asano K, Kuroda T, Tanaka K, Masuyama T, Hori M, Fujii K. 2003. Association between hyperglycemia and the no-reflow phenomenon in patients with acute myocardial infarction. J Am Coll Cardiol 41 (1): 1-7. DOI: 10.1016/s0735-1097(02)02626-8.

Jiang Y, Yue R, Liu G, Liu J, Peng B, Yang M, Zhao L, Li Z. 2024. Garlic (*Allium sativum* L.) in diabetes and its complications: Recent advances in mechanisms of action. Crit Rev Food Sci Nutr 64 (16):5290-5340. doi: 10.1080/10408398.2022.2153793.

Khatun MM, Sapan MA, Hossain MS, Islam MR. 2015. Antidiabetic activity of *Piper betle* in alloxan induced type 1 diabetic model rats. Intl J Pharm Sci Res 7 (2): 675-680. DOI: 10.13040/IJPSR.0975-8232.7(2).675-80.

Kim YM, Wang MH, Rhee HI. 2004. A novel α-glucosidase inhibitor from pine bark, Carbohydr Res 339 (3): 715-717. DOI: 10.1016/j.carres.2003.11.005.

Konishi K, Watanabe N, Saito M, Nakajima N, Sakaki T, Katayama T, Enomoto T. 2012. Isolation of a new phlorotannin, a potent inhibitor of carbohydrate hydrolyzing enzymes, from the brown alga *Sargassum patens*. J Agr Food Chem 60: 5565-5570. DOI: 10.1021/jf300165j.

Lu J, Li N, Li S, Liu W, Li M, Zhang M, Chen H. 2023. Biochemical composition, antioxidant activity and antiproliferative effects of different processed garlic products. Molecules 28 (2): 804. DOI: 10.3390/molecules28020804.

Mahmoud MR, Abdalla AM. 2011. ypoglycemic and anti-apoptotic effects of aqueous garlic extract in streptozotocin-induced diabetic rats. Egypt J Biochem Mol Biol 29 (2): 393-406. DOI: 10.4314/ejbmb.v29i2.72446.

Mahmud T, Hasan R, Islam K, Alam MJ. 2023. Inhibition of key digestive enzymes linked to type 2 diabetes mellitus by *Piper betle* L. leaf extracts to manage diabetes in an alternative way. Curr Nutr Food Sci 19 (6): e280922209221. DOI: 10.2174/1573401318666220928091823.

Masjedi F, Gol A, Dabiri S. 2013. The preventive effect of garlic juice on serum biochemical factors and histopathology of pancreas and liver in streptozotocin-induced diabetic rats. Iran J Basic Med Sci 16 (9): 1012-1019.

Mnayer D, Fabiano TA, Petitcolas E, Hamieh T, Nehme N, Ferrant C, Fernandez X, Chemat F. 2014. Chemical composition, antibacterial and antioxidant activities of six essential oils from the Alliaceae family. Molecules 19 (12): 20034-20053. DOI: 10.3390/molecules191220034.

Nickavar B, Yousefian N. 2009. Inhibitory effects of six *Allium* species on α-Amylase enzyme activities. Iran J Pharm Res 8: 53-57.

Orhan N, Aslan M, Süküroğlu M, Orhan D. 2013. In vivo and in vitro antidiabetic effect of *Cistus laurifolius* L. and detection of major phenolic compounds by UPLC-TOF-MS analysis. J Ethnopharmacol 146: 859-865. DOI: 10.1016/j.jep.2013.02.016.

Panwar H, Calderwood D, Grant IR, Grover S, Green BD. 2015. *Lactobacillus* strains isolated from infant faeces possess potent inhibitory activity against intestinal α- and beta-glucosidases suggesting anti-diabetic potential. Eur J Nutr 53: 1465-1474. DOI: 10.1007/s00394-013-0649-9.

Paul JS, Gupta N, Beliya E, Tiwari S, Jadhav SK. 2021. Aspects and Recent Trends in Microbial α-Amylase: A review. Appl Biochem Biotechnol. 193 (8):2649-2698. doi: 10.1007/s12010-021-03546-4. Epub 2021 Mar 14. PMID: 33715051.

Phan ADT, Netzel G, Chhim P, Netzel ME, Sultanbawa Y. 2019. Phytochemical characteristics and antimicrobial activity of Australian grown garlic (*Allium sativum* L.) cultivars. Foods 8 (9): 358. DOI: 10.3390/foods8090358.

Poovitha S, Parani M. 2016. *In vitro* and *in vivo* α-amylase and α-glucosidase inhibiting activities of the protein extracts from two varieties of bitter gourd (*Momordica charantia* L.). BMC Complement Altern Med 16 (1): 185. DOI: 10.1186/s12906-016-1085-1.

Rahmani AH. 2015. *Cassia fistula* L.: Potential candidate in the health management. Pharmacognosy Res 7 (3): 217-24. DOI: 10.4103/0974-8490.157956. PMID: 26130932; PMCID: PMC4471647.

Rowley WR, Bezold C, Arikan Y, Byrne E, Krohe S. 2017. Diabetes2030: Insights from yesterday, today and future trends. Popul Health Manag 20 (1): 6-12. DOI: 10.1089/pop.2015.0181.

Sadeghi M, Moradi M, Madanchi H, Johari B. 2021. In silico study of garlic (*Allium sativum* L.)-derived compounds molecular interactions with α-glucosidase. In silico Pharmacol 9 (1): 11. DOI: 10.1007/s40203-020-00072-9.

Sani DH, Munna AN, Alam MJ, Salim M, Alam MJ. 2020. Evaluation of α-amylase inhibition and cytotoxic activities of the *Arachis hypogaea* and *Cinnamomum tamala*. Curr Nutr Food Sci 17 (3): 328-336. DOI: 10.2174/1573401316999200728183434.

Sani DH, Sarker P, Alam MJ. 2024. Restraint of starch-hydrolyzing enzyme in the management of postprandial blood glucose level: An alternative approach. Lett Drug Des Discov 21 (10): e170423215853. DOI: 10.2174/1570180820666230417083840.

Sarker P, Sani DH, Miah MF, Alam MJ. 2024. Curbing key digestive enzymes by three plant extracts for sustainable management of postprandial hyperglycemia. Lett Drug Des Discov 21 (11): e180523217037. DOI: 10.2174/1570180820666230518100900.

Sathishkumar T, Anitha S, Sharon RE, Santhi V, Sukanya M, Kumaraesan K, Rapheal V. 2015. Evaluation of *in vitro* invertase inhibitory activity of *Manilkara zapota* seeds – A novel strategy to manange diabetes mellitus. J Food Biochem 2015: 12157. DOI: 10.1111/jfbc.12157.

Teng H, Chen L. 2017. α-Glucosidase and α-amylase inhibitors from seed oil: A review of liposoluble substance to treat diabetes. Crit Rev Food Sci Nutr 57 (16):3438-3448. doi: 10.1080/10408398.2015.1129309.

Thakre D, Dhamodar K, Khan ND, Khan ZH, Mular SM, Khan B. 2017. *In vitro* assy of alpha amylase inhibitory activity of *Piper* species. Biosci Discov 8 (2): 125-128.

Vazquez-Armenta FJ, Cruz-Valenzuela MR, Ayala-Zavala JF. 2016. Onion (*Allium cepa*) essential oils. In: Preedy VR (eds). Essential Oils in Food, Preservation, Flavor and Safety. Academic Press, London. DOI: 10.1016/B978-0-12-416641-7.00070-5.

Wu J, Wang Y, Li S, Wu T, Liu R, Sui W, Zhang M. 2023. Black garlic melanoidins inhibit *in vitro* α-amylase and α-glucosidase activity: The role of high-molecular-weight fluorescent compounds. J Sci Food Agric 103 (11): 5376-5387. DOI: 10.1002/jsfa.12634.

Ye M, Liu C, Chen S, Niu C, Wang J, Zheng F, Xu X, Li Q. 2023. Screening of strains with potential hypoglycemic effect and its application in fermented garlic production. Syst Microbiol Biomanufacturing 3: 602-614. DOI: 10.1007/s43393-022-00129-0.

Yibchok-Anun S, Adisakwattana S, Yao CY, Sangvanich P, Roengsumran S, Hsu WH. 2006. Slow acting protein extract from fruit pulp of *Momordica charantia* with insulin secretagogue and insulinomimetic activities. Biol Pharm Bull 29 (6): 1126-1131. DOI: 10.1248/bpb.29.1126.

Zafar M, Shahid SMA, Alshammari RF, Kausar MA, Ginawi TAN, Hatim AW, Wadi AM, Ali H, Hamed AA, Al-Zahrani MS, Hussain A, Alduhaim AS, Mohammed A. 2022. Association of thyroid disorders with diabetes: A cross-sectional study. Nusantara Biosci 14: 135-140. DOI: 10.13057/nusbiosci/n140201.

Zhao X, Cheng T, Xia H, Yang Y, Wang S. 2024. Effects of garlic on glucose parameters and lipid profile: A systematic review and meta-analysis on randomized controlled trials. Nutrients 16 (11): 1692. DOI: 10.3390/nu16111692.

ASIAN J NAT PROD BIOCHEM
Volume 23, Number 2, December 2025
Pages: 131-145

P-ISSN: 2775-4189
E-ISSN: 2775-4197
DOI: 10.13057/biofar/f230205

Comparative HPLC fingerprinting of flavonoid profiles in *Selaginella* species

AHMAD DWI SETYAWAN[1,2,♥], TATIK CHIKMAWATI[3], MIFTAHUDIN[3], PUSPA DEWI N. LOTULUNG[4], SUTARNO[5], SUGIYARTO[5], SUNARTO[1]

[1]Department of Environmental Science, Faculty of Mathematics and Natural Sciences, Universitas Sebelas Maret. Jl. Ir. Sutami 36A, Surakarta 57126, Central Java, Indonesia. Tel./fax.: +62-271-663375, ♥email: volatileoils@gmail.com
[2]Biodiversity Research Group, Universitas Sebelas Maret. Jl. Ir. Sutami 36A, Surakarta 57126, Central Java, Indonesia
[3]Department of Biology, Faculty of Mathematics and Natural Sciences, Institut Pertanian Bogor. Jl. Raya Dramaga, Bogor 16680, West Java, Indonesia
[4]Research Center for Pharmaceutical Ingredients and Traditional Medicine, National Research and Innovation Agency. KST BJ Habibie Puspiptek Area, Jl. Raya Serpong, Muncul, Setu, South Tangerang 15314, Banten, Indonesia
[5]Department of Biology, Faculty of Mathematics and Natural Sciences, Universitas Sebelas Maret. Jl. Ir. Sutami 36A, Surakarta 57126, Central Java, Indonesia

Manuscript received: 26 March 2025. Revision accepted: 3 November 2025.

Abstract. *Setyawan AD, Chikmawati T, Miftahudin, Lotulung PDN, Sutarno, Sugiyarto, Sunarto. 2025. Comparative HPLC fingerprinting of flavonoid profiles in* Selaginella *species. Asian J Nat Prod Biochem 23: 131-145.* Flavonoids are among the most prominent secondary metabolites in *Selaginella*, yet comparative information on flavonoid composition across multiple species remains limited. Most existing phytochemical studies focus on individual species or isolated compounds, providing little insight into interspecific chemical relationships within the genus. This study applies RT-based HPLC fingerprinting to comparatively assess flavonoid profile variation among 20 samples representing 17 *Selaginella* species collected from diverse ecological and geographical settings in Indonesia. Methanolic extracts were analyzed under standardized chromatographic conditions, and flavonoid-related peaks were aligned using a retention time tolerance of ±0.2 min to construct a binary presence-absence fingerprint matrix comprising 11 RT-defined features. Interspecific similarity was evaluated using Sørensen and Jaccard coefficients, followed by hierarchical clustering (UPGMA) and complementary ordination to visualize chemical relationships among samples. The results reveal pronounced qualitative differences in flavonoid fingerprints among species, characterized by both shared and species-specific chromatographic features. Conspecific samples collected from different localities exhibited stable core flavonoid profiles with additional site-related variation, while interspecific comparisons showed substantial heterogeneity. Similarity patterns were not strictly associated with geographic proximity, suggesting that flavonoid composition primarily reflects intrinsic biochemical traits rather than purely environmental effects. This study provides an effective qualitative framework for interspecific discrimination and chemotaxonomic assessment in *Selaginella*. Although compound identity and abundance were not resolved, the approach offers a practical foundation for future targeted phytochemical, bioactivity-oriented, and integrative chemotaxonomic investigations.

Keywords: Chemotaxonomy, flavonoids, HPLC fingerprinting, retention time, *Selaginella*

INTRODUCTION

Selaginella is one of the most diverse genera of lycophytes, comprising more than 700 species distributed predominantly in tropical and subtropical regions (Jermy 1990; Banks 2009; Weststrand and Korall 2016a). As an early-diverging lineage of vascular plants, *Selaginella* exhibits distinctive physiological and biochemical traits that have attracted increasing scientific interest, particularly in relation to secondary metabolites (Banks et al. 2011). Among these, flavonoids represent one of the most prominent and chemically diverse groups reported from the genus (Cao et al. 2010; Setyawan 2011).

Flavonoids in *Selaginella* are dominated by biflavonoids and related phenolic compounds, which have been associated with a wide range of bioactivities, including antioxidant, anti-inflammatory, cytotoxic, and neuroprotective effects (Chikmawati et al. 2012; Zheng et al. 2012; Křížkovská et al. 2020). In addition to their pharmacological relevance, flavonoids play important ecological roles in UV protection, stress tolerance, and defense against herbivores and pathogens, particularly in species inhabiting exposed or heterogeneous environments (Close and McArthur 2002; Mierziak et al. 2014). This dual functional relevance places flavonoids at the intersection of chemical ecology, adaptive biology, and applied phytochemistry in *Selaginella*.

Despite growing interest, most flavonoid studies on *Selaginella* have focused on individual species or a limited number of taxa, primarily emphasizing compound isolation and structural elucidation (Shim et al. 2018; Muema et al. 2022). While these studies provide valuable information on compound diversity, they offer limited insight into broader interspecific patterns of flavonoid composition. Consequently, current knowledge remains fragmented, underscoring the need for comparative approaches capable of capturing chemical variation across multiple *Selaginella* species within a unified analytical framework.

Phytochemical investigations of *Selaginella* have traditionally relied on targeted strategies, including

spectroscopic identification and LC-MS-based profiling aimed at known flavonoids (Cao et al. 2010; Almeida et al. 2013; Shim et al. 2018). Although indispensable for structural and bioactivity studies, such approaches are less effective for comparative analysis across numerous species, as they often prioritize dominant or previously reported compounds. Moreover, the lack of standardized comparative matrices hampers holistic assessment of chemical similarity, species discrimination, and chemotaxonomic interpretation within the genus, particularly in species-rich tropical regions where chemical diversity may parallel ecological differentiation (Wolfender et al. 2003; Kim et al. 2010; Allard et al. 2016).

From a methodological perspective, the application of chromatographic fingerprinting remains surprisingly scarce in *Selaginella* research. Comparative RT-based flavonoid fingerprinting across multiple *Selaginella* species is still poorly explored, and few studies have constructed retention time matrices or applied similarity indices and clustering analyses to evaluate interspecific chemical relationships (Liang et al. 2004; Tistaert et al. 2011; Goodarzi et al. 2013). As a result, chemotaxonomic signals and interspecific chemical affinities within *Selaginella* remain insufficiently resolved.

High-Performance Liquid Chromatography (HPLC) fingerprinting offers a robust and reproducible approach for comparative analysis of complex phytochemical mixtures by emphasizing overall chromatographic patterns rather than individual compound identities (Gong et al. 2003; Xie et al. 2006). Retention time-based fingerprinting is particularly suitable for multi-species comparisons, as it facilitates pattern recognition, similarity assessment, and clustering analysis across large datasets (Xie et al. 2006; D'Orazio et al. 2016). In the context of *Selaginella*, this approach provides a practical strategy to overcome the limitations of compound-centered studies and to support comparative, chemotaxonomic, and exploratory screening objectives.

The present study aims to comparatively evaluate flavonoid profiles across multiple *Selaginella* species using Retention Time (RT)-based HPLC fingerprinting. Specifically, this study seeks to (i) construct a retention time matrix of flavonoid peaks, (ii) identify shared and species-specific chromatographic features, and (iii) assess interspecific chemical similarity and clustering patterns using similarity indices and multivariate analysis. We hypothesized that RT-based HPLC flavonoid fingerprints would exhibit (i) stable species-level core patterns across samples of the same *Selaginella* species collected from different localities, and (ii) significant interspecific differentiation in flavonoid composition that is not strictly associated with geographic proximity, reflecting intrinsic biochemical traits rather than environmental factors alone. The novelty of this study lies in its integrative multi-species design, representing one of the first applications of RT-based HPLC fingerprinting combined with similarity and cluster analyses to explore flavonoid diversity within *Selaginella*. By adopting a comparative framework, this work contributes to improved chemotaxonomic understanding and provides a methodological foundation for future studies linking chemical diversity with bioactivity screening and evolutionary interpretation.

MATERIALS AND METHODS

Plant materials and species identification

Plant materials used in this study consisted of multiple *Selaginella* species representing a range of habitats and elevational zones. Species selection was designed to capture interspecific variation in flavonoid profiles across contrasting ecological settings, including lowland, montane, and high-altitude environments. Details of the analyzed species, sampling localities, habitat characteristics, and elevation ranges are summarized in Table 1.

Field sampling was conducted across different geographic locations, with site selection based on the natural distribution of each *Selaginella* species (Alves and Rosa 2007). For each species, healthy and mature aerial parts were collected to ensure sufficient biomass for phytochemical analysis, following recommended botanical collection practices (Hudson et al. 2021). Habitat descriptions were recorded in situ, including dominant vegetation type, light conditions, and substrate characteristics, as these factors may influence secondary metabolite production (Gershenzon 1984). Elevation was determined using a handheld GPS device or altimeter and is reported in meters above sea level (masl) to provide ecological context for each species (Hijmans et al. 2005).

Species identification was conducted using a combination of diagnostic morphological characters, including leaf arrangement, the shape and dimorphism of lateral and median leaves, stem architecture, and overall growth form. Identification *Selaginella* followed the earliest and authoritative taxonomic from the Malay Archipelago, particularly by Alston (1934, 1935a, b, 1937, 1940). Specimens were further compared with authenticated collections housed at Herbarium Bogoriense (BO), Indonesia, with special emphasis on specimens determined by A.G.H. Alston. Additional confirmation was obtained by consulting more recent taxonomic references covering *Selaginella* in the Malay Archipelago and adjacent regions, including Wong (1982, 2010), Tsai and Shieh (1994), Li and Tan (2005), Chang et al. (2012), Setyawan (2012), et al. (2013), and Zhang et al. (2013).

Voucher specimens for all analyzed species were prepared and deposited at the Herbarium of Universitas Sebelas Maret, Indonesia (UNS; herbarium code: SO) to ensure reproducibility and taxonomic verifiability of the study. Each voucher specimen was assigned a unique collection number and labeled with detailed locality information, collector name, and collection date. Duplicate specimens (selected herbarium copies) will be forwarded to Herbarium Bogoriense (BO) for reference and long-term curation. Voucher accession numbers corresponding to each species are provided in Table 1. The deposition of voucher specimens ensures that future studies can re-examine the taxonomic identity of the analyzed material and facilitates integration of phytochemical data with taxonomic and ecological research.

Table 1. List of *Selaginella* species, collection sites, and ecological characteristics

Species name	Collection locality	Province (Indonesia)	Habitat type	Elevation (masl)	Voucher specimen
Selaginella opaca	Karangtengah: Sikidang Crater	Central Java	*Albizia lophantha* forest above a volcanic crater	2,124	ADS 22
S. remotifolia	Karangtengah: Sikidang Crater	Central Java	Dirt inspection road of the geothermal steam pipeline	2,071	ADS 23
S. intermedia-01	Citalahab-Malasari: Nirmala Tea Plantation	West Java	Forest trail and tea plantation margin	1,118	ADS 117
S. subalpina-01	Banyukuning: Gedongsongo Temple	Central Java	Shaded area under the bamboo canopy	1,309	ADS 45
S. involvens-01	Kledung Village: Temporary tobacco field	Central Java	Drainage edge of the tobacco field	1,493	ADS 38
S. wildenowii	Citalahab-Malasari: Nirmala Tea Plantation	West Java	Forest trail and tea plantation margin	1,118	ADS 116
S. mayeri	Bogor Botanical Gardens	West Java	Wild growth among botanical garden collections	262	ADS 111
S. ornata	Citalahab-Malasari: Nirmala Tea Plantation	West Java	Forest trail and tea plantation margin	1,118	ADS 118
S. plana	Gondowido: Lake Ngebel	East Java	Lake margin	786	ADS 52
S. frondosa	Bogor Botanical Gardens	West Java	Wild growth among botanical garden collections	262	ADS 112
S. subalpina-02	Gunung Bunder 2: Mount Halimun Salak National Park	West Java	Cliff in Damar Forest	869	ADS 136
S. intermedia-02	Gunung Bunder 2: Mount Halimun Salak National Park	West Java	Cliff in Damar Forest	869	ADS 135
S. aristata	Berjo: Ngargoyoso Grand Forest Park	Central Java	Roadside cliff	1,220	ADS 8
S. ciliaris	Gentan: Batuseribu Park	Central Java	Small river cliff	182	ADS 46
S. repanda	Kulurejo: Riparian agroforestry	Central Java	Hills near a small stream	185	ADS 134
S. involvens-02	Baturiti: Batu Kahu Nature Reserve	Bali	Montane forest floor	1,403	ADS 155
S. ketra-ayam	Mount Menumbing	Bangka Belitung Islands	Hill forest	400	ADS 146
S. velutina	Cycloops Mountain Nature Reserve	Papua	Lower montane forest	281	ADS 141
Selaginella sp. (Mt. Meja)	Mount Meja Protected Forest	West Papua	Lowland protected forest	102	ADS 145
S. caudata	Mount Meja Protected Forest	West Papua	Lowland protected forest	102	ADS 144

Note: Numeric suffixes (e.g., -01, -02) indicate distinct samples of the same species collected from different localities or collection events, following the original sample labeling. Elevation is expressed in meters above sea level (masl)

Sample preparation and flavonoid extraction

Plant materials of each *Selaginella* sample were processed following a standardized protocol to ensure comparability of flavonoid profiles across species. Fresh aerial parts, including stems and leaves, were cleaned to remove adhering soil and debris, then air-dried under shade at ambient temperature to minimize degradation of phenolic compounds. Dried samples were subsequently ground into a fine powder using a laboratory mill and stored in airtight containers at room temperature until extraction.

Flavonoid extraction was carried out using a solvent-based maceration method commonly employed in phytochemical studies (Stalikas 2007; Azmir et al. 2013). Approximately 0.5 g of powdered plant material was extracted with 10 mL of analytical-grade methanol, selected for its effectiveness in solubilizing flavonoid and other phenolic compounds (Dai and Mumper 2010). The mixture was sonicated for 30 min at room temperature to enhance extraction efficiency, followed by static maceration for 24 h in the dark (Shehzadi et al. 2025). After centrifugation at 4,000 rpm for 10 min, the supernatant was collected for subsequent analysis (Stalikas 2007).

To ensure sample consistency, all extracts were filtered through 0.45 µm PTFE syringe filters prior to HPLC analysis to remove particulates and protect the chromatographic system (Stalikas 2007; Snyder et al. 2010). Filtrates were transferred into amber vials and stored at 4°C to minimize degradation of phenolic compounds before analysis (Dai and Mumper 2010). No further purification or fractionation was applied, as the aim was to obtain holistic flavonoid fingerprints rather than isolated compounds, thereby preserving the overall chromatographic pattern and enabling direct comparison of retention time-based profiles among samples (Liang et al. 2004; Xie et al. 2006).

Extraction conditions, solvent type, sample-to-solvent ratio, and filtration procedures were kept identical for all samples to minimize methodological bias. Such standardization is essential for reliable interpretation of interspecific differences in flavonoid fingerprints derived from HPLC analysis.

HPLC instrumentation and analytical conditions

The HPLC analysis of flavonoid extracts was performed using a reversed-phase system equipped with a quaternary pump, an autosampler, a column oven, and a photodiode array (PDA) detector. Chromatographic separation was achieved on a C18 reversed-phase column (250 × 4.6 mm, 5 µm particle size), which is commonly employed for the analysis of flavonoids and related phenolic compounds due to its robustness and broad applicability (Snyder et al. 2010).

The gradient system and mobile phase composition followed commonly applied RP-HPLC conditions for flavonoid fingerprinting (Liang et al. 2004; Stalikas 2007). The mobile phase consisted of solvent A (water containing 0.1% formic acid) and solvent B (acetonitrile). A linear gradient elution was applied to ensure adequate separation of flavonoid constituents with varying polarities. The gradient program was as follows: 10% B at 0 min, increased to 30% B over 15 min, then to 50% B at 30 min, and finally to 70% B at 45 min, followed by a 5 min re-equilibration to initial conditions. The flow rate was maintained at 1.0 mL min^{-1}, the column temperature was set at 30°C, and the injection volume was 10 µL.

Detection was carried out using a PDA detector, with chromatograms recorded at 270 nm, a wavelength commonly applied for monitoring flavonoid aglycones and biflavonoids due to their strong UV absorbance in this region (Liang et al. 2004; Stalikas 2007). For fingerprint analysis, chromatograms obtained at 270 nm were primarily used, providing adequate sensitivity for comparative assessment of major flavonoid constituents across samples. Representative chromatograms presented in this study were selected to reflect the range of profile complexity observed across the entire dataset.

To support RT stability and analytical consistency across runs, a reference standard of amentoflavone was analyzed under identical chromatographic conditions (Figure 1). The standard produced a single, well-resolved peak with a consistent retention time (≈7.27 min), serving as an external RT reference to monitor system performance and alignment reliability. The use of this reference was intended solely to support RT reproducibility and calibration, not for compound identification within sample chromatograms.

Method reproducibility was further evaluated through replicate injections of selected samples under identical chromatographic conditions. Retention time stability was assessed by calculating the Relative Standard Deviation (RSD) of major peak retention times, which consistently remained below 2%, indicating that the analytical conditions were sufficiently stable to support reliable comparison of RT-based flavonoid fingerprints across all Selaginella samples (Xie et al. 2006).

Peak detection and RT alignment

Peak detection was conducted on HPLC chromatograms obtained under standardized analytical conditions using the instrument's integrated chromatographic software. A consistent signal-to-noise threshold was applied uniformly across all samples, and only peaks with well-defined shapes and intensities clearly exceeding baseline noise were retained to minimize the inclusion of artefacts.

The RT alignment was performed to enable accurate comparison of chromatographic features among samples. Minor RT shifts arising from instrumental variability or matrix effects were accommodated by applying a general tolerance window of ±0.2 min for peak matching across chromatograms. Peaks falling within this tolerance range were treated as representing the same chromatographic feature, a criterion commonly adopted in chromatographic fingerprinting studies to balance alignment robustness and sensitivity (Liang et al. 2004; Xie et al. 2006).

For RT-based fingerprint construction, a narrow RT bin (7.25-7.40 min) was defined as an operational alignment feature (RT3) corresponding to the elution region of the amentoflavone reference peak. This restricted window was intentionally selected to capture only consistently aligned peaks and to exclude borderline signals occurring slightly earlier or later than the reference RT. The use of a narrow RT bin is critical for preserving feature homology across samples and for preventing artificial inflation of similarity values in subsequent similarity, clustering, and ordination analyses. Accordingly, RT3 represents a conservative alignment feature rather than an exhaustive indicator of amentoflavone occurrence.

Aligned peaks were further inspected visually to confirm consistency in peak shape and relative elution order across samples. This semi-automated approach reduced the risk of misalignment associated with fully automated algorithms, particularly when handling complex plant extracts.

The resulting aligned RT dataset formed the basis for constructing a binary presence–absence fingerprint matrix used in subsequent similarity and clustering analyses. By focusing on RT-defined features rather than absolute peak areas, this approach emphasizes qualitative pattern recognition and interspecific comparability, which are central to the objectives of this study.

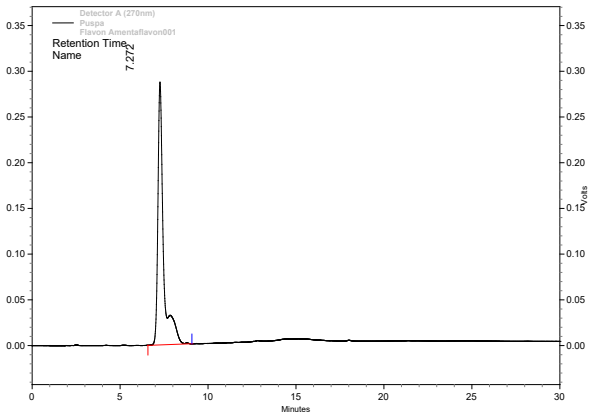

Figure 1. HPLC chromatogram of amentoflavone reference standard (270 nm) showing a single peak at RT 7.27 min under the chromatographic conditions applied in this study

Construction of RT-based fingerprint matrix

An RT-based fingerprint matrix was constructed using aligned chromatographic data to facilitate comparative analysis of flavonoid profiles across *Selaginella* species. Retention Times (RTs) of detected peaks were compiled for all samples, and a tolerance threshold of ±0.2 min was applied to define equivalent chromatographic features among different samples. Peaks eluting within this RT window were considered to represent the same flavonoid-related signal, following established practices in chromatographic fingerprinting studies (Liang et al. 2004; Xie et al. 2006).

Based on this criterion, a binary presence-absence matrix was generated, in which each row corresponded to an individual *Selaginella* sample and each column represented a distinct RT-defined peak. The presence of a peak within the defined RT window was coded as "1," while its absence was coded as "0." Peak intensity or area was not included in the matrix to avoid bias arising from concentration differences or matrix effects, thereby emphasizing qualitative pattern recognition rather than quantitative abundance.

The resulting RT matrix summarizes the distribution of flavonoid-related chromatographic features across all analyzed species and samples. This matrix is presented in Table 2, which serves as the primary dataset for subsequent similarity analysis and cluster construction. By standardizing RT thresholds and using a binary scoring approach, the fingerprint matrix provides a robust and reproducible framework for evaluating interspecific similarities and differences in flavonoid profiles among *Selaginella* species.

Similarity analysis and multivariate statistics

Similarity analysis was performed using the RT-based binary fingerprint matrix derived from aligned chromatographic peaks. Pairwise similarity among *Selaginella* samples was quantified using both Sørensen and Jaccard similarity coefficients, which are widely applied to presence-absence data in comparative chemical and ecological studies (Jaccard 1901; Sørensen 1948). These indices emphasize shared features between samples while minimizing the influence of joint absences, making them suitable for RT-based chromatographic fingerprints.

The Sørensen coefficient was calculated as $2a/(2a+b+c)$, whereas the Jaccard coefficient was computed as $a/(a+b+c)$, where a represents the number of shared RT-defined peaks between two samples, and b and c represent peaks unique to each sample. Similarity matrices generated from these coefficients formed the basis for subsequent multivariate analyses.

Hierarchical cluster analysis was conducted to visualize patterns of chemical relatedness among *Selaginella* species. Clustering was performed using the Unweighted Pair Group Method with Arithmetic (UPGMA) mean based on the similarity matrices, a method commonly used for chemotaxonomic and fingerprinting studies due to its interpretability and robustness (Everitt et al. 2011; Legendre and Legendre 2012). The resulting dendrogram illustrates the grouping of samples according to overall flavonoid fingerprint similarity and was used to identify major chemotypic clusters among the analyzed species.

To complement hierarchical clustering and to provide an ordination-based visualization of overall similarity patterns, Non-Metric Multidimensional Scaling (NMDS) was additionally applied to the RT-based binary fingerprint matrix. NMDS was performed using a Sørensen dissimilarity matrix, which is appropriate for presence-absence data and emphasizes shared chromatographic features while minimizing the influence of joint absences. The analysis was conducted in a two-dimensional solution, and ordination quality was evaluated using the stress value as a measure of goodness-of-fit. NMDS was employed as an exploratory visualization tool rather than a formal hypothesis-testing framework, with the aim of assessing whether major similarity patterns observed in clustering analysis were consistently reflected in an ordination space.

RESULTS AND DISCUSSION

Overview of HPLC chromatographic profiles

The HPLC chromatographic profiles of flavonoid extracts from the analyzed *Selaginella* species exhibited pronounced qualitative differences in peak distribution, profile complexity, and overall chromatographic architecture. Representative chromatograms illustrating these interspecific variations are shown in Figure 2. All samples produced multiple resolved peaks under identical extraction and analytical conditions, confirming that flavonoids constitute a prominent component of the secondary metabolite profiles across the genus.

Clear variation was observed in the number and distribution of peaks along the retention time axis. Several species displayed complex chromatographic profiles characterized by numerous peaks distributed across mid to late retention times, indicating a diverse assemblage of flavonoid-related constituents. In contrast, other species exhibited simpler profiles dominated by a limited number of peaks, reflecting a more restricted flavonoid composition. These differences suggest substantial heterogeneity in flavonoid profiles among *Selaginella* species, even when methodological variables are fully standardized.

Samples representing the same nominal species but collected from different localities, as indicated by numerical suffixes, generally shared a similar overall chromatographic framework. Major retention time regions were often conserved between conspecific samples, while additional peaks or minor shifts in peak occurrence contributed to subtle intra-specific variation. This pattern indicates that species-level flavonoid fingerprints are broadly stable, with local environmental conditions potentially influencing the presence of secondary or low-frequency peaks without altering the core chromatographic structure.

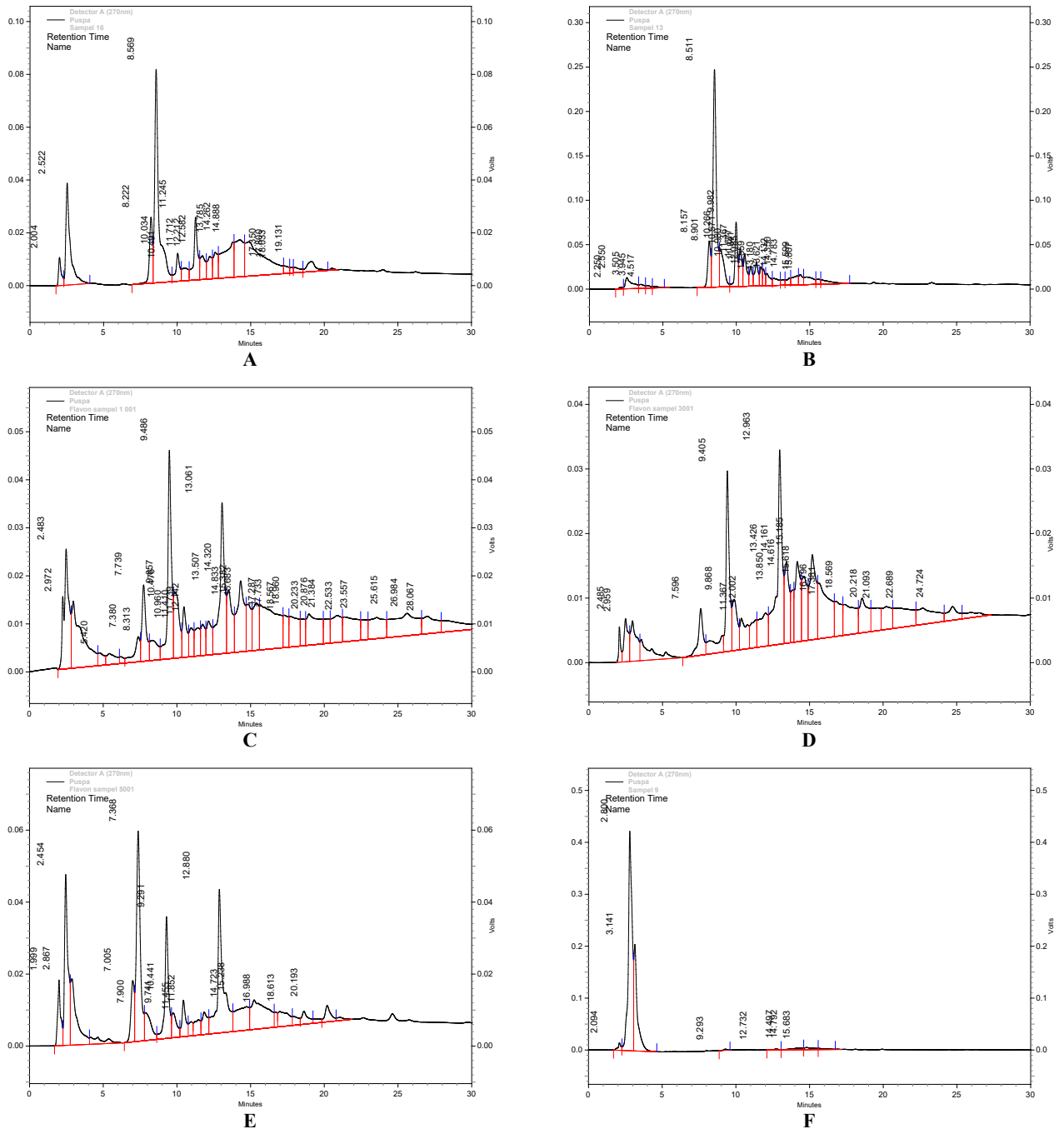

Figure 2. Representative HPLC chromatograms of flavonoid extracts from selected *Selaginella* species recorded at 270 nm. A. *S. ciliaris*, B. *S. aristata*, C. *S. opaca*, D. *S. intermedia*-01, E. *S. involvens*-01, F. *S. plana*

Across the dataset, several retention time regions were recurrently occupied by prominent peaks in multiple species, suggesting the presence of shared flavonoid-related components within the genus. At the same time, distinct peaks confined to one or a few species contributed to unique chromatographic signatures. Together, these patterns demonstrate that HPLC-based profiling effectively captures both shared and species-specific features of flavonoid composition in *Selaginella* and provides a qualitative foundation for subsequent RT-based fingerprint matrix construction and similarity analysis.

RT-based flavonoid fingerprint matrix

Alignment of HPLC chromatographic peaks across all *Selaginella* samples resulted in a discrete set of 11 RT-defined flavonoid features, representing chromatographic signals that are either shared among multiple species or restricted to particular taxa. Using a tolerance window of ±0.2 min, peaks eluting within the same RT interval were treated as equivalent features and compiled into a binary RT-based fingerprint matrix (Table 2). This matrix summarizes the qualitative presence-absence distribution of flavonoid-related peaks across all analyzed samples and

constitutes the primary dataset for subsequent similarity and clustering analyses.

As shown in Table 2, the RT-based fingerprint matrix reveals clear heterogeneity in flavonoid composition among *Selaginella* species. Several of the 11 RT features are detected in multiple species, indicating the occurrence of shared flavonoid components that may reflect conserved biosynthetic traits within the genus. In contrast, other RT features are present only in one or a few species, highlighting species-specific or low-frequency flavonoid constituents that contribute to distinct chromatographic signatures.

Conspecific samples collected from different localities, such as *Selaginella intermedia*-01 versus -02 and *S. involvens*-01 versus -02, exhibit partially overlapping RT profiles within the 11-feature matrix (Table 2). These samples share a set of core RT peaks while differing in the presence of auxiliary peaks, indicating intraspecific variability superimposed on broader interspecific differentiation. This pattern suggests that species-level flavonoid fingerprints are generally stable, with additional variation likely influenced by local environmental or microhabitat factors.

The RT-based fingerprint matrix comprising 11 aligned RT bins provides a standardized qualitative framework for evaluating similarities and differences in flavonoid profiles across *Selaginella* species. By explicitly resolving shared and unique RT features (Table 2), this matrix forms the analytical basis for similarity coefficient calculation and hierarchical clustering presented in subsequent sections.

Similarity matrix among *Selaginella* species

Pairwise similarity among all Selaginella samples was quantified using Sørensen and Jaccard coefficients derived from the RT-based binary fingerprint matrix. Both indices yielded comparable patterns of qualitative chemical relatedness; therefore, the Sørensen similarity matrix is presented as the primary result to represent overall similarity relationships among samples, while Jaccard values are used as complementary support in the interpretation (Table 3).

Similarity values spanned a broad range across sample pairs, indicating substantial heterogeneity in flavonoid fingerprint composition within the dataset. Conspecific samples collected from different localities, such as *S. intermedia*-01 versus -02 and *S. involvens*-01 versus -02, consistently exhibited moderate to high similarity values, reflecting the presence of shared core flavonoid features accompanied by additional variation at the individual level.

In contrast, comparisons among ecologically and geographically distinct samples generally resulted in lower similarity values, suggesting pronounced differentiation in overall flavonoid composition. Nevertheless, several sample pairs displayed relatively high similarity coefficients despite geographic separation, indicating the presence of chemical affinities that are not strictly structured by spatial proximity. Such patterns suggest that RT-based flavonoid fingerprints may capture chemotaxonomic signals that extend beyond local environmental variation.

Table 2. RT-based flavonoid fingerprint matrix across *Selaginella* species

Species	RT1 (2.05-2.25)	RT2 (2.45-2.60)	RT3 (7.25-7.40)	RT4 (8.45-8.55)	RT5 (9.90-10.05)	RT6 (11.30-11.45)	RT7 (12.25-12.35)	RT8 (13.45-13.55)	RT9 (14.30-14.40)	RT10 (14.75-14.85)	RT11 (15.60-15.75)
Selaginella opaca	1	1	1	0	1	1	0	1	1	1	1
S. remotifolia	0	1	0	0	1	0	1	1	0	1	1
S. intermedia-01	0	1	0	0	1	0	1	1	1	0	0
S. subalpina-01	1	1	1	0	1	0	1	0	1	1	0
S. involvens-01	1	1	0	0	1	0	0	0	0	1	0
S. wildenowii	1	1	0	0	1	0	0	0	1	1	0
S. mayeri	1	1	0	0	1	0	0	0	1	0	0
S. ornata	1	1	0	0	0	0	0	0	1	0	0
S. plana	1	0	0	0	0	0	0	0	0	0	0
S. frondosa	1	1	0	0	1	0	1	0	1	1	0
S. subalpina-02	1	1	0	1	0	1	1	0	1	1	0
S. intermedia-02	1	1	0	1	0	1	0	0	1	1	0
S. aristata	1	1	0	1	1	1	0	0	1	1	1
S. ciliaris	1	1	1	1	1	1	1	0	1	1	1
S. repanda	1	0	0	0	0	0	0	0	1	0	0
S. involvens-02	1	1	0	1	1	1	0	0	1	1	0
S. ketra-ayam	1	1	0	1	1	0	0	0	1	1	0
S. velutina	0	1	0	1	1	1	1	0	1	1	1
Selaginella sp. (Mt. Meja)	1	1	0	0	0	0	0	0	1	1	0
S. caudata	1	1	0	0	0	0	0	0	1	1	0

Note: Binary scores (1/0) indicate the presence or absence of a chromatographic peak within each RT bin for a given species, based on aligned HPLC chromatograms using a tolerance of ±0.2 min. RT3 corresponds to the retention time of the amentoflavone reference peak (~7.27 min) and was used as an alignment anchor. The matrix represents qualitative RT-based features and does not imply compound identity beyond the reference anchor

Table 3. Sørensen similarity matrix of RT-based flavonoid fingerprints among 20 *Selaginella* samples

Species	No.	1	2	3	4	5	6	7	8	9	10	11	12	13	14	15	16	17	18	19	20
Selaginella opaca	1	1.000	0.667	0.571	0.750	0.615	0.714	0.615	0.500	0.200	0.667	0.625	0.667	0.824	0.842	0.364	0.750	0.667	0.706	0.615	0.615
S. remotifolia	2	0.667	1.000	0.727	0.615	0.600	0.545	0.400	0.222	0.000	0.667	0.462	0.333	0.571	0.625	0.000	0.462	0.500	0.714	0.400	0.400
S. intermedia-01	3	0.571	0.727	1.000	0.667	0.444	0.600	0.667	0.500	0.000	0.727	0.500	0.364	0.462	0.533	0.286	0.500	0.545	0.615	0.444	0.444
S. subalpina-01	4	0.750	0.615	0.667	1.000	0.727	0.833	0.727	0.600	0.250	0.923	0.714	0.615	0.667	0.824	0.444	0.714	0.769	0.667	0.727	0.727
S. involvens-01	5	0.615	0.600	0.444	0.727	1.000	0.889	0.750	0.571	0.400	0.800	0.545	0.600	0.667	0.571	0.333	0.727	0.800	0.500	0.750	0.750
S. wildenowii	6	0.714	0.545	0.600	0.833	0.889	1.000	0.889	0.750	0.333	0.909	0.667	0.727	0.769	0.667	0.571	0.833	0.909	0.615	0.889	0.889
S. mayeri	7	0.615	0.400	0.667	0.727	0.750	0.889	1.000	0.857	0.400	0.800	0.545	0.600	0.667	0.571	0.667	0.727	0.800	0.500	0.750	0.750
S. ornata	8	0.500	0.222	0.500	0.600	0.571	0.750	0.857	1.000	0.500	0.667	0.600	0.667	0.545	0.462	0.800	0.600	0.667	0.364	0.857	0.857
S. plana	9	0.200	0.000	0.000	0.250	0.400	0.333	0.400	0.500	1.000	0.286	0.250	0.286	0.222	0.182	0.667	0.250	0.286	0.000	0.400	0.400
S. frondosa	10	0.667	0.667	0.727	0.923	0.800	0.909	0.800	0.667	0.286	1.000	0.769	0.667	0.714	0.750	0.500	0.769	0.833	0.714	0.800	0.800
S. subalpina-02	11	0.625	0.462	0.500	0.714	0.545	0.667	0.545	0.600	0.250	0.769	1.000	0.923	0.800	0.824	0.444	0.857	0.769	0.800	0.727	0.727
S. intermedia-02	12	0.667	0.333	0.364	0.615	0.600	0.727	0.600	0.667	0.286	0.667	0.923	1.000	0.857	0.750	0.500	0.923	0.833	0.714	0.800	0.800
S. aristata	13	0.824	0.571	0.462	0.667	0.667	0.769	0.667	0.545	0.222	0.714	0.800	0.857	1.000	0.889	0.400	0.933	0.857	0.875	0.667	0.667
S. ciliaris	14	0.842	0.625	0.533	0.824	0.571	0.667	0.571	0.462	0.182	0.750	0.824	0.750	0.889	1.000	0.333	0.824	0.750	0.889	0.571	0.571
S. repanda	15	0.364	0.000	0.286	0.444	0.333	0.571	0.667	0.800	0.667	0.500	0.444	0.500	0.400	0.333	1.000	0.444	0.500	0.200	0.667	0.667
S. involvens-02	16	0.750	0.462	0.500	0.714	0.727	0.833	0.727	0.600	0.250	0.769	0.857	0.923	0.933	0.824	0.444	1.000	0.923	0.800	0.727	0.727
S. ketra-ayam	17	0.667	0.500	0.545	0.769	0.800	0.909	0.800	0.667	0.286	0.833	0.769	0.833	0.857	0.750	0.500	0.923	1.000	0.714	0.800	0.800
S. velutina	18	0.706	0.714	0.615	0.667	0.500	0.615	0.500	0.364	0.000	0.714	0.800	0.714	0.875	0.889	0.200	0.800	0.714	1.000	0.500	0.500
Selaginella sp. (Mt. Meja)	19	0.615	0.400	0.444	0.727	0.750	0.889	0.750	0.857	0.400	0.800	0.727	0.800	0.667	0.571	0.667	0.727	0.800	0.500	1.000	1.000
S. caudata	20	0.615	0.400	0.444	0.727	0.750	0.889	0.750	0.857	0.400	0.800	0.727	0.800	0.667	0.571	0.667	0.727	0.800	0.500	1.000	1.000

Note: Similarity values were calculated using the Sørensen coefficient based on the RT-based presence–absence fingerprint matrix (Table 2). Numeric suffixes indicate distinct samples of the same species collected from different localities

Conversely, samples characterized by simplified RT profiles or a limited number of shared chromatographic features showed consistently low similarity values when compared with most other taxa. The Sørensen similarity matrix provides a quantitative foundation for evaluating qualitative chemical relationships among Selaginella samples and serves as the basis for subsequent hierarchical clustering analysis.

Cluster analysis of flavonoid fingerprints

Hierarchical cluster analysis was performed to visualize patterns of chemical relatedness among Selaginella samples based on the Sørensen similarity matrix derived from the RT-based flavonoid fingerprint data (Table 3). Clustering was conducted using the Unweighted Pair Group Method with Arithmetic mean (UPGMA), which is widely applied in chemotaxonomic and fingerprinting studies due to its interpretability and suitability for similarity-based datasets. The resulting clustering pattern is illustrated in Figure 3.

The dendrogram reveals several distinct clusters that reflect differences and affinities in flavonoid fingerprint composition among samples and species. Samples belonging to the same nominal species but collected from different localities, such as *S. intermedia*-01 and -02, as well as *S. involvens*-01 and -02, were consistently grouped within the same or closely adjacent clusters. This pattern indicates that core species-level flavonoid signatures are generally preserved at the individual level despite site-specific variation, supporting the robustness of RT-based fingerprinting for comparative analysis.

At a broader level, clusters comprised multiple species sharing relatively high similarity values, suggesting the presence of broad chemotypic affinities that are not strictly aligned with geographic origin. Several samples collected from different regions were positioned within the same major cluster, indicating that flavonoid composition may capture intrinsic biochemical traits that are not exclusively structured by spatial proximity. Conversely, samples characterized by simplified RT profiles or a limited number of shared peaks tended to form isolated branches, reflecting their distinct flavonoid fingerprints.

The clustering pattern provides an integrated visualization of qualitative chemical relationships among Selaginella samples, which can be interpreted at the species level when conspecific samples exhibit consistent grouping. When interpreted together with the RT-based fingerprint matrix and similarity analysis, the dendrogram highlights the potential of flavonoid fingerprinting to contribute to chemotaxonomic assessment and comparative phytochemical studies within the genus.

NMDS ordination of RT-based flavonoid fingerprints

The NMDS ordination based on the Sørensen dissimilarity matrix provided a low-dimensional visualization of similarity relationships among Selaginella samples derived from the RT-based flavonoid fingerprint matrix (Figure 4). The ordination was constructed using the full Sørensen dissimilarity matrix (Table 3), and the two-dimensional solution yielded a low stress value (Stress-1 ≈ 0.087), indicating that the ordination adequately represents the multivariate similarity structure of the dataset.

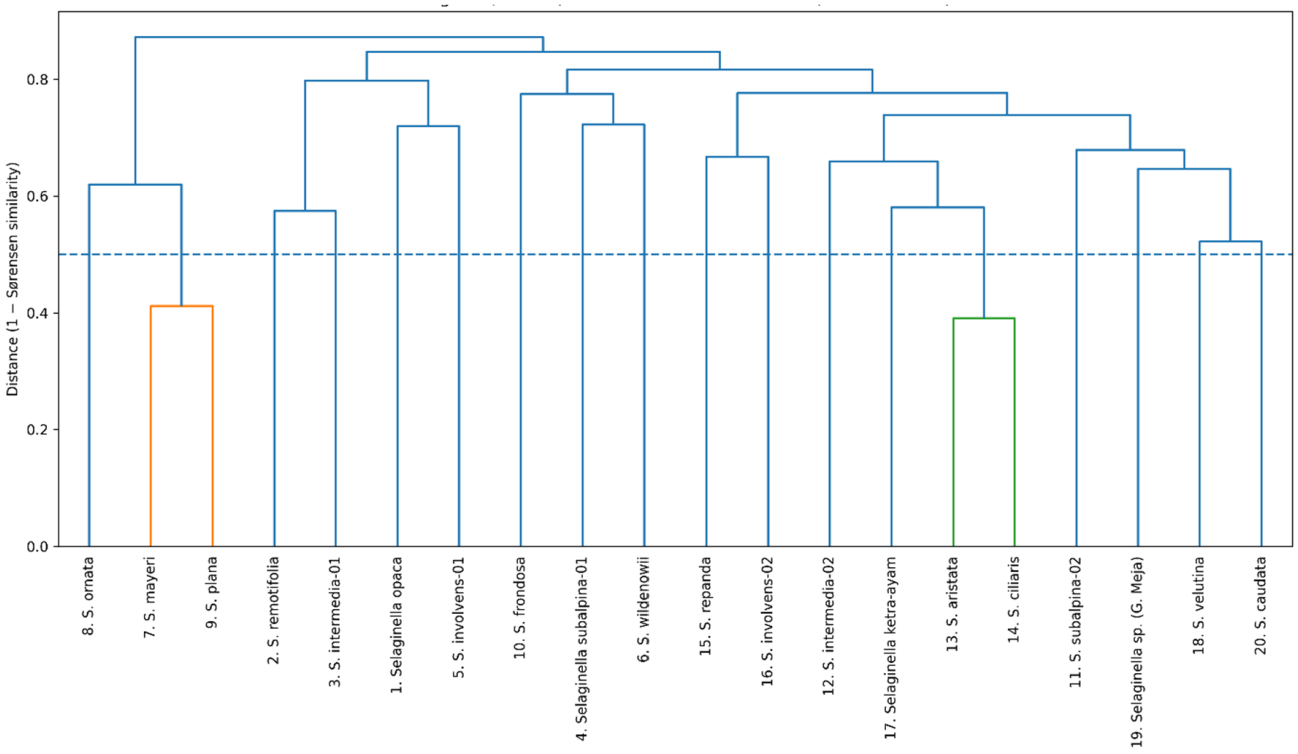

Figure 3. Dendrogram (UPGMA) showing hierarchical clustering of *Selaginella* species based on Sørensen similarity of RT-based flavonoid fingerprints (cut-off = 0.45)

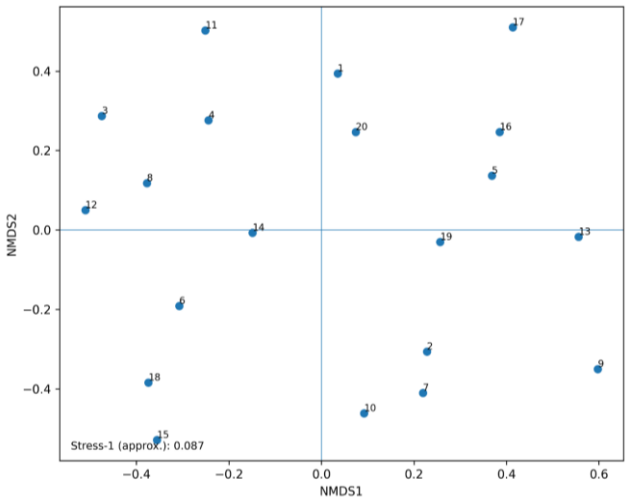

Figure 4. NMDS ordination of *Selaginella* samples based on Sørensen dissimilarity of RT-based flavonoid fingerprints (presence-absence matrix). Each point represents one sample (1-20), and inter-point distances reflect overall qualitative similarity in RT-defined features. The ordination is presented as an exploratory visualization complementary to hierarchical clustering. Stress-1 (approx.) = 0.087. Sample codes: 1. *S. opaca*, 2. *S. remotifolia*, 3. *S. intermedia*-01, 4. *S. subalpina*-01, 5. *S. involvens*-01, 6. *S. wildenowii*, 7. *S. mayeri*, 8. *S. ornata*, 9. *S. plana*, 10. *S. frondosa*, 11. *S. subalpina*-02, 12. *S. intermedia*-02, 13. *S. aristata*, 14. *S. ciliaris*, 15. *S. repanda*, 16. *S. involvens*-02, 17. *S. ketra-ayam*, 18. *S. velutina*, 19. *Selaginella* sp. (Mt. Meja), 20. *S. caudata*

Overall, samples that clustered closely in the UPGMA dendrogram also tended to occupy proximate positions in the NMDS ordination space. Conspecific samples collected from different localities showed partial overlap or close proximity, reflecting shared core flavonoid features with limited divergence. In contrast, samples characterized by simplified RT profiles tended to be positioned toward the periphery of the ordination, consistent with their lower similarity values observed in pairwise comparisons.

The NMDS ordination did not reveal a clear separation of samples based on geographic origin, supporting the inference that overall flavonoid fingerprint similarity is not primarily structured by spatial proximity. Instead, the ordination reflects broad qualitative chemical similarity among samples, in agreement with the clustering analysis, and is interpreted here as a complementary visualization rather than evidence of discrete chemotypic boundaries.

Summary of flavonoid fingerprint variation across *Selaginella* species

The integrated results of chromatographic profiling, RT-based fingerprint construction, similarity analysis, and hierarchical clustering collectively reveal structured patterns of qualitative flavonoid variation among the analyzed Selaginella samples. Visual comparison of chromatographic profiles demonstrated pronounced interspecific and inter-individual differences in peak distribution and overall profile complexity, indicating heterogeneous flavonoid compositions across the genus (Figure 2). These qualitative differences provided the empirical basis for subsequent RT alignment and comparative analysis.

The RT-based fingerprint matrix captures the distribution of aligned flavonoid-related peaks across all analyzed samples and highlights the coexistence of conserved and variable chemical features (Table 2). Several RT-defined peaks were consistently detected across multiple species, suggesting the presence of shared flavonoid components within Selaginella. In contrast, numerous peaks were restricted to a limited number of species or individual samples, contributing to distinct chromatographic signatures. This pattern reflects a dual structure of flavonoid diversity, comprising both genus-level conserved elements and species- or sample-specific differentiation.

Quantitative similarity analysis based on the Sørensen coefficient translated these qualitative patterns into measurable similarity relationships among samples (Table 3). Conspecific samples collected from different localities exhibited moderate to high similarity values, indicating that core flavonoid fingerprints are generally stable at the species level. At the same time, lower similarity values observed between ecologically or taxonomically distinct samples underscore pronounced divergence in overall flavonoid composition, reinforcing the discriminatory power of RT-based fingerprinting.

Hierarchical clustering analysis integrates these findings by providing a coherent visualization of chemical relatedness among *Selaginella* samples (Figure 3). The resulting dendrogram reveals clusters that group samples and species with similar flavonoid fingerprints, while also identifying chemically distinct taxa that form isolated branches. Importantly, these chemotypic groupings are not strictly aligned with geographic origin, suggesting that intrinsic biochemical characteristics play a substantial role in shaping flavonoid profiles.

The combined results demonstrate that RT-based HPLC fingerprinting provides a robust qualitative framework for assessing interspecific flavonoid diversity based on individual-level chemical data in Selaginella. Chromatographic profiles, fingerprint matrices, similarity indices, and clustering analysis consistently reveal patterns of shared and species-specific chemical variation, providing a basis for interpreting comparative chemotaxonomic patterns and exploratory ecological implications.

Discussion

Flavonoid fingerprinting as a tool for interspecific discrimination

The results of this study demonstrate that RT-based HPLC flavonoid fingerprinting provides an effective qualitative tool for discriminating among *Selaginella* species based on their secondary metabolite profiles. Distinct chromatographic patterns observed across species, as reflected in peak distribution, profile complexity, and similarity relationships, indicate that flavonoid fingerprints capture biologically meaningful variation at the interspecific level. This finding is consistent with previous phytochemical studies showing that flavonoid composition

often exhibits species-specific patterns linked to genetic background and evolutionary history (Markham 1988; Harborne and Williams 2000).

In vascular plants, flavonoids have long been recognized as valuable chemotaxonomic markers due to their structural diversity, relative stability, and taxonomic consistency (Harborne 1994; Harborne and Williams 2000). In pteridophytes, including *Selaginella*, flavonoids are among the most frequently reported secondary metabolites, yet their application for comparative and chemotaxonomic purposes has remained limited. Most existing studies on *Selaginella* flavonoids have focused on the isolation and structural elucidation of individual compounds or on targeted LC-MS screening of selected taxa (Cao et al. 2010; Zhao et al. 2013). While such approaches provide detailed chemical information, they are less suited for broad interspecific comparisons across multiple taxa.

The RT-based fingerprinting approach adopted in this study addresses this limitation by emphasizing holistic chromatographic patterns rather than individual compound identities. Similar fingerprinting strategies have been widely applied in medicinal plant authentication, species discrimination, and quality control, particularly when dealing with complex phytochemical mixtures (Gong et al. 2003; Liang et al. 2004; Xie et al. 2006). The present results align with these studies by showing that reproducible retention time patterns can be translated into binary matrices and similarity indices that effectively differentiate species based on overall chemical composition.

The moderate to high similarity values observed among conspecific samples collected from different localities further support the utility of flavonoid fingerprints for species-level discrimination. Such stability of core chromatographic features suggests that flavonoid profiles are largely governed by intrinsic biochemical and genetic factors, with environmental variation contributing secondary modifications. Comparable patterns have been reported in fingerprint-based studies of other plant groups, where interspecific variation exceeds intraspecific variability when standardized analytical protocols are applied (Zhao et al. 2006; Smillie and Khan 2010).

Importantly, the clustering patterns derived from similarity analysis reveal chemical affinities that are not strictly correlated with geographic proximity. This observation suggests that flavonoid fingerprinting may capture deeper chemotaxonomic signals reflecting shared evolutionary or biosynthetic traits among species, rather than merely environmental influences. Similar findings have been reported in chemotaxonomic studies of ferns and lycophytes, where flavonoid distribution patterns were found to complement morphological and molecular evidence (Wollenweber et al. 1998; Vetter 2018).

Taken together, these results highlight the value of RT-based HPLC flavonoid fingerprinting as a practical and informative approach for interspecific discrimination in *Selaginella*. By enabling comparative analysis across multiple species without reliance on full compound identification, this method provides a robust framework for exploring chemical diversity, supporting chemotaxonomic inference, and guiding the selection of taxa for further bioactivity-oriented phytochemical studies.

Chemotaxonomic implications of flavonoid variation in Selaginella

The observed patterns of flavonoid fingerprint variation among *Selaginella* species carry important implications for chemotaxonomic interpretation within the genus. The coexistence of shared and species-specific RT-defined peaks suggests that flavonoid composition reflects both conserved biochemical traits and lineage-specific differentiation. Such dual patterns are characteristic of secondary metabolite systems that are shaped by evolutionary constraints as well as diversification processes, making flavonoids particularly informative for chemotaxonomic assessment (Harborne 1994; Wink 2003).

In chemotaxonomy, the value of flavonoids lies not only in the presence of particular compounds but also in broader distributional patterns across taxa. In this study, several RT regions were consistently represented across multiple *Selaginella* species, indicating the presence of common flavonoid-related components at the genus level. These shared features may reflect conserved biosynthetic pathways that have been maintained throughout the evolutionary history of *Selaginella*, one of the earliest diverging lineages of vascular plants (Banks 2009; Weststrand and Korall 2016a, b). Comparable genus-level conservation of flavonoid patterns has been reported in ferns and other lycophytes, where flavonoid classes show phylogenetically structured distributions (Wollenweber et al. 1998; Vetter 2018).

At the same time, the occurrence of distinct RT peaks restricted to specific species or small species groups highlights the potential of flavonoid fingerprints to resolve finer-scale taxonomic relationships. Species-specific or narrowly distributed flavonoid features have long been recognized as valuable chemotaxonomic markers, particularly in groups where morphological differentiation is subtle or convergent (Wollenweber et al. 1998; Harborne and Williams 2000). In *Selaginella*, morphological plasticity and ecological adaptation often complicate species delimitation, suggesting that complementary chemical evidence may provide additional resolution when integrated with morphological and molecular data.

The clustering patterns observed in this study further support the chemotaxonomic relevance of flavonoid fingerprints. Species grouped within the same chemical clusters did not always share close geographic proximity, implying that chemical similarity is not merely a reflection of local environmental conditions. Instead, these groupings may correspond to shared evolutionary or biosynthetic traits, consistent with the view that secondary metabolite profiles can retain phylogenetic signals across broad spatial scales (Wink and Waterman 1999; Wink 2008). Similar chemotaxonomic clustering based on flavonoid profiles has been reported in fern genera and other plant groups, where chemical affinities complement phylogenetic reconstructions based on DNA sequence data (Zhao et al. 2006; Smillie and Khan 2010).

Nevertheless, it is important to recognize that chemotaxonomic interpretation based on fingerprinting approaches remains inherently qualitative. RT-based fingerprints capture overall compositional patterns but do not directly resolve compound identity or biosynthetic pathways. As such, the chemotaxonomic signals inferred here should be viewed as complementary rather than definitive. Integration with molecular phylogenetic frameworks and targeted structural identification of key flavonoid markers would further strengthen taxonomic inference in future studies (Wink and Waterman 1999; Xie et al. 2006; Burleigh et al. 2009).

The flavonoid fingerprint variation documented in this study supports the utility of secondary metabolite profiling as a chemotaxonomic tool in *Selaginella*. By revealing patterns of chemical similarity and differentiation that align imperfectly with geography, RT-based HPLC fingerprinting provides independent evidence of biochemical structuring within the genus. These findings reinforce the value of combining chemical, morphological, and molecular data to achieve a more comprehensive understanding of species relationships and evolutionary diversification in *Selaginella*.

Ecological and adaptive significance of flavonoid diversity in Selaginella

The observed diversity of flavonoid fingerprints among *Selaginella* species also carries important ecological and adaptive implications. Flavonoids are multifunctional secondary metabolites that play key roles in plant-environment interactions, including protection against ultraviolet radiation, oxidative stress, pathogens, and herbivores, as well as mediation of physiological responses to abiotic stress (Agati et al. 2012; Brunetti et al. 2013). In early-diverging vascular plants such as *Selaginella*, these functions may be particularly critical for survival across heterogeneous habitats.

The qualitative variation in flavonoid fingerprints documented in this study, reflected in differences in peak number, distribution, and species-specific features, suggests that adaptive responses to local environmental conditions may shape flavonoid composition. *Selaginella* species occupy a wide range of ecological settings, from shaded montane forests to open, seasonally dry, or disturbed habitats. Such environmental heterogeneity is likely to impose different selective pressures on secondary metabolite production, resulting in distinct flavonoid profiles optimized for specific ecological contexts (Winkel-Shirley 2002; Treutter 2005).

Conspecific samples collected from different localities exhibited broadly similar core flavonoid fingerprints, yet with additional variation in minor or low-frequency peaks. This pattern suggests that while fundamental flavonoid biosynthetic pathways are genetically conserved at the species level, fine-scale modulation of flavonoid expression may occur in response to microhabitat conditions such as light intensity, moisture availability, and temperature regimes. Similar patterns of environmentally modulated flavonoid variation have been reported in ferns and angiosperms, where stress-related flavonoids increase under high irradiance or nutrient limitation without altering the core metabolite profile (Close and McArthur 2002; Agati and Tattini 2010).

The lack of strict correspondence between chemical similarity and geographic proximity further indicates that spatial factors do not solely determine flavonoid diversity in *Selaginella*. Instead, adaptive convergence may occur among species occupying comparable ecological niches in different regions, leading to chemically similar flavonoid fingerprints despite geographic separation. Such convergence has been documented in other plant groups, where similar environmental pressures result in parallel secondary metabolite profiles across unrelated or distantly distributed taxa (Wink 2003; Lattanzio et al. 2006).

The flavonoid fingerprint variation observed in this study supports the view that flavonoids contribute to the ecological flexibility and adaptive capacity of *Selaginella*. While RT-based fingerprinting does not directly resolve functional mechanisms, the detected patterns provide indirect evidence that flavonoid diversity is linked to environmental adaptation. These findings underscore the importance of considering ecological context when interpreting phytochemical variation and highlight the potential of comparative flavonoid profiling for exploring adaptive strategies in early vascular plant lineages.

Methodological strengths and limitations of RT-based HPLC fingerprinting

RT-based HPLC fingerprinting offers several methodological advantages for comparative phytochemical studies, particularly when dealing with multiple species and complex metabolite mixtures such as those found in *Selaginella*. One of the principal strengths of this approach lies in its ability to capture holistic chemical profiles without requiring full structural identification of individual compounds. By focusing on reproducible retention time patterns, fingerprinting enables efficient interspecific comparison and pattern recognition across large datasets (Liang et al. 2004; Xie et al. 2006).

The standardized analytical conditions applied in this study, including consistent extraction procedures, chromatographic parameters, and retention time alignment thresholds, contributed to the reproducibility of the resulting fingerprints. The use of a binary presence-absence matrix further reduced the influence of peak intensity variability, which can be affected by extraction efficiency, sample handling, or detector sensitivity. As a result, the RT-based fingerprints provided a robust qualitative framework for similarity analysis and clustering, suitable for chemotaxonomic and comparative purposes (Gong et al. 2003).

The methodological robustness of RT alignment was further strengthened by the inclusion of an amentoflavone reference standard, which served as an external retention time anchor for biflavonoid-rich regions of the chromatogram. Although amentoflavone was not introduced as an internal standard into each extract, its reproducible elution under identical chromatographic conditions confirms the stability and comparability of retention time patterns across analytical runs. This external

calibration approach enhances confidence in RT-based fingerprint interpretation while remaining consistent with the qualitative objectives of chromatographic fingerprinting.

Another methodological strength of RT-based fingerprinting is its scalability. Compared with targeted compound identification using LC-MS or NMR, fingerprinting requires less analytical time and interpretative effort, making it particularly useful for preliminary screening of chemical diversity across multiple taxa. This characteristic is especially relevant for understudied groups such as lycophytes, where comprehensive phytochemical coverage across species remains limited (Xie et al. 2006).

Despite these advantages, several limitations of the RT-based fingerprinting approach must be acknowledged. Retention time alone does not provide direct information on compound identity, structural class, or biosynthetic origin. Consequently, different compounds with similar chromatographic behavior may contribute to the same RT-defined peak, potentially obscuring finer chemical distinctions. In addition, minor shifts in retention time can occur due to column aging or subtle changes in mobile phase composition, necessitating careful calibration and alignment procedures (Gong et al. 2003).

Furthermore, the qualitative nature of binary scoring precludes quantitative assessment of relative flavonoid abundance. While this approach is appropriate for interspecific discrimination and pattern recognition, it cannot address questions related to metabolite concentration, dominance, or dose-dependent bioactivity. Therefore, RT-based fingerprinting should be viewed as a complementary tool rather than a replacement for targeted quantitative or structural analyses (Xie et al. 2006).

RT-based HPLC fingerprinting represents a methodologically sound and efficient strategy for comparative analysis of flavonoid diversity in *Selaginella*. When combined with rigorous analytical standardization, external RT referencing, and cautious interpretation, this approach provides valuable insights into interspecific chemical variation while laying the groundwork for subsequent targeted phytochemical and bioactivity-oriented investigations.

The inclusion of NMDS ordination further supports the robustness of the similarity patterns derived from RT-based fingerprinting. NMDS was applied conservatively as a complementary visualization tool, and yielded ordination patterns broadly consistent with hierarchical clustering results, with a low stress value indicating an adequate two-dimensional representation of the qualitative similarity structure. Importantly, the absence of sharp group boundaries or strong gradients in the ordination space reinforces the qualitative nature of the dataset and cautions against overinterpretation of fine-scale chemical distances. In this context, NMDS serves to confirm general similarity relationships rather than to infer discrete chemotypes or environmental drivers, which would require quantitative metabolite data or targeted compound identification.

Comparison with previous phytochemical studies on Selaginella

Previous phytochemical investigations on *Selaginella* have substantially expanded knowledge of flavonoid diversity within the genus, particularly through the isolation and structural elucidation of individual compounds. Numerous studies have reported biflavonoids, flavones, and related phenolic compounds from selected *Selaginella* species, often emphasizing their pharmacological potential, such as antioxidant, anti-inflammatory, and cytotoxic activities (Lin et al. 2000; Cao et al. 2010; Zhao et al. 2013; Shim et al. 2018). While these studies provide detailed chemical characterization, their scope has generally been limited to one or a few species and has rarely addressed comparative patterns across multiple taxa.

Targeted LC-MS-based studies have further contributed to flavonoid identification in *Selaginella* by enabling the detection of known compounds and their derivatives in complex extracts (Zhang et al. 2013; Yao et al. 2017; Křížkovská et al. 2021). However, such approaches typically rely on predefined metabolite classes and reference standards, which limit their applicability for holistic chemical comparison among diverse species (Dunn et al. 2013; Wolfender et al. 2013). Consequently, interspecific chemical relationships and broader patterns of flavonoid distribution within *Selaginella* remain insufficiently explored in the existing literature.

In contrast to these compound-centered approaches, the present study adopts a fingerprint-based strategy that emphasizes overall chromatographic patterns rather than individual metabolite identities. This methodological shift allows direct comparison of flavonoid profiles across a wider set of *Selaginella* species under standardized analytical conditions. By constructing an RT-based fingerprint matrix and applying similarity and clustering analyses, this study provides a comparative framework that complements earlier phytochemical reports and addresses a gap in genus-wide chemical assessment, consistent with established chromatographic fingerprinting approaches (Liang et al. 2004; Xie et al. 2006).

Comparative fingerprinting approaches have been successfully applied in other plant groups, particularly in medicinal plants and ferns, where they have proven effective for species discrimination, chemotaxonomic inference, and preliminary screening of chemical diversity (Liang et al. 2004; Zhao et al. 2006; Smillie and Khan 2010). The present results demonstrate that similar strategies are equally applicable to *Selaginella*, a lineage that has received relatively limited attention from a comparative phytochemical perspective.

The findings of this study do not contradict previous reports on flavonoid composition in *Selaginella*, but rather contextualize them within a broader comparative framework. Species previously reported to contain diverse flavonoid classes also tend to exhibit complex chromatographic fingerprints, while species with fewer documented compounds often show simpler profiles. This correspondence suggests that RT-based fingerprinting captures meaningful chemical signals consistent with

existing phytochemical knowledge, while extending it to a multi-species comparative scale (Harborne and Williams 2000; Xie et al. 2006).

This study complements earlier phytochemical investigations by shifting the analytical focus from isolated compounds to comparative flavonoid patterns across species. In doing so, it provides a foundation for integrating fingerprint-based screening with targeted structural and bioactivity studies, thereby advancing a more comprehensive understanding of flavonoid diversity and its taxonomic, ecological, and applied significance within *Selaginella*.

In conclusion, this study demonstrates that RT-based HPLC flavonoid fingerprinting provides a robust qualitative framework for comparing flavonoid profiles across *Selaginella* species. Analysis of 20 samples yielded a binary fingerprint matrix comprising 11 aligned RT-defined features generated using a retention time tolerance of ±0.2 min. Chromatographic profiles exhibited pronounced interspecific variation, while conspecific samples from different localities showed moderate to high similarity, indicating the presence of stable species-level core flavonoid signatures. Similarity and clustering analyses, supported by complementary NMDS ordination, further revealed broader chemical affinities that are not strictly associated with geographic origin, suggesting that flavonoid composition reflects intrinsic biochemical traits shaped by evolutionary history, with additional modulation by local environmental conditions. Although RT-based fingerprinting does not resolve compound identity, structural variation, or metabolite abundance, it effectively captures holistic chemical patterns and supports comparative and chemotaxonomic assessment. As a qualitative screening approach, it provides a practical foundation for future studies integrating LC-MS/MS dereplication, quantitative profiling, and molecular phylogenetic analyses to clarify the biosynthetic, functional, and evolutionary significance of flavonoid diversity in *Selaginella*.

ACKNOWLEDGEMENTS

The authors thank all field assistants and local collaborators who supported plant collection and documentation. We also acknowledge colleagues and staff of herbarium and laboratory facilities for their assistance and technical support in specimen curation and chromatographic analysis. Several analytical components of this study, including reference materials and access to instrumentation, were made possible through academic collaboration. This work was conducted as part of an academic research activity and did not involve a dedicated research grant allocated specifically for this study.

REFERENCES

Agati G, Azzarello E, Pollastri S, Tattini M. 2012. Flavonoids as antioxidants in plants: Location and functional significance. Plant Sci 196: 67-76. DOI: 10.1016/j.plantsci.2012.07.014.

Agati G, Tattini M. 2010. Multiple functional roles of flavonoids in photoprotection. New Phytol 186 (4): 786-793. DOI: 10.1111/j.1469-8137.2010.03269.x.

Allard PM, Péresse T, Bisson J, Gindro K, Marcourt L, Pham VC, Roussi F, Litaudon M, Wolfender JL. 2016. Integration of molecular networking and in-silico MS/MS fragmentation for natural products dereplication. Anal Chem 88 (6): 3317-3323. DOI: 10.1021/acs.analchem.5b04804.

Almeida JR, Sá P, Macedo L, Siqueira Filho J, Oliveira V, Barbosa Filho J. 2013. Phytochemistry of the genus *Selaginella* (Selaginellaceae). J Med Plant Res 7: 1858-1866. DOI: 10.5897/JMPR12.1223

Alston AHG. 1934. The genus *Selaginella* in the Malay Peninsula. Gard Bull Strait Settl 8: 41-62.

Alston AHG. 1935a. The *Selaginella* of the Malay Islands: I. Java and the Lesser Sunda Islands. Bull Jard Bot Buitenzorg 3 (13): 432-442.

Alston AHG. 1935b. The Philippine species of *Selaginella*. Philippines J Sci 58: 359-383.

Alston AHG. 1937. The *Selaginella* of the Malay Islands: II. Sumatra. Bull Jard Bot Buitenzorg 3 (14): 175-186.

Alston AHG. 1940. The *Selaginella* of the Malay Islands: III. Celebes and the Maluku. Bull Jard Bot Buitenzorg 3 (16): 343-350.

Alves RR, Rosa IM. 2007. Biodiversity, traditional medicine, and public health: Where do they meet? J Ethnobiol Ethnomed 3: 14. DOI: 10.1186/1746-4269-3-14.

Azmir J, Zaidul ISM, Rahman MM, Sharif KM, Mohamed A, Sahena F, Jahurul MHA, Ghafoor K, Norulaini NAN, Omar AKM. 2013. Techniques for extraction of bioactive compounds from plant materials: A review. J Food Eng 117 (4): 426-436. DOI: 10.1016/j.jfoodeng.2013.01.014.

Banks JA, Nishiyama T, Hasebe M, et al. 2011. The *Selaginella* genome identifies genetic changes associated with the evolution of vascular plants. Science 332 (6032): 960-963. DOI: 10.1126/science.1203810.

Banks JA. 2009. *Selaginella* and 400 million years of separation. Ann Rev Plant Biol 60: 223-238. DOI: 10.1146/annurev.arplant.59.032607.092851.

Brunetti C, Di Ferdinando M, Fini A, Pollastri S, Tattini M. 2013. Flavonoids as antioxidants and developmental regulators: Relative significance in plants and humans. Intl J Mol Sci 14 (2): 3540-3555. DOI: 10.3390/ijms14023540.

Burleigh JG, Hilu KW, Soltis DE. 2009. Inferring phylogenies with incomplete data sets: A 5-gene, 567-taxon analysis of angiosperms. BMC Evol Biol 9: 61. DOI: 10.1186/1471-2148-9-61.

Cao Y, Tan NH, Chen JJ, Zeng GZ, Ma YB, Wu YP, Yan H, Yang J, Lu LF, Wang Q. 2010. Bioactive flavones and biflavones from *Selaginella moellendorffii* Hieron. Fitoterapia 81 (4): 253-258. DOI: 10.1016/j.fitote.2009.09.007.

Chang HM, Chiou WL, Wang JC. 2012. Flora of Taiwan: Selaginellaceae. Endemic Species Research Institute, Nantou, Taiwan.

Chikmawati T, Setyawan AD, Miftahudin M. 2012. Phytochemical composition of *Selaginella* spp. from Java Island, Indonesia. Makara J Sci 16 (2): 121-128. DOI: 10.7454/mss.v16i2.1408.

Close DC, McArthur C. 2002. Rethinking the role of many plant phenolics: Protection from photodamage, not herbivores? Oikos 99 (1): 166-172. DOI: 10.1034/j.1600-0706.2002.990117.x.

D'Orazio G, Asensio-Ramos M, Fanali C, Hernández-Borges J, Fanali S. 2016. Capillary electrochromatography in food analysis. TrAC Trends Anal Chem 82: 250-267. DOI: 10.1016/j.trac.2016.06.012.

Dai J, Mumper RJ. 2010. Plant phenolics: Extraction, analysis, and their antioxidant and anticancer properties. Molecules 15 (10): 7313-7352. DOI: 10.3390/molecules15107313.

Dunn WB, Erban A, Weber RJM et al. 2013. Mass appeal: Metabolite identification in mass spectrometry-focused untargeted metabolomics. Metabolomics 9 (Suppl 1): 44-66. DOI: 10.1007/s11306-012-0434-4.

Everitt BS, Landau S, Leese M, Stahl D. 2011. Cluster Analysis. 5th ed. Wiley Series in Probability and Statistics, Wiley, Chichester. DOI: 10.1002/9780470977811.

Gershenzon J. 1984. Changes in the levels of plant secondary metabolites under water and nutrient stress. In: Timmermann BN, Steelink C, Loewus FA (eds). Phytochemical Adaptations to Stress. Recent Advances in Phytochemistry, Vol. 18. Springer, Boston. DOI: 10.1007/978-1-4684-1206-2_10.

Gong F, Liang YZ, Xie PS, Chau FT. 2003. Information theory applied to the chromatographic fingerprint of herbal medicine for quality control. J Chromatogr A 1002 (1-2): 25-40. DOI: 10.1016/S0021-9673(03)00648-4.

Goodarzi M, Russell PJ, Vander Heyden Y. 2013. Similarity analyses of chromatographic herbal fingerprints: A review. Anal Chim Acta 804: 16-28. DOI: 10.1016/j.aca.2013.09.017.

Harborne JB, Williams CA. 2000. Advances in flavonoid research since 1992. Phytochemistry 55 (6): 481-504. DOI: 10.1016/S0031-9422(00)00235-1.

Harborne JB. 1994. The Flavonoids: Advances in Research Since 1986. Chapman and Hall, London. DOI: 10.1007/978-1-4899-2911-2.

Hijmans RJ, Cameron SE, Parra JL, Jones PG, Jarvis A. 2005. Very high resolution interpolated climate surfaces for global land areas. Int J Climatol 25 (15): 1965-1978. DOI: 10.1002/joc.1276.

Hudson A, Smith P, Gori B, Sharrock S. 2021. Botanic garden collections—An under-utilised resource. Am J Plant Sci 12 (9): 1291-1305. DOI: 10.4236/ajps.2021.129101.

Jaccard P. 1901. Étude comparative de la distribution florale dans une portion des Alpes et du Jura. Bull Soc Vaudoise Sci Nat 37: 547-579.

Jermy AC. 1990. Selaginellaceae. In: Kramer KU, Green PS (eds). The Families and Genera of Vascular Plants, Vol. 1. Springer, Berlin.

Kim HK, Choi YH, Verpoorte R. 2010. NMR-based metabolomic analysis of plants. Nat Protoc 5 (3): 536-549. DOI: 10.1038/nprot.2009.237.

Křížkovská B, Kumar R, Řehořová K, Sýkora D, Dobiasová S, Kučerová D, Tan MC, Linis V, Oyong G, Ruml T, Lipov J, Viktorová J. 2021. Comparison of chemical composition and biological activities of eight *Selaginella* species. Pharmaceuticals 14 (1): 16. DOI: 10.3390/ph14010016.

Lattanzio V, Lattanzio VMT, Cardinali A. 2006. Role of phenolics in the resistance mechanisms of plants against fungal pathogens and insects. In: Imperato F (eds). Phytochemistry: Advances in Research. Research Signpost, Trivandrum, India.

Legendre P, Legendre L. 2012. Numerical Ecology. 3rd ed. Developments in Environmental Modelling. Elsevier, Amsterdam.

Li ZJ, Tan BC. 2005. A review of the species diversity of *Selaginella* in Fujian Province of China. Acta Phytotax Sin 43 (1): 50-59. DOI: 10.1360/aps040081.

Liang YZ, Xie P, Chan K. 2004. Quality control of herbal medicines. J Chromatogr B 812 (1-2): 53-70. DOI: 10.1016/j.jchromb.2004.08.041.

Lin LC, Kuo YC, Chou CJ. 2020. Cytotoxic biflavonoids from *Selaginella delicatula.* J Nat Prod 63 (5): 627-630. DOI: 10.1021/np990538m.

Markham KR. 1988. Distribution of flavonoids in the lower plants and its evolutionary significance. In: Harborne JB (eds). The Flavonoids: Advances in Research Since 1980. Academic Press, New York. DOI: 10.1007/978-1-4899-2913-6_12.

Mierziak J, Kostyn K, Kulma A. 2014. Flavonoids as important molecules of plant interactions with the environment. Molecules 19 (10): 16240-16265. DOI: 10.3390/molecules191016240.

Muema FW, Liu Y, Zhang Y, Chen G, Guo M. 2022. Flavonoids from *Selaginella doederleinii* Hieron and their antioxidant and antiproliferative activities. Antioxidants 11 (6): 1189. DOI: 10.3390/antiox11061189.

Setyawan AD, Sutarno S, Sugiyarto S. 2013. Species diversity of *Selaginella* in Mount Lawu, Java, Indonesia. Biodiversitas 14 (1): 1-9. DOI: 10.13057/biodiv/d140101.

Setyawan AD. 2011. Review: Recent status of *Selaginella* (Selaginellaceae) research in Nusantara. Biodiversitas 12: 151-158. DOI: 10.13057/biodiv/d120209.

Setyawan AD. 2012. Altitudinal distribution of *Selaginella* in southern Central Java, Indonesia. Proc Soc Indones Biodivers Intl Conf 1: 153-157.

Shehzadi F, Shoaib M, Munir S, Abdi G. 2025. Ultrasound-assisted extraction of bioactive compounds from pomegranate peel and seed: A comprehensive review of key parameters and optimization strategies. Ultrason Sonochem 124: 107722. DOI: 10.1016/j.ultsonch.2025.107722.

Shim SY, Lee SG, Lee M. 2018. Biflavonoids isolated from *Selaginella tamariscina* and their anti-inflammatory activities via ERK1/2 signaling. Molecules 23 (4): 926. DOI: 10.3390/molecules23040926.

Smillie TJ, Khan IA. 2010. A comprehensive approach to identifying and authenticating botanical products. Clin Pharmacol Ther 87 (2): 175-186. DOI: 10.1038/clpt.2009.287.

Snyder LR, Kirkland JJ, Dolan JW. 2010. Introduction to modern liquid chromatography. Wiley, Hoboken. DOI: 10.1002/9780470508183.

Sørensen T. 1948. A method of establishing groups of equal amplitude in plant sociology based on similarity of species content and its application to analyses of the vegetation on Danish commons. Biol Skr Dan Vid Selsk 5: 1-34.

Stalikas CD. 2007. Extraction, separation, and detection methods for phenolic acids and flavonoids. J Sep Sci 30 (18): 3268-3295. DOI: 10.1002/jssc.200700261.

Tistaert C, Dejaegher B, Vander Heyden Y. 2011. Chromatographic separation techniques and data handling methods for herbal fingerprints: A review. Anal Chim Acta 690 (2): 148-161. DOI: 10.1016/j.aca.2011.02.023.

Treutter D. 2005. Significance of flavonoids in plant resistance and enhancement of their biosynthesis. Plant Biol 7 (6): 581-591. DOI: 10.1055/s-2005-873009.

Tsai JL, Shieh WC. 1994. Selaginellaceae. In: Huang TC (eds). Flora of Taiwan, Vol. 1. 2nd ed. Department of Botany, National Taiwan University, Taipei.

Vetter J. 2018. Secondary metabolites of ferns. In: Fernández H (eds). Current Advances in Fern Research. Springer, Cham. DOI: 10.1007/978-3-319-75103-0_15.

Weststrand S, Korall P. 2016a. Phylogeny of Selaginellaceae: There is value in morphology after all. Am J Bot 103 (12): 2136-2159. DOI: 10.3732/ajb.1600156.

Weststrand S, Korall P. 2016b. A subgeneric classification of *Selaginella* (Selaginellaceae). Am J Bot 103 (12): 2160-2169. DOI: 10.3732/ajb.1600288.

Wink M, Waterman P. 1999. Chemotaxonomy in relation to molecular phylogeny of plants. In: Wink M (eds). Biochemistry of Plant Secondary Metabolism. Annual Plant Reviews, Vol. 2. Sheffield Academic Press, Sheffield. DOI: 10.1177/1934578X0800300801.

Wink M. 2003. Evolution of secondary metabolites from an ecological and molecular phylogenetic perspective. Phytochemistry 64 (1): 3-19. DOI: 10.1016/S0031-9422(03)00300-5.

Wink M. 2008. Plant secondary metabolism: Diversity, function, and its evolution. Nat Prod Commun 3: 1205-1216.

Winkel-Shirley B. 2002. Biosynthesis of flavonoids and effects of stress. Curr Opin Plant Biol 5 (3): 218-223. DOI: 10.1016/S1369-5266(02)00256-X.

Wolfender JL, Ndjoko K, Hostettmann K. 2003. Liquid chromatography with ultraviolet absorbance-mass spectrometric detection and with nuclear magnetic resonance spectroscopy: A powerful combination for the on-line structural investigation of plant metabolites. J Chromatogr A 1000(1-2): 437-455. DOI: 10.1016/S0021-9673(03)00303-0.

Wollenweber E, Dörr M, Mues R. 1998. Flavonoids and other phenolics in ferns: Distribution and chemotaxonomic significance. Biochem Syst Ecol 26 (7): 735-750. DOI: 10.1016/S0305-1978(98)00043-2

Wong KM. 1982. Critical observations on Peninsular Malaysian *Selaginella*. Gard Bull Sing 35(2): 107-135.

Wong KM. 2010. Selaginellaceae. In: Parris BS, Kiew R, Chung RKC, Saw LG, Soepadmo E (eds). Flora of Peninsular Malaysia, Series 1. Ferns and Lycophytes. Malayan Forest Records No. 48. FRIM, Kepong.

Xie P, Chen S, Liang YZ, Wang X, Tian R, Upton R. 2006. Chromatographic fingerprint analysis—a rational approach for quality assessment of traditional Chinese herbal medicine. J Chromatogr A 1112 (1-2): 171-180. DOI: 10.1016/j.chroma.2005.12.091.

Yao H, Chen B, Zhang Y, Ou H, Li Y, Li S, Shi P, Shi S, Lin X. 2017. Analysis of the total biflavonoids extract from *Selaginella doederleinii* by HPLC-QTOF-MS and its in vitro and in vivo anticancer effects. Molecules 22 (2): 325. DOI: 10.3390/molecules22020325.

Zhang XC, Nooteboom HP, Kato M. 2013. Selaginellaceae. In: Wu ZY, Raven PH, Hong DY (eds). Flora of China, Vol. 2-3 (Pteridophytes). Science Press, Beijing and Missouri Botanical Garden Press, St. Louis.

Zhao Q, Wang CX, Li YL, Liu CY, Rong YH. 2013. Chemical constituents from *Selaginella doederleinii* and their bioactivities. Chinese Traditional and Herbal Drugs 44 (23): 3270-3275. DOI: 10.7501/j.issn.0253-2670.2013.23.004.

Zhao Z, Hu Y, Liang Z, Yuen JP, Jiang Z, Leung KS. 2006. Authentication is fundamental for the standardization of Chinese medicines. Planta Med 72 (10): 865-874. DOI: 10.1055/s-2006-947209.

Zheng XK, Li KK, Feng WS. 2012. Advances in the research of chemical constituents in the genus *Selaginella*. Chin J New Drugs 21: 124-133.

ASIAN J NAT PROD BIOCHEM
Volume 23, Number 2, December 2025
Pages: 146-152

P-ISSN: 2775-4189
E-ISSN: 2775-4197
DOI: 10.13057/biofar/f230206

Rosemary-loaded nanolipid carriers for multifunctional antioxidant, anti-inflammatory, and antifungal therapy enhancement

SADHANA PADMANABHAN, BOOPATHI PRIYA DHARSHINI, SURESH VASUGI, ELANGOVAN DILIPAN♥
Marine Genomics and Proteomics Lab, Department of Physiology, Saveetha Dental College and Hospitals, Saveetha Institute of Medical and Technical Sciences, Saveetha University. Chennai 600077, Tamil Nadu, India. Tel.: +91-44-2680-1050, +91-44-2680-0892, Ext. 9772,
♥email: gerberadilip@gmail.com

Manuscript received: 30 August 2025. Revision accepted: 20 December 2025.

Abstract. *Padmanabhan S, Dharshini BP, Vasugi S, Dilipan E. 2025. Rosemary-loaded nanolipid carriers for multifunctional antioxidant, anti-inflammatory, and antifungal therapy enhancement. Asian J Nat Prod Biochem 23: 146-152.* We developed and characterized rosemary-loaded Nanostructured Lipid Carriers (NLCs) and evaluated their multifunctional bioactivity. Rosemary extract (Soxhlet, 80% methanol) was incorporated into a lipid matrix via a microemulsion route. Physicochemical analyses confirmed successful encapsulation and stability: X-ray diffraction showed a semi-crystalline/disordered matrix consistent with efficient loading, and FTIR revealed characteristic bands (O–H, C–H, C=O/C–O–C) indicating compatible interactions between extract and lipids. In vitro bioassays demonstrated strong, concentration-dependent effects. Anti-inflammatory activity (protein-denaturation model) rose from 44% inhibition at 50 µg to 94% at 200 µg. Antioxidant capacity (DPPH) increased from 52.32% at 50 µg to 89.47% at 200 µg. Antifungal testing against *Candida albicans* showed dose-dependent zones of inhibition, with maximal effects at the highest tested volume (100 µL). Collectively, these data indicate that NLC encapsulation enhances the functional performance of rosemary bioactive across complementary therapeutic axes anti-inflammatory, antioxidant, and antifungal while maintaining structural integrity of the carrier system. The eco-friendly formulation strategy, relying on biocompatible lipids and surfactants, supports improved bioavailability and stability and is well-suited for translation to topical wound care, infection control, and targeted drug-delivery applications. Future work will optimize particle attributes and release kinetics and benchmark efficacy against standard comparators in relevant preclinical models.

Keywords: Bioactive compounds, drug delivery system, lipid-based nanocarriers, rosemary extract, therapeutic potential

INTRODUCTION

A Nanostructured Lipid Carrier (NLC) is a solid matrix–based drug delivery system at room temperature, composed of physiological, biodegradable, and biocompatible lipids with surfactants. Approved by regulatory bodies for various drug delivery modalities, NLCs are considered a superior alternative to Solid Lipid Nanoparticles (SLNs) because the inclusion of liquid oil droplets within the solid matrix increases drug loading capacity and minimizes drug mobility. Compared with polymeric nanoparticles, NLCs offer distinct advantages such as reduced toxicity, biodegradability, drug protection, controlled release, and solvent-free production. They have been extensively explored for delivering both hydrophilic and hydrophobic compounds (Iqbal et al. 2012) and are regarded as highly promising solubilizing systems (Chinsriwongkul et al. 2012). Key therapeutic benefits include enhanced solubility, improved stability, higher permeability and bioavailability, reduced side effects, prolonged half-life, and targeted tissue distribution (Fang et al. 2013; Afeeza et al. 2025).

Several preparation methods have been established, with solvent diffusion and hot high-pressure homogenization (≥80°C) being the most effective for scalable synthesis (Selvamuthukumar and Velmurugan 2012). Stability during storage remains critical to ensure chemical, physical, and microbiological integrity (Obeidat et al. 2010). The nanoscale size and lipid matrix also allow NLCs to penetrate biological barriers, including the brain, offering controlled release, high drug loading, biocompatibility, and scalability (Agrawal et al. 2020). Their clinical utility has been demonstrated in wound healing, where reduced particle size, enhanced solubility, and prolonged release improve therapeutic efficacy and sustain dosing at the wound site (Wathoni et al. 2024). By modulating lipid composition, NLCs can maintain their solid state while incorporating both solid and liquid lipids, ensuring effective drug immobilization and preventing particle agglomeration (Jaiswal et al. 2016). Beyond conventional therapy, NLCs have gained attention in cancer treatment due to their precision delivery and reduced side effects (Naseem et al. 2024), as well as in nutraceuticals to improve the stability and distribution of antioxidants (Gunawan and Boonkanokwong 2024).

Plant-derived bioactive compounds are increasingly explored as alternatives or complements to synthetic drugs due to their broad pharmacological activities and relatively low side-effect profiles. However, many phytochemicals suffer from poor aqueous solubility, low chemical stability, and limited bioavailability, which restrict their clinical translation (Aziz et al. 2021). Nanoencapsulation using lipid-based carriers such as NLCs has proven effective in addressing these limitations by shielding bioactives from

degradation, improving solubilization, and enabling sustained release (Lacatusu et al. 2010; Soleimanifard et al. 2019).

Rosemary (*Rosmarinus officinalis* L., Lamiaceae) is a medicinal plant rich in flavonoids, recognized for its broad-spectrum bioactivities including antioxidant, antibacterial, and antitumoral effects (Lacatusu et al. 2010). Widely used as a food additive in Europe, America, and Asia, rosemary possesses therapeutic potential against infections, diabetes, obesity, and cancer (Khatoon et al. 2020), and has been studied for dermatological applications such as preventing age-related skin damage (Montenegro et al. 2017). It is also applied as a natural preservative in food systems, reducing oxidative spoilage (Kaur et al. 2024), and exhibits antifungal, anti-aflatoxigenic, and herbicidal activities (Hendel et al. 2024).

Inflammation and oxidative stress are closely interrelated pathological processes implicated in the progression of chronic diseases, infections, and tissue damage (Afeeza et al. 2025). Protein denaturation is a widely accepted in vitro model for assessing anti-inflammatory activity, while the DPPH radical scavenging assay remains a standard method for evaluating antioxidant potential (Aksoy et al. 2013; Gunathilake et al. 2018). Furthermore, fungal infections caused by *Candida albicans* pose a significant clinical challenge, particularly due to rising antifungal resistance and limited efficacy of existing therapies (Ross et al. 2008). Plant-based antifungal agents delivered through nanocarrier systems represent a promising alternative approach to address these challenges.

In this context, the present study aims to develop rosemary extract-loaded nanostructured lipid carriers using an eco-friendly microemulsion technique and to evaluate their multifunctional biological activities. Structural characterization of the formulated NLCs was performed using X-Ray Diffraction (XRD) and Fourier-Transform Infrared Spectroscopy (FTIR) to confirm successful encapsulation and molecular interactions. The anti-inflammatory, antioxidant, and antifungal properties of the rosemary-loaded NLCs were systematically investigated through in vitro assays. This study seeks to establish rosemary-loaded NLCs as a promising nanotechnology-based platform for enhanced therapeutic applications in inflammation control, oxidative stress management, and antifungal therapy.

MATERIALS AND METHODS

Collection of samples

The Rosemary plant (*R. officinalis*) was collected from Salem District, Tamil Nadu, India and transported to laboratory. After being washed well the plant material was shade dried for 10-16 days. In shade drying, the sample was dried in air at normal room temperature without sunlight to avoid abiotic stress. After drying, the plant material was continuously monitored and maintained to prevent unwanted things and moisture content.

Preparation of extraction

Approximately 10 grams of powdered rosemary were accurately weighed and placed into a Soxhlet extraction thimble. The round-bottom flask of the Soxhlet apparatus was filled with 80% methanol as the extraction solvent for 4 hrs at 80°C. Following the extraction process, the resulting solution was filtered through Whatman No. 1 filter paper to eliminate insoluble plant debris and particulate matter. The concentrated extract was subsequently transferred to a clean, sterile vial, and stored at 4°C for storage prior to further analysis.

Synthesis of Nanostructured Lipid Carriers (NLCs)

Nanostructured Lipid Carriers (NLCs) were synthesized utilizing the microemulsion method. Initially, a Tris buffer solution (pH 6.8) was prepared, to which a few drops of coconut oil and 16 mg of beeswax were added to 10 mL of the buffer. The mixture was heated to 70°C with continuous stirring until the beeswax completely melted, resulting in a uniform lipid phase. Concurrently, in a separate beaker, 100 mg of Polyvinyl Alcohol (PVA) was dissolved in 10 mL of Tris buffer, and 0.5% w/v Sodium Dodecyl Sulfate (SDS) was incorporated, stirring until fully dissolved. The lipid phase was subsequently and gradually introduced into the aqueous phase while maintaining continuous stirring at 70°C for two hours, ensuring the formation of a stable emulsion. Following this, 100 mg of rosemary extract was introduced to the emulsion, and thorough mixing was conducted to ensure the even distribution of the bioactive compounds. The emulsion was then allowed to cool to room temperature and was stored at -20°C overnight to stabilize the NLCs. After 24 hours, the container was transferred to -80°C for additional freezing, ensuring complete solidification of the lipid particles. Ultimately, the emulsion was subjected to lyophilization, resulting in stable NLCs that are suitable for further characterization and analysis (Garg et al. 2022).

X-Ray Diffraction (XRD)

The dried mixture of nanolipid carriers containing rosemary extract was subjected to analysis using an X'Pert Pro X-ray diffractometer (PANalytical BV, The Netherlands) to confirm the incorporation of the extract within the carriers. The instrument was operated at a voltage of 40 kV and a current of 30 mA, employing Cu Kα radiation to ensure precise measurements. The analysis was conducted in a standard configuration, facilitating the identification of crystalline phases and structural patterns. This method provides valuable insights into the molecular arrangement and stability of the rosemary extract integrated within the nanolipid carrier matrix (Sarvesh et al. 2024).

FTIR analysis

The dried mixture of nanolipid carriers containing rosemary extract was subjected to analysis via a Fourier-Transform Infrared (FTIR) spectrophotometer (Nicolet b6700 FTIR, Thermo Scientific) to identify the functional groups present within the sample. The instrument operated with a resolution of 4 cm^{-1}, encompassing a spectral range of 4000-400 cm^{-1}, thereby ensuring high precision in the

detection of molecular vibrations and chemical bonds. This analysis yielded comprehensive information regarding the interactions between the rosemary extract and the nanolipid carrier matrix, thereby confirming the incorporation and stability of the extract. The FTIR spectra facilitated the identification of characteristic peaks corresponding to the functional groups present in the sample (Dilipan et al. 2023).

Protein denaturation assay

The protein denaturation experiment was conducted with slight modifications to a previously reported method (Gunathilake et al. 2018). A 5 mL reaction mixture was prepared, consisting of 0.2 µL of 1% bovine serum albumin, 4.78 mL of phosphate-buffered saline (PBS, pH 6.4), and the lyophilized sample at a concentration of 10 mg/mL. The mixture was incubated in a water bath at 37°C for 15 minutes and then heated to 70°C for 5 minutes to induce denaturation. After cooling, the turbidity was measured at 660 nm using a UV/VIS spectrometer (Optima SP-3000, Tokyo, Japan).

A phosphate buffer served as the control. The inhibition percentage of protein denaturation was calculated using the formula: % inhibition = 100 × (1 - A2/A1), where A1 is the control sample absorption and A2 is the test sample absorption.

2,2-diphenyl-1-picrylhydrazyl (DPPH) assay

The radical scavenging activity of the test sample was assessed utilizing the DPPH (2,2-diphenyl-1-picrylhydrazyl) assay (Aksoy et al. 2013). The procedure entailed the combination of the sample with DPPH solution, followed by incubation in the dark at 37°C for 30 minutes to facilitate the reaction. Subsequent to the incubation period, the absorbance of the DPPH solution was measured at 517 nm employing a UV-VIS spectrophotometer, with ascorbic acid employed as a positive control (Ramachandran et al. 2021).

$$\text{DPPH scavenging effect} = ((A0 - A1)/A0) \times 100,$$

Where A0 is the absorbance of the control and A1 is the absorbance of the sample.

Antifungal activity

Antifungal activity was assessed using the agar well diffusion method. The inoculum of *C. albicans* was prepared by culturing the strain in Sabouraud Dextrose Broth (SDB) at 37°C for 24 hours, with turbidity standardized to the 0.5 McFarland standard. Subsequently, Sabouraud Dextrose Agar (SDA) plates were uniformly inoculated with the prepared suspension, and wells measuring 6 mm in diameter were created using a sterile gel punch. Test samples were introduced into the wells in varying volumes (50 µL, 75 µL, and 100 µL). The plates were then incubated at room temperature for a duration of 24 to 48 hours, after which the zones of inhibition surrounding the wells were measured to evaluate antifungal activity (Ross et al. 2008).

Statistically analysis

All experiments were performed in triplicate, and results were expressed as mean ± Standard Error of the Mean (SEM). Statistical analyses were conducted using OriginPro software. Pearson correlations and one-way ANOVA were applied to evaluate the significance of parameters and treatments. Additional analyses were performed using SPSS version 21.0, with $p<0.05$ considered statistically significant.

RESULTS AND DISCUSSION

X-Ray Diffraction

The X-Ray Diffraction (XRD) analysis of the Nanostructured Lipid Carrier (NLC) infused with rosemary extract revealed distinct peaks that substantiate its semi-crystalline nature (Figure 1). Notable diffraction peaks were observed at 2θ values of 11.21°, 16.54°, 22.03°, 22.59°, 26.24°, 31.14°, and 41.84°. The sharp and intense peak at 22.59° indicates a highly ordered crystalline region, suggesting an alignment of lipid molecules and effective encapsulation of rosemary extract within the carrier. In contrast, the broader peaks with lower intensities, such as those at 11.21° and 16.54°, indicate amorphous regions, which are essential for enhancing drug-loading efficiency and promoting sustained release properties of the carrier. These findings confirm that the rosemary extract was integrated into the lipid matrix without compromising its structural integrity.

Fourier-Transform Infrared spectroscopy

The FTIR spectrum of the Nanostructured Lipid Carrier (NLC) infused with rosemary extract reveals essential functional groups and molecular interactions, thereby confirming the successful incorporation of the extract into the lipid matrix (Figure 2). The broad peaks at 3348 cm^{-1} and 3289 cm^{-1} are indicative of O–H stretching vibrations, signifying the presence of hydroxyl groups from both the lipid carrier and the rosemary extract. These bands suggest the occurrence of hydrogen bonding, which contributes to the stabilization of the system. The peaks at 2916 cm^{-1} and 2848 cm^{-1} are attributed to C–H stretching vibrations from the alkyl chains of the lipids, further affirming the lipid nature of the carrier. The sharp peak at 1589 cm^{-1} corresponds to C=C stretching vibrations characteristic of the aromatic rings present in the phenolic compounds of rosemary extract. Additionally, the peaks at 1402 cm^{-1} and 1287 cm^{-1} indicate C–H bending and aromatic interactions, thereby further substantiating the presence of bioactive compounds in rosemary. A strong band at 1218 cm^{-1} represents C–O stretching, which is associated with esters or phenolic ethers in either the carrier or the extract. Notable absorption bands at 1082 cm^{-1} and 1024 cm^{-1} are attributed to C–O–C stretching vibrations, thereby confirming the existence of ester linkages within the lipid matrix. The peaks at 789 cm^{-1}, 627 cm^{-1}, and 526 cm^{-1} suggest out-of-plane bending vibrations associated with the aromatic structures and lipid functional groups. The FTIR spectrum demonstrates the successful encapsulation of

rosemary extract within the nanolipid carrier, revealing stable molecular interactions that preserve the functional integrity of both components. This confirms the system's potential for pharmaceutical and therapeutic applications.

Anti-inflammatory activity: Protein denaturation assay

The protein denaturation assay for the NLC infused with rosemary extract demonstrates its substantial anti-inflammatory activity, as evidenced by the percentage of inhibition observed at various concentrations (Figure 3). The data presented in the graph illustrate a concentration-dependent inhibition of protein denaturation, which serves as a critical marker of anti-inflammatory properties. At a concentration of 50 µg, the NLC exhibited a 44% inhibition, indicating moderate anti-inflammatory activity. This effect significantly increased at higher concentrations, reaching 56.5% inhibition at 100 µg and 81.5% at 150 µg. The highest concentration tested, 200 µg, exhibited a remarkable inhibition of 94%, thereby confirming the formulation's considerable anti-inflammatory potential.

Antioxidant activity: 2,2-diphenyl-1-picrylhydrazyl (DPPH) assay

The results of the DPPH assay for the NLC infused with rosemary extract indicate substantial antioxidant activity, as demonstrated by the percentage of inhibition observed at various concentrations (Figure 4). The data reveal a distinct concentration-dependent enhancement in the scavenging activity of the NLC. At a lower concentration of 50 µg, the system exhibited moderate inhibition of 52.32%, suggesting the presence of bioactive antioxidant compounds. As the concentration increased to 100 µg, the inhibition rose to 67.05%, reflecting an improved capacity for free radical scavenging. At 150 µg, the NLC achieved significant inhibition of 78.84%, underscoring its potent antioxidant potential. The highest concentration tested, 200 µg, recorded an impressive 89.47% inhibition, nearing complete neutralization of free radicals. This progressive increase in antioxidant activity with concentration is attributed to the bioactive compounds present in rosemary extract, including phenolic acids, flavonoids, and terpenoids, which are well-documented for their free radical scavenging properties.

Antifungal activity

The antifungal activity of the NLC infused with rosemary extract was evaluated using the agar well diffusion method (Figure 5). The results indicated a strong efficacy against *C. albicans*. The zones of inhibition surrounding the wells increased in size with escalating concentrations of the NLC, demonstrating a concentration-dependent antifungal effect. At a lower concentration of 50 µL, the zone of inhibition was moderate, signifying initial antifungal activity. Conversely, as the concentration increased to 75 µL and 100 µL, the zones of inhibition expanded significantly, illustrating enhanced efficacy at higher doses.

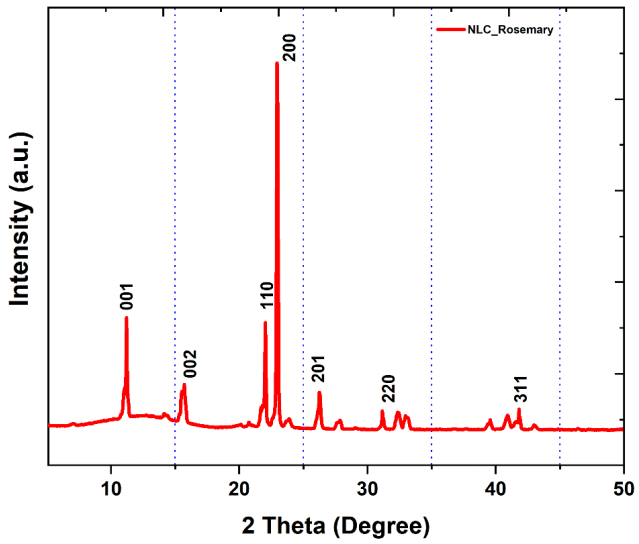

Figure 1. X-Ray Diffraction (XRD) pattern of Rosemary extract-loaded Nanostructured Lipid Carriers (NLCs). The diffractogram shows reduced crystalline peaks of rosemary extract within the lipid matrix, indicating successful encapsulation and transformation to a more amorphous state

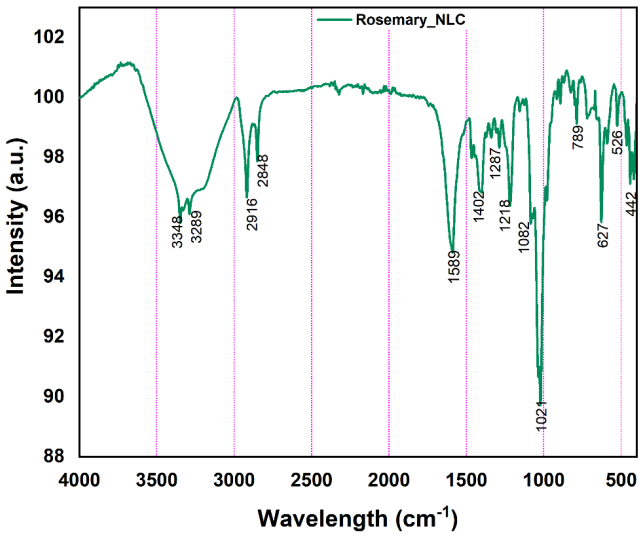

Figure 2. Fourier-Transform Infrared Spectroscopy (FTIR) spectral analysis of rosemary extract-loaded Nanostructured Lipid Carriers (NLCs)

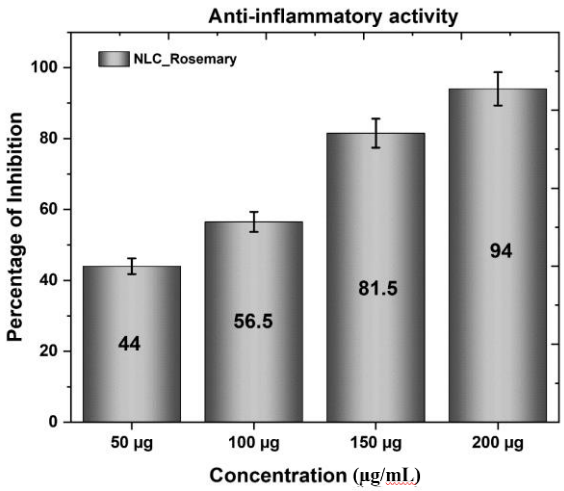

Figure 3. Anti-inflammatory activity of rosemary extract-loaded Nanostructured Lipid Carriers (NLCs)

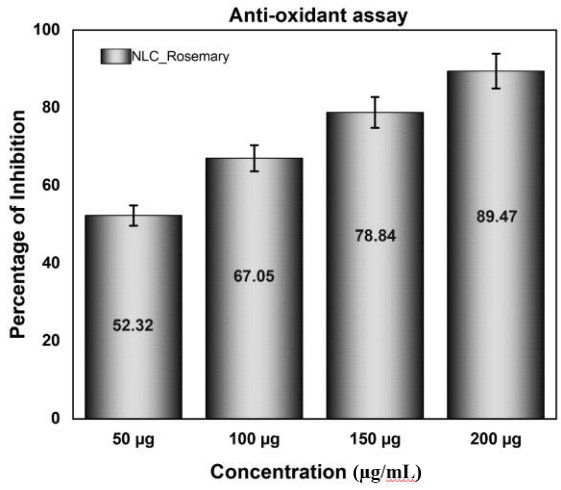

Figure 4. Antioxidant activity of rosemary extract-loaded Nanostructured Lipid Carriers (NLCs)

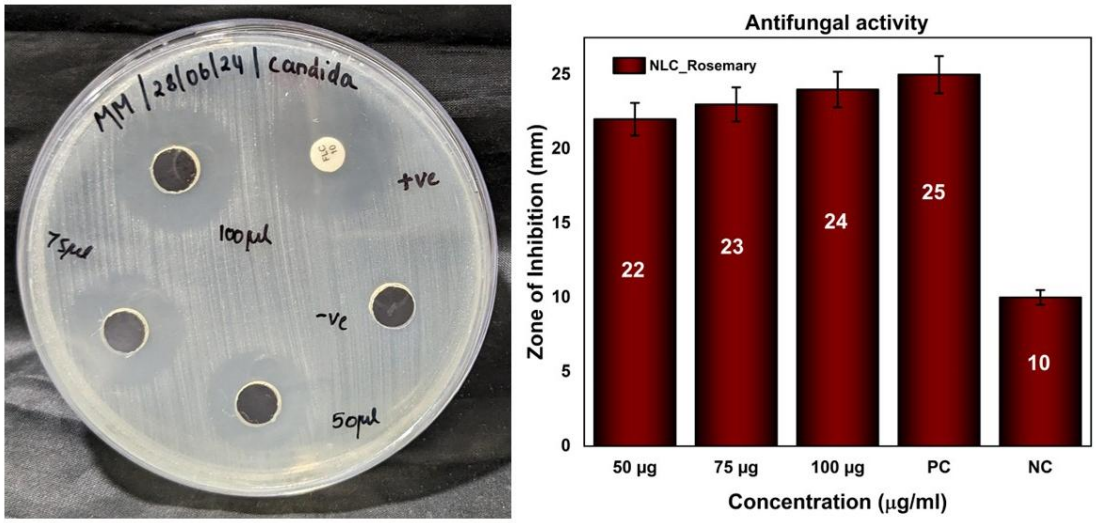

Figure 5. Antifungal activity of rosemary extract-loaded Nanostructured Lipid Carriers (NLCs)

Discussion

The present study demonstrates that Nanostructured Lipid Carriers (NLCs) markedly enhance the therapeutic potential of rosemary extract compared to its free form or conventional delivery systems. Encapsulation improved the stability of bioactive compounds, sustained their release, and enhanced their bioavailability, thereby maximizing antioxidant, anti-inflammatory, and antifungal effects (Javed et al. 2024). These findings are particularly significant given that free rosemary extract is often limited by rapid degradation, low solubility, and reduced bioactivity under physiological conditions (Aziz et al. 2021). By contrast, the rosemary-NLC formulation provided a protective lipid matrix that preserved phenolic compounds such as rosmarinic and carnosic acid, while simultaneously improving their therapeutic delivery.

The XRD and FTIR analyses confirmed the semi-crystalline structure and stable encapsulation of rosemary bioactives, features that explain the superior drug-loading capacity and release kinetics observed in this study. The coexistence of crystalline and amorphous lipid domains has been shown to enhance solubility and facilitate controlled release, consistent with previous reports on lipid-based systems (Soleimanifard et al. 2019; Malekmohammadi et al. 2023). Furthermore, the absence of significant spectral shifts in FTIR suggests that the encapsulation process preserved the chemical integrity of bioactive compounds, preventing degradation (Musuc et al. 2013). Together, these structural features provide mechanistic insight into the observed pharmacological efficacy.

The biological assays further underscore the advantages of rosemary-NLCs. The formulation achieved strong anti-inflammatory activity, likely through improved

stabilization and delivery of rosmarinic and carnosic acid, which are known to suppress pro-inflammatory mediators (Al-Sereiti et al. 1999). Likewise, the enhanced antioxidant activity can be attributed to the sustained release of phenolics such as caffeic acid and flavonoids, which effectively neutralize free radicals (Rašković et al. 2014). The antifungal efficacy against *C. albicans* was also potentiated, most likely due to improved penetration of terpenoids such as cineole and camphor across fungal membranes, an effect facilitated by the lipid carrier system (Agrawal et al. 2020). Collectively, these results highlight the multifaceted therapeutic advantages of NLC encapsulation over free rosemary extract and other conventional carriers.

Despite these promising outcomes, certain limitations must be acknowledged. The present work was confined to in vitro evaluations, and the absence of in vivo or clinical validation restricts the generalizability of findings. Moreover, issues such as large-scale manufacturing, batch-to-batch consistency, and long-term stability remain unresolved, and these represent key barriers to clinical translation. Regulatory challenges surrounding the safety assessment of nanocarrier systems must also be addressed before rosemary-NLCs can be adopted for therapeutic use.

In this study, rosemary-loaded NLCs offer a superior delivery platform that enhances the stability, bioavailability, and therapeutic performance of rosemary bioactives. While these findings provide a strong proof of concept, future work should focus on in vivo validation, pharmacokinetic profiling, and clinical evaluation to bridge the gap between experimental outcomes and practical biomedical applications.

In conclusion, rosemary extract-loaded Nanostructured Lipid Carriers (NLCs) demonstrate considerable biomedical potential, highlighting their multifunctional therapeutic properties. X-Ray Diffraction (XRD) analysis elucidates the structural complexity and disordered polymeric nature of the NLCs, while Fourier-Transform Infrared Spectroscopy (FTIR) confirms the presence of functional groups such as alcohols, amines, and esters, which contribute to their bioactivity. The NLCs exhibit significant anti-inflammatory activity, achieving 94% inhibition of protein denaturation at a concentration of 200 µg/mL, alongside remarkable antioxidant efficacy, scavenging 89.47% of DPPH radicals at the same concentration. Additionally, the NLCs manifest antifungal activity against *C. albicans*, with effective inhibition further enhanced by the encapsulation of rosemary extract. These findings suggest that the incorporation of rosemary extract into NLCs enhances bioavailability, stability, and therapeutic efficiency. This study underscores the potential of rosemary-loaded NLCs as a cost-effective and environmentally friendly nanotechnology platform for various biomedical applications, including drug delivery, wound healing, antioxidant therapy, and disease management. This innovative approach paves the way for further exploration and clinical applications of plant-based nanocarriers.

REFERENCES

Afeeza KLG, Priyadharshini B, Vasugi S, Dilipan E. 2025. Exploring the therapeutic potential of biosynthetic enzymes in cancer treatment: Innovations and implications. Intl J Biol Macromol 292: 139171. DOI: 10.1016/j.ijbiomac.2024.139171.

Agrawal M, Saraf S, Saraf S, Dubey SK, Puri A, Patel RJ, Ajazuddin, Ravichandiran V, Murty US, Alexander A. 2020. Recent strategies and advances in the fabrication of nano lipid carriers and their application towards brain targeting. J Control Release 321: 372-415. DOI: 10.1016/j.jconrel.2020.02.020.

Aksoy L, Kolay E, Ağılönü Y, Aslan Z, Kargıoğlu M. 2013. Free radical scavenging activity, total phenolic content, total antioxidant status, and total oxidant status of endemic *Thermopsis turcica*. Saudi J Biol Sci 20 (3): 235-239. DOI: 10.1016/j.sjbs.2013.02.003.

Al-Sereiti MR, Abu-Amer KM, Sen P. 1999. Pharmacology of rosemary (*Rosmarinus officinalis* Linn.) and its therapeutic potentials. Indian J Exp Biol 37: 124-130.

Aziz E, Batool R, Akhtar W, Shahzad T, Malik A, Shah MA, Iqbal S, Rauf A, Zengin G, Bouyahya A, Rebezov M, Dutta N, Khan MU, Khayrullin M, Babaeva M, Goncharov A, Shariati MA, Thiruvengadam M. 2021. Rosemary species: A review of phytochemicals, bioactivities and industrial applications. S Afr J Bot 151: 3-18. DOI: 10.1016/j.sajb.2021.09.026.

Chinsriwongkul A, Chareanputtakhun P, Ngawhirunpat T, Rojanarata T, Sila-on W, Ruktanonchai U, Opanasopit P. 2012. Nanostructured Lipid Carriers (NLC) for parenteral delivery of an anticancer drug. AAPS PharmSciTech 13 (1): 150-158. DOI: 10.1208/s12249-011-9733-8.

Dilipan E, Sivaperumal P, Kamala K, Ramachandran M, Vivekanandhan P. 2023. Green synthesis of silver nanoparticles using seagrass *Cymodocea serrulata* (R.Br.) Asch. & Magnus, characterization, and evaluation of anticancer, antioxidant, and antiglycemic index. Biotechnol Appl Biochem 70 (3): 1346-1356. DOI: 10.1002/bab.2444.

Fang CL, Al-Suwayeh SA, Fang JY. 2013. Nanostructured lipid carriers (NLCs) for drug delivery and targeting. Recent Pat Nanotechnol 7 (1): 41-55. DOI: 10.2174/187221013804484827.

Garg J, Pathania K, Sah SP, Pawar SV. 2022. Nanostructured lipid carriers: A promising drug carrier for targeting brain tumours. Future J Pharm Sci 8 (1): 25. DOI: 10.1186/s43094-022-00414-8.

Gunathilake KDPP, Ranaweera KKDS, Rupasinghe HPV. 2018. In vitro anti-inflammatory properties of selected green leafy vegetables. Biomedicines 6 (4): 107. DOI: 10.3390/biomedicines6040107.

Gunawan M, Boonkanokwong V. 2024. Current applications of solid lipid nanoparticles and nanostructured lipid carriers as vehicles in oral delivery systems for antioxidant nutraceuticals: A review. Colloids Surf B Biointerfaces 233: 113608. DOI: 10.1016/j.colsurfb.2023.113608.

Hendel N, Sarri D, Sarri M, Napoli E, Palumbo Piccionello A, Ruberto G. 2024. Phytochemical analysis and antioxidant and antifungal activities of powders, methanol extracts, and essential oils from *Rosmarinus officinalis* L. and *Thymus ciliatus* Desf. Benth. Intl J Mol Sci 25 (14): 7989. DOI: 10.3390/ijms25147989.

Iqbal MA, Md S, Sahni JK, Baboota S, Dang S, Ali J. 2012. Nanostructured lipid carriers system: Recent advances in drug delivery. J Drug Target 20 (10): 813-830. DOI: 10.3109/1061186X.2012.71684.

Jaiswal P, Gidwani B, Vyas A. 2016. Nanostructured lipid carriers and their current application in targeted drug delivery. Artif Cells Nanomed Biotechnol 44 (1): 27-40. DOI: 10.3109/21691401.2014.909822.

Javed S, Mangla B, Salawi A, Sultan MH, Almoshari Y, Ahsan W. 2024. Essential oils as dermocosmetic agents, their mechanism of action and nanolipidic formulations for maximized skincare. Cosmetics 11 (6): 210. DOI: 10.3390/cosmetics11060210.

Kaur R, Gupta TB, Bronlund J, Singh J, Kaur L. 2024. Synthesis and characterisation of Mānuka and rosemary oil-based nano-entities and their application in meat. Food Chem 436: 137600. DOI: 10.1016/j.foodchem.2023.137600.

Khatoon R, Alam MA, Sharma PK. 2020. A comprehensive study of pharmacological behaviors, nano-formulations, and applications of rosemary. Nat Prod J 11 (5): 629-647. DOI: 10.2174/2210315510999201104165058.

Lacatusu I, Badea N, Murariu A, Nichita C, Bojin D, Meghea A. 2010. Antioxidant capacity of lipid nanoparticles loaded with rosemary extract. Mol Cryst Liq Cryst 523 (1): 260-272. DOI: 10.1080/15421401003719886.

Malekmohammadi M, Ghanbarzadeh B, Hanifian S, Kafil HS, Gharekhani M, Falcone PM. 2023. The gelatin-coated Nanostructured Lipid Carrier (NLC) containing Salvia officinalis extract: Optimization by combined D-optimal design and its application to improve the quality parameters of beef burger. Foods 12 (20): 3737. DOI: 10.3390/foods12203737.

Montenegro L, Pasquinucci L, Zappalà A, Chiechio S, Turnaturi R, Parenti C. 2017. Rosemary essential oil-loaded lipid nanoparticles: In vivo topical activity from gel vehicles. Pharmaceutics 9 (4): 48. DOI: 10.3390/pharmaceutics9040048.

Musuc AM, Badea-Doni M, Jecu L, Rusu A, Popa TV. 2013. FTIR, XRD, and DSC analysis of the rosemary extract effect on polyethylene structure and biodegradability. J Therm Anal Calorim 114: 169-177. DOI: 10.1007/s10973-012-2909-y.

Naseem N, Kushwaha P, Haider F. 2024. Leveraging nanostructured lipid carriers to enhance targeted delivery and efficacy in breast cancer therapy: A comprehensive review. Naunyn Schmiedebergs Arch Pharmacol 398 (1): 449-468. DOI: 10.1007/s00210-024-03408-w.

Obeidat WM, Schwabe K, Müller RH, Keck CM. 2010. Preservation of Nanostructured Lipid Carriers (NLC). Eur J Pharm Biopharm 76 (1): 56-67. DOI: 10.1016/j.ejpb.2010.05.001.

Ramachandran M, Arulbalachandran D, Dilipan E, Ramya S. 2021. Comparative analysis of abscisic acid recovery on two varieties of rice (*Oryza sativa* L.) under drought condition. Biocatal Agric Biotechnol 33: 102006. DOI: 10.1016/j.bcab.2021.102006.

Rašković A, Milanović I, Pavlović N, Ćebović T, Vukmirović S, Mikov M. 2014. Antioxidant activity of rosemary (*Rosmarinus officinalis* L.) essential oil and its hepatoprotective potential. BMC Complement Altern Med 14: 225. DOI: 10.1186/1472-6882-14-225.

Ross C, Puglisi MP, Paul VJ. 2008. Antifungal defenses of seagrasses from the Indian River Lagoon, Florida. Aquat Bot 88 (2): 134-141. DOI: 10.1016/j.aquabot.2007.09.003.

Sarvesh N, Afeeza K, Suresh V, Dilipan E. 2024. Development of the antioxidant property of seagrass extract-based hydrogel for dental application. Cureus 16 (2): e54544. DOI: 10.7759/cureus.54544.

Selvamuthukumar S, Velmurugan R. 2012. Nanostructured lipid carriers: A potential drug carrier for cancer chemotherapy. Lipids Health Dis 11: 159. DOI: 10.1186/1476-511X-11-159.

Soleimanifard M, Sadeghi Mahoonak A, Sepahvand A, Heydari R, Farhadi S. 2019. Spanish olive leaf extract-loaded nanostructured lipid carriers: Production and physicochemical characterization by Zetasizer, FT-IR, DTA/TGA, FE-SEM and XRD. J Food Process Preserv 43 (7): e13994. DOI: 10.1111/jfpp.13994.

Wathoni N, Suhandi C, Elamin KM, Lesmana R, Hasan N, Mohammed AFA, El-Rayyes A, Wilar G. 2024. Advancements and challenges of nanostructured lipid carriers for wound healing applications. Intl J Nanomed 19: 8091-8113. DOI: 10.2147/IJN.S478964.

ASIAN J NAT PROD BIOCHEM
Volume 23, Number 2, December 2025
Pages: 153-163

P-ISSN: 2775-4189
E-ISSN: 2775-4197
DOI: 10.13057/biofar/f230207

Natural dye plants in traditional batik production and their potential as plant-derived pigments

ANDARA NADIEN HAPSARI[1], ANGGITA YULIA NURRIZQI[1], ANIS NABILA NURROSIDAH[1], AYU CITRA MAHARANI[1], MUHAMMAD INDRAWAN[1], SURAPON SAENSOUK[2], AHMAD DWI SETYAWAN[1,3,♥]

[1]Department of Environmental Science, Faculty of Mathematics and Natural Sciences, Universitas Sebelas Maret. Jl. Ir. Sutami 36A, Surakarta 57126, Central Java, Indonesia. Tel./fax.: +62-271-663375, ♥email: volatileoils@gmail.com
[2]Walai Rukhavej Botanical Research Institute, Mahasarakham University. Kantarawichai District, Maha Sarakham 44150, Thailand
[3]Biodiversity Research Group, Universitas Sebelas Maret. Jl. Ir. Sutami 36A, Surakarta 57126, Central Java, Indonesia

Manuscript received: 20 September 2025. Revision accepted: 24 December 2025.

Abstract. *Hapsari AN, Nurrizqi AY, Nurrosidah AN, Maharani AC, Indrawan M, Saensouk S, Setyawan AD. 2025. Natural dye plants in traditional batik production and their potential as plant-derived pigments. Asian J Nat Prod Biochem 23: 153-163.* Plant-derived natural dyes have attracted renewed interest as alternative pigment sources due to growing concerns over the environmental and health implications of synthetic dyes. Traditional dyeing practices offer process-based systems in which pigment extraction, transformation, and application are achieved using low-input operational controls. This study documents plant species used as natural dyes in traditional batik production at Batik Tjap Tiga Negeri, Laweyan Batik Village, Surakarta, Central Java, Indonesia, and discusses their relevance as plant-derived pigment sources within a natural product and biochemical context. Observations were conducted during active dye production to record plant species utilized, plant parts used, extraction methods, dye application procedures, and handling of residual materials. A total of seven plant species were identified as components of the dyeing system, including *Indigofera tinctoria*, *Caesalpinia sappan*, *Cudrania javanensis*, *Swietenia mahagoni*, *Symplocos fasciculata*, *Tectona grandis*, and *Acacia* spp. Dye extraction involved fermentation or aqueous heat-based processes, while dye application relied on repeated dipping and drying cycles. Variation in color intensity was associated with differences in dyeing duration and the number of application cycles. The results indicate that traditional dyeing systems function as low-input pigment processing frameworks in which color outcomes are regulated through process variables such as fermentation, pH adjustment, and repeated application. Literature-based synthesis further shows that the documented dye plants are associated with reported pigment classes, including indigoids, homoisoflavonoids, flavonoid-related pigments, and tannin-rich polyphenols. Although no chemical analyses were performed, the study highlights traditional dyeing systems as low-input pigment processing models and identifies candidate plant sources for future biochemical characterization and natural product research.

Keywords: Batik dyeing, natural pigments, plant-derived dyes, process-controlled coloration, traditional dyeing systems

INTRODUCTION

Synthetic dyes have been extensively used in the textile industry due to their color uniformity, reproducibility, and high production efficiency. However, their widespread application has raised serious environmental and health concerns, particularly related to the release of non-biodegradable effluents, high Chemical Oxygen Demand (COD), Biological Oxygen Demand (BOD), and the formation of toxic aromatic amines during degradation (Ardila-Leal et al. 2021; Al-Tohamy et al. 2022; Islam et al. 2023). These issues have motivated increasing regulatory pressure and scientific interest in developing safer and more sustainable alternatives for textile coloration. Recent studies emphasize that synthetic dye residues contribute significantly to aquatic toxicity and long-term ecosystem degradation, especially in regions dominated by small-scale textile industries with limited wastewater treatment infrastructure (Moreira et al. 2022; Periyasamy 2024).

In response to these challenges, plant-derived natural pigments have re-emerged as promising alternatives due to their renewable origin, lower toxicity, and potential biodegradability. Advances in green chemistry and sustainable materials research highlight natural pigments as key components in environmentally responsible production systems (Fried et al. 2022; Pizzicato et al. 2023; Renita et al. 2023). In addition to their environmental advantages, plant-based pigments are increasingly valued for their aesthetic complexity and compatibility with eco-friendly processing routes. Reviews published in some scientific journals consistently report growing scientific and industrial interest in natural colorants derived from higher plants (Bechtold and Mussak 2009; Shahid et al. 2013).

Despite these advantages, the large-scale adoption of natural pigments remains constrained by variability in color yield, stability, and processing efficiency. Consequently, understanding traditional dyeing systems that have historically optimized plant pigment use under low-input conditions may provide valuable insights for contemporary natural product and biochemical research.

Several plant species traditionally used in textile dyeing are well documented in the literature as sources of chemically distinct pigment classes. *Indigofera tinctoria* is widely recognized as a primary source of indigoid pigments, particularly indigo and indirubin, which are

formed through enzymatic hydrolysis and subsequent oxidation of indican precursors (Fried et al. 2022; Castillo-Suárez et al. 2023). Indigoid compounds have attracted biochemical interest due to their redox behavior and chromophoric properties (Maugard et al. 2001; Bechtold et al. 2003).

Caesalpinia sappan has been reported as a major source of brazilin and its oxidized derivative brazilein, phenolic pigments responsible for red to reddish-brown hues. These compounds belong to the homoisoflavonoid group and are known for their pH-dependent color transitions and metal-binding behavior, making them relevant to studies on pigment stability and mordant interactions (Pizzicato et al. 2023; Wouyou et al. 2025). Similarly, *Cudrania javanensis* and related dye plants have been associated with flavonoid-related yellow pigments, which contribute to color diversity and exhibit sensitivity to processing conditions (Alegbe and Uthman 2024).

Importantly, these pigment associations are reported in the literature and are not derived from chemical analyses conducted in the present study. Nevertheless, identifying plant species traditionally selected for dyeing provides an empirical basis for linking botanical sources with known pigment classes of biochemical relevance.

Traditional textile dyeing systems rely on process variables that directly influence pigment release, transformation, and fixation onto textile fibers. Fermentation is commonly employed to convert precursor compounds into chromophoric forms, particularly in indigo-based systems where microbial or enzymatic activity facilitates pigment solubilization prior to oxidation. Another critical variable is pH adjustment, often achieved through the addition of alkaline materials such as calcium oxide (CaO). The pH plays a decisive role in pigment ionization, solubility, and affinity for textile fibers, thereby affecting color intensity and stability (Shahid et al. 2013). Repeated dipping and drying cycles further enhance pigment deposition by promoting gradual accumulation and fixation.

Viewed from a natural product perspective, these traditional practices can be conceptualized as integrated pigment processing systems governed by fermentation, pH control, and repeated application. Understanding these process-dependent effects is essential for translating traditional knowledge into biochemical and natural product research frameworks.

This study aims to document plant species used as natural dyes in traditional batik production and to discuss their potential relevance as plant-derived pigment sources for natural product and biochemical studies. We hypothesized that color intensity in traditional batik dyeing increases with longer dyeing duration and a higher number of repeated dipping cycles, reflecting process-controlled modulation of plant-derived pigments rather than chemical modification of pigment composition.

MATERIALS AND METHODS

Study site and dye production system

The study was conducted at Batik Tjap Tiga Negeri, a traditional batik production unit located in Laweyan, Surakarta, Central Java, Indonesia. The site represents an active batik workshop that applies plant-based natural dyes as part of its regular production process. Observations were carried out during ongoing dyeing activities to capture operational practices under real production conditions.

The dye production system at the study site is characterized by small-scale, manual processing and the use of plant-derived materials prepared on-site. Natural dyes are processed through a sequence of steps that include plant material preparation, aqueous extraction or fermentation, dye bath conditioning, and repeated application to textile fibers. All procedures are conducted under ambient conditions without the use of synthetic auxiliaries or industrial-scale equipment.

Plant materials used for dyeing are sourced from cultivated plants or local suppliers, depending on availability. Dye preparation methods vary according to plant species and targeted color outcomes and include fermentation, boiling, decoction, soaking, or grinding. In indigo-based dyeing, alkaline conditions are achieved through the controlled addition of calcium oxide to facilitate dye application prior to oxidation. These procedures form an integrated dye production system in which color development is regulated through operational control rather than chemical modification.

The dye application process involves repeated immersion and air-drying cycles to achieve gradual color accumulation on textile fibers. Adjustments in dyeing duration and repetition are made empirically by practitioners based on visual assessment of color development. Handling of residual materials is incorporated into routine production activities and does not involve secondary chemical treatment.

The study site was treated as a process-oriented unit of analysis, focusing on the operational steps relevant to pigment extraction, transformation, and application. Historical, cultural, and spatial aspects were not included, as the primary objective was to document dyeing practices with relevance to plant-derived pigment research.

Plant material identification

Plant species used as natural dye sources were identified based on direct observation of dye preparation and application activities at the study site, combined with information provided by practitioners regarding local plant names and plant parts utilized. The identification process focused on establishing the correct scientific names of plant taxa relevant to dye production.

Initial identification was conducted using regional and national floristic references, including standard botanical handbooks and floras relevant to Indonesian plant taxa (Backer and van den Brink 1980; Whitmore et al. 1986; Suheryanto 2017). These printed sources were used to match local plant names with macroscopic morphological

descriptions and accepted scientific names prior to verification using online taxonomic databases.

To ensure taxonomic accuracy and nomenclatural consistency, scientific names were subsequently verified using authoritative online plant taxonomic resources, including Plants of the World Online (POWO 2026; https://powo.science.kew.org), the Global Biodiversity Information Facility (GBIF 2026; https://www.gbif.org), and the International Plant Names Index (IPNI 2026; https://www.ipni.org). These databases were consulted to confirm accepted names, authorship, and higher-level taxonomic placement.

Plant identification was limited to species actively used in the dyeing process during the observation period. No plant specimens were collected for herbarium deposition, and no microscopic or molecular identification was performed. Consequently, species determination relied on macroscopic morphological characteristics, local usage information, and cross-validation with floristic literature and online taxonomic references.

This identification approach aimed to produce a validated list of plant species relevant to the dyeing system while maintaining methodological transparency appropriate for a process-oriented natural product study.

Observation of dye preparation and application

Observation of dye preparation and application was conducted through direct, non-intrusive monitoring of routine dyeing activities at the study site. The observations aimed to document operational steps and key process variables involved in the use of plant-based natural dyes under real production conditions, without measuring pigment composition or performance quantitatively. This approach is commonly used in process-oriented studies of traditional dyeing systems to capture practice-based knowledge (Cardon 2007; Bechtold and Mussak 2009).

The observation covered sequential stages of dyeing activities, including plant material preparation, dye extraction or fermentation, dye bath conditioning, and application of dyes to textile fibers. For indigo-based dyeing, particular attention was given to leaf fermentation, alkalization, and oxidation, as these stages regulate pigment availability and dye uptake in traditional indigo systems (Maugard et al. 2001; Bechtold et al. 2003; Castillo-Suárez et al. 2023).

For non-indigo dye plants, observations focused on aqueous extraction methods such as boiling or decoction of bark, wood, or leaves. Heat-assisted extraction is widely reported as an effective approach for releasing phenolic and flavonoid-related pigments from plant tissues used in natural dyeing (Vankar 2000; Samanta and Agarwal 2009). Extraction duration and handling of dye solutions prior to application were recorded descriptively to characterize process variability.

The use of plant-based mordants was also noted, including the sequence and timing of mordant application relative to dyeing. Natural mordants derived from plant materials have been reported to influence pigment-fiber interactions without the use of synthetic additives (Shahid et al. 2013).

Dye application was observed during repeated immersion and air-drying cycles. Key variables recorded included dyeing duration, number of dipping cycles, and general dye bath conditions such as perceived alkalinity. Repeated application is known to facilitate gradual pigment accumulation and improved color fixation in plant-based dyeing systems (Pizzicato et al. 2023; Renita et al. 2023).

All observations were conducted under ambient production conditions without intervention, aligning with established process-based investigations of traditional dyeing systems (Cardon 2007; Fried et al. 2022).

Data analysis

Data analysis was conducted using a descriptive and process-oriented framework to synthesize observational information related to plant species utilization, dye preparation procedures, and dye application practices. The analytical approach was designed to organize field observations systematically without applying quantitative statistical inference or laboratory-based pigment measurements.

Information obtained from observations was categorized according to major components of the dyeing system, including plant material characteristics, extraction or fermentation techniques, application procedures, and handling of residual materials. Process variables such as dyeing duration, number of dipping cycles, and general dye bath conditions were documented to enable comparison across different dye types. This form of qualitative categorization is widely used in studies aiming to understand traditional production systems and process-driven material behavior (Bechtold and Mussak 2009; Ling et al. 2022).

Color intensity was assessed using an observational ordinal scale based on visual evaluation during routine production. Such qualitative scaling methods are commonly employed in traditional dyeing studies where color outcomes are controlled empirically and instrumental colorimetric measurements are not available (Renita et al. 2023; Negi 2025). The analysis focused on identifying consistent patterns between operational variables and observed color development rather than on quantifying pigment concentration or color metrics.

Comparative interpretation of dyeing practices emphasized process-response relationships, allowing evaluation of how variations in operational control influenced dye application outcomes. Interpretation was limited to patterns observable across repeated production cycles and did not extend to causal or mechanistic claims at the molecular level. This constraint ensured a clear distinction between observational findings and literature-based biochemical interpretation.

Literature-based synthesis was applied separately during the discussion stage to relate observed dye plants and processing practices to reported pigment classes and biochemical behavior. By maintaining this separation, the analytical framework preserved methodological transparency and avoided conflation between primary observational data and secondary literature interpretation (Snyder et al. 2019; Fried et al. 2022; Pizzicato et al. 2023).

RESULTS AND DISCUSSION

Plant species used as natural dye sources

Observation of dye production activities at Batik Tjap Tiga Negeri identified a set of plant species consistently used as sources of natural dyes in traditional batik production. These species represent the primary botanical materials employed for generating different color tones and for supporting dye fixation during the dyeing process. The documented plant species, plant parts used, color outcomes, and extraction methods are summarized in Table 1.

A total of seven plant species were recorded as active components of the dyeing system. The species utilized include *I. tinctoria*, *C. sappan*, *C. javanensis*, *Swietenia mahagoni*, *Symplocos fasciculata*, *Tectona grandis*, and *Acacia* spp. Each species was associated with a distinct role within the dyeing process, either as a primary source of color or as a supporting material for color fixation.

Leaves of *I. tinctoria* were used as the sole source of blue coloration. The dye preparation involved a fermentation-based process followed by oxidation, resulting in a characteristic indigo hue applied as a base layer in the dyeing sequence. Other dye plants primarily utilized woody tissues, including bark or heartwood, which were processed through boiling or decoction to obtain aqueous dye solutions. These species contributed red, yellow, brown, or dark brown tones depending on the plant material and extraction method employed.

In addition to pigment-producing plants, *S. fasciculata* bark was recorded as a natural mordant source. Rather than contributing a distinct color, this species was used to support dye fixation through alum-related compounds released during grinding and soaking. The inclusion of a plant-based mordant highlights the integrated nature of the dyeing system, in which color development and fixation are achieved using botanical materials.

Across all documented species, extraction methods were limited to low-input aqueous processes, including fermentation, boiling, decoction, grinding, and soaking. No synthetic chemicals or industrial additives were applied during plant material processing. The recorded plant species and associated extraction techniques together form the botanical foundation of the natural dyeing system observed in this study.

Dye extraction and application processes

The dye extraction and application processes observed at Batik Tjap Tiga Negeri followed a structured sequence of plant material preparation, aqueous extraction or fermentation, dye bath conditioning, and repeated application to textile fibers. Although specific procedures varied among plant species, the overall workflow showed consistent operational stages across different dye types.

For indigo-based dyeing derived from *I. tinctoria*, dye preparation involved a fermentation stage using fresh leaves immersed in water. The fermentation process produced a soluble dye intermediate, which was subsequently subjected to oxidation during application. Prior to dyeing, alkaline conditions were established through the addition of small amounts of calcium oxide (CaO) to the dye bath. This step facilitated pigment solubilization before oxidation and application. The sequential stages of fermentation, alkalization, oxidation, and dye application were consistently applied during indigo dyeing, as illustrated in Figure 1.

Extraction of dyes from non-indigo plant species relied primarily on aqueous heat-based methods. Woody materials such as the bark or wood of *C. sappan*, *C. javanensis*, *S. mahagoni*, and *Acacia* spp. were processed through boiling or decoction to release color-bearing compounds into the dye solution. Following extraction, solid residues were removed by simple filtration, and the resulting dye solutions were used directly for fabric dyeing without further modification.

In the case of *S. fasciculata*, bark material was processed by grinding and soaking to obtain a solution used as a natural mordant. This solution was applied prior to or in conjunction with dyeing to support color fixation. The mordanting step was integrated into the dyeing sequence without the use of synthetic additives.

Application of natural dyes to textiles involved repeated dipping and air-drying cycles. Each cycle allowed gradual accumulation of color on the fabric surface, while intermediate drying facilitated fixation. Dyeing was conducted under ambient conditions, and the duration and number of dipping cycles were adjusted according to the desired color depth. Variations in these parameters were recorded as part of the observation process and are addressed in subsequent sections.

To synthesize the observed dye preparation and application procedures, the individual operational steps were integrated into a simplified workflow representing the general structure of plant-based dyeing systems. This workflow is summarized in Figure 2, highlighting common stages shared across different dye types.

Table 1. Plant species used as natural dye sources in traditional batik production

Scientific name	Local name	Plant part used	Color obtained	Extraction method
Indigofera tinctoria	Indigo / Tarum	Leaves	Blue	Fermentation followed by oxidation
Caesalpinia sappan	Secang	Wood	Red	Boiling
Cudrania javanensis	Tegeran	Wood	Yellow	Decoction
Swietenia mahagoni	Mahoni	Bark	Brown	Boiling
Symplocos fasciculata	Jambal	Bark	Mordant source (alum)	Grinding and soaking
Tectona grandis	Jati	Leaves	Reddish brown	Hot extraction
Acacia spp.	Kayu akasia	Bark	Dark brown	Boiling

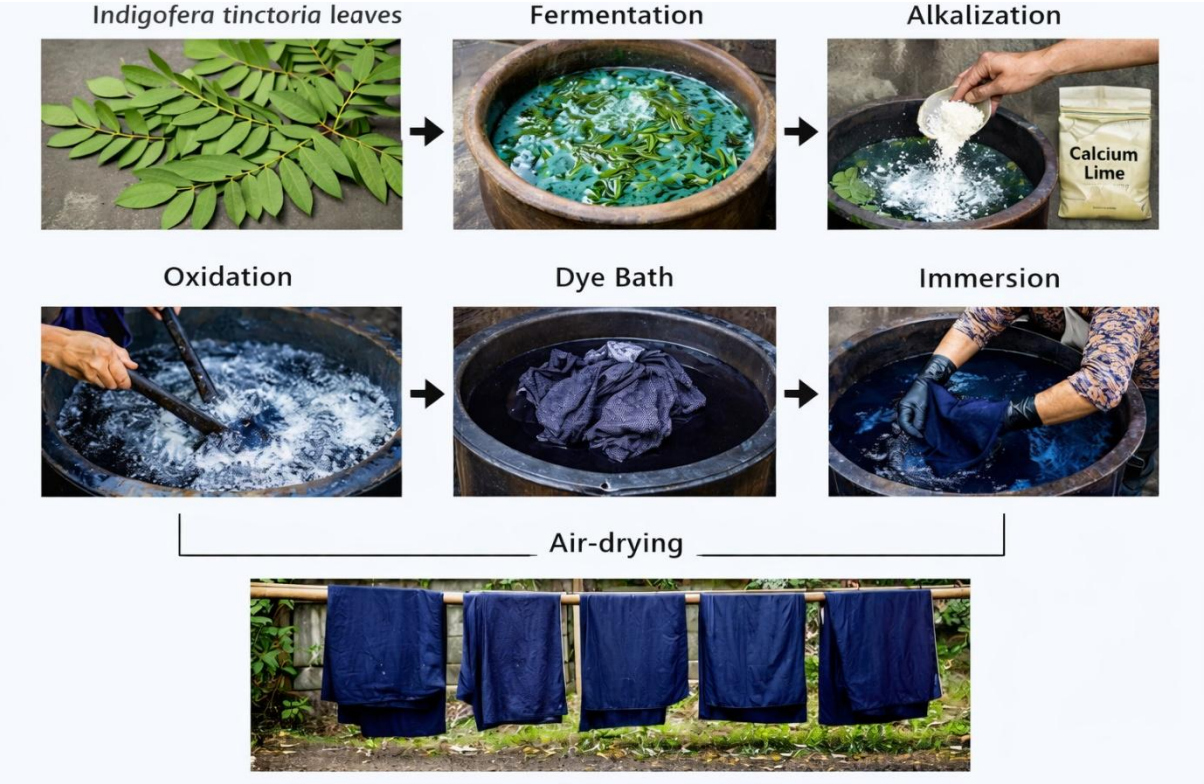

Figure 1. Indigo-based dye preparation and application process derived from *Indigofera tinctoria*

Figure 2. Simplified workflow of plant-based natural dye preparation and application in traditional batik production

Influence of processing parameters on color intensity

Variation in color intensity observed during natural dyeing was closely associated with differences in processing parameters, particularly dyeing duration and the number of repeated dipping cycles. Practitioners consistently adjusted these parameters to achieve the desired color depth across different dye types. Observed relationships between processing conditions and resulting color intensity are summarized in Table 2.

Across all dye plants, increased dyeing duration and a higher number of dipping cycles were associated with progressively deeper color tones. Fabrics subjected to a

single or limited number of dipping cycles generally exhibited lighter coloration, whereas repeated application resulted in darker and more saturated hues. This pattern was most pronounced in indigo-based dyeing, where incremental color buildup was achieved through successive dipping and oxidation cycles.

For non-indigo dye plants, including *C. sappan*, *C. javanensis*, and *S. mahagoni*, color development followed a similar trend, although the rate of intensity increases varied among species. Short extraction and dyeing times produced pale or moderate tones, while extended exposure and repeated application enhanced color depth. These observations indicate that color intensity is not solely dependent on plant species but is strongly influenced by operational control during dye application.

Color intensity was recorded using an observational ordinal scale, reflecting practical assessments made during routine production. This scale captured relative differences in color depth rather than quantitative pigment concentration. The summarized relationships between dyeing duration, dipping frequency, and observed color intensity are presented in Table 2, while a visual representation of these trends is provided in Figure 3.

The observed patterns demonstrate that traditional dyeing systems rely on process-based modulation to control color outcomes. Rather than altering dye composition through chemical modification, practitioners achieve color variation by adjusting exposure time and repetition, allowing gradual pigment accumulation on textile fibers. These findings highlight the role of processing parameters as key determinants of color intensity within plant-based dyeing systems.

Handling of residual dye materials within the dyeing process

Handling of residual materials generated during the dyeing process was systematically documented based on the type of residue produced and the applied handling practice. Residual materials were classified into liquid and solid forms originating from different stages of dye preparation and application. The observed types of residual materials and their corresponding handling practices are summarized in Table 3.

Table 2. Observed the relationship between processing parameters and color intensity in natural dyeing

Dye plant source	Dyeing duration	Number of dipping cycles	Observed color intensity*
Indigofera tinctoria	Short	Low	Light blue
Indigofera tinctoria	Moderate	Medium	Medium blue
Indigofera tinctoria	Extended	High	Deep blue
Caesalpinia sappan	Short	Low	Light red
Caesalpinia sappan	Moderate	Medium	Medium red
Caesalpinia sappan	Extended	High	Dark red
Cudrania javanensis	Short	Low	Pale yellow
Cudrania javanensis	Moderate	Medium	Yellow
Cudrania javanensis	Extended	High	Deep yellow

Note: *: Color intensity was assessed using an observational ordinal scale based on routine production evaluation

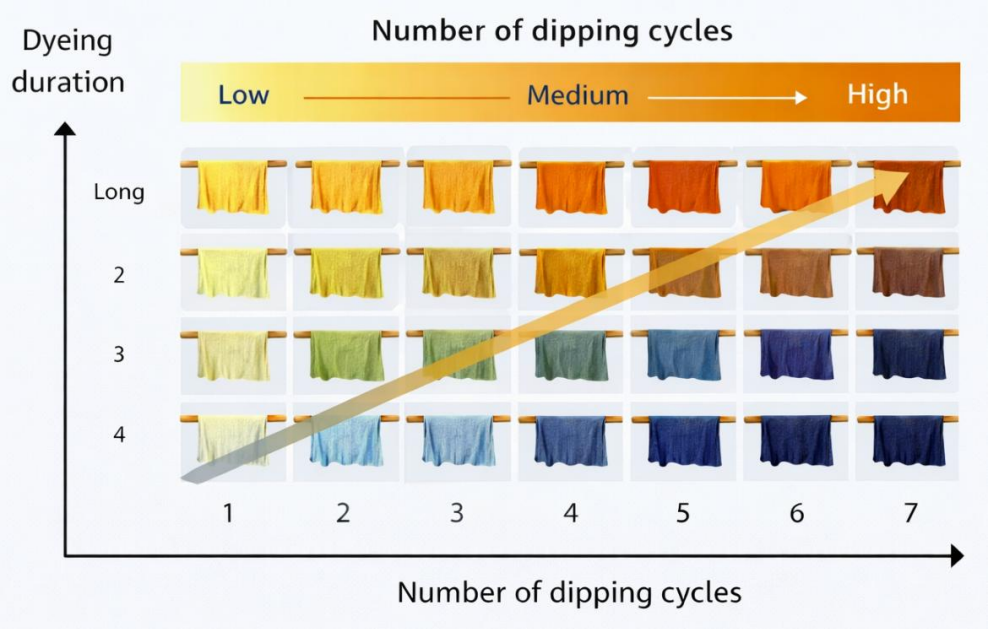

Figure 3. Relationship between dyeing duration, number of dipping cycles, and observed color intensity in plant-based natural dyeing

Table 3. Types of residual materials generated during dyeing and their observed handling practices

Residual type	Source process	Physical form	Observed handling practice
Spent indigo dye solution	Leaf fermentation and dyeing	Liquid	Reused when possible; settled before discharge
Spent dye solution (non-indigo)	Boiling/decoction of plant materials	Liquid	Settled before discharge
Fermented leaf residues	Indigo dye preparation	Solid	Manually removed; disposed of as organic waste
Bark and wood residues	Boiling/decoction processes	Solid	Manually removed; disposed of as organic waste

Liquid residues consisted primarily of spent dye solutions derived from indigo fermentation and aqueous extraction of non-indigo dye plants. These residues were temporarily retained and reused when visible color potential remained, particularly in indigo-based dyeing systems. Once reuse was no longer feasible, liquid residues were subjected to basic settling prior to discharge.

Solid residues included spent leaves, bark, and wood fragments remaining after fermentation or boiling processes. These materials were manually separated from dye solutions and handled as organic waste. No chemical additives or secondary processing steps were applied to either liquid or solid residues during handling.

The classification presented in Table 3 demonstrates that residual material handling was embedded within routine dyeing operations and followed consistent, low-input practices across different dye types.

Discussion

Reported pigment classes associated with dye plants

The plant species documented in this study as natural dye sources (Table 1) are widely reported in the literature to contain distinct classes of plant-derived pigments with biochemical relevance. Although no chemical analyses were conducted in the present work, linking the observed dye plants with previously reported pigment classes provides a contextual framework for interpreting traditional dyeing practices within natural product research.

Indigofera tinctoria is consistently reported as a primary source of indigoid pigments, particularly indigo and indirubin. These pigments originate from indican precursors that undergo enzymatic hydrolysis followed by oxidation, yielding the characteristic blue chromophore widely used in natural dyeing systems. Indigoid compounds are of long-standing interest in pigment chemistry due to their redox-dependent color expression and stability under alkaline conditions (Maugard et al. 2001; Bechtold et al. 2003). The exclusive use of *I. tinctoria* for blue coloration observed in this study aligns with these well-documented biochemical properties.

Caesalpinia sappan has been extensively reported as a source of brazilin and its oxidized derivative brazilein, belonging to the homoisoflavonoid group. These phenolic pigments exhibit pronounced color changes depending on oxidation state and pH, producing red to reddish-brown hues commonly exploited in traditional dyeing. Beyond their chromophoric role, brazilin-type compounds have attracted attention due to their metal-binding behavior and sensitivity to processing conditions (Pizzicato et al. 2023; Vij et al. 2023). The use of *C. sappan* wood as a red dye source in the present study is therefore consistent with reported pigment chemistry.

Yellow dyes derived from *C. javanensis* have been associated in previous studies with flavonoid-related pigments, a broad class of polyphenolic compounds known for their structural diversity and color variability. Flavonoids typically display yellow coloration resulting from conjugated aromatic systems and are sensitive to extraction method and pH conditions (Mansour 2018). Although the exact pigment composition of *C. javanensis* was not analyzed here, its application as a yellow dye source corresponds with these reported characteristics.

Other dye plants recorded in this study, including *S. mahagoni*, *T. grandis*, and *Acacia* spp., are reported to contain phenolic compounds and tannin-related pigments that contribute to brown or dark color tones. Tannins and related polyphenols are commonly associated with bark- and wood-derived dyes and are known for their affinity to textile fibers and role in color fixation (Samanta and Konar 2011; Pisitsak et al. 2016). The use of these species as sources of brown coloration observed in the present work reflects this broader pattern.

In addition to pigment-producing plants, *S. fasciculata* is widely reported as a natural source of alum-related mordant compounds, rather than as a direct pigment source. Its inclusion in the dyeing system supports color fixation by enhancing pigment-fiber interactions, a role well documented in traditional dyeing literature (Shahid et al. 2013). This functional distinction underscores the integrated use of different plant materials within traditional dyeing systems.

The reported pigment classes associated with each dye plant documented in this study are summarized in Table 4. Importantly, this table represents a synthesis of published literature rather than the results of chemical characterization conducted in the present work. By explicitly distinguishing observational findings from literature-based pigment associations, this study maintains methodological transparency while situating traditional dye plants within a biochemical and natural product context.

Table 4. Reported pigment classes associated with plant species used as natural dyes

Plant species	Plant part used	Reported pigment class	Representative compounds (reported)	Key literature sources
Indigofera tinctoria	Leaves	Indigoid pigments	Indigo, indirubin	Bechtold et al. (2003), Maugard et al. (2001) and Arista et al. (2024)
Caesalpinia sappan	Wood	Homoisoflavonoids	Brazilin, brazilein	Vij et al. (2023) and Pizzicato et al. (2023)
Cudrania javanensis	Wood	Flavonoid-related pigments	Flavones, flavonols	Darshi et al. (2019) and Maula et al. (2025)
Swietenia mahagoni	Bark	Phenolic compounds/ tannins	Condensed tannins	Syame et al. (2022) and Bakar et al. (2023)
Tectona grandis	Leaves	Phenolic pigments	Anthraquinone- and flavonoid-related compounds	Godghate and Sawant (2014) and Montri et al. (2025)
Acacia spp.	Bark	Tannin-rich polyphenols	Catechin-based tannins	Haslam (1989), Seigler (2003) and Pizzi (2008)
Symplocos fasciculata	Bark	Alum-related mordant compounds	Aluminum-containing mineral complexes	Cardon (2007) and Laksono and Subiyati (2021)

Traditional dyeing as a low-input pigment processing system

Traditional dyeing practices observed in this study can be interpreted as low-input pigment processing systems, in which color development and fixation are achieved through the manipulation of physical and chemical process variables rather than through synthetic modification of dye molecules. Fermentation, pH adjustment, and repeated dye application function collectively to regulate pigment solubility, transformation, and deposition on textile fibers. This process-based control mechanism distinguishes traditional dyeing from industrial dye production, where pigment properties are typically standardized through chemical synthesis and auxiliary additives.

Fermentation plays a central role in indigo-based dyeing systems and represents a biologically mediated transformation process. In indigo dyeing, enzymatic or microbial hydrolysis converts precursor compounds into soluble intermediates that can later be oxidized to form the insoluble indigo pigment. Similar fermentation-driven transformations have been described in traditional dyeing systems across Asia and Africa, where microbial activity governs pigment availability under ambient conditions (Maugard et al. 2001; Bechtold et al. 2003; Cardon 2007). From a biochemical perspective, such systems provide natural examples of redox-controlled pigment chemistry occurring without external catalysts or high-energy inputs.

Adjustment of dye bath pH, commonly achieved using alkaline materials such as calcium oxide, represents another key variable influencing pigment behavior. pH governs pigment ionization state, solubility, and affinity for textile fibers, thereby directly affecting color intensity and stability. Numerous studies on plant-derived pigments have demonstrated strong pH sensitivity, particularly for indigoids, flavonoids, and phenolic compounds (Vankar 2000; Saxena and Raja 2014; Mansour 2018). In traditional dyeing, pH adjustment is conducted empirically, yet the observed outcomes mirror fundamental principles of pigment chemistry described in laboratory-based studies.

Repeated dipping and drying cycles further illustrate how traditional systems achieve color modulation through incremental pigment accumulation. Rather than relying on high pigment concentrations in a single application, color depth is gradually built through successive exposure and oxidation or fixation steps. This approach parallels adsorption-based models of pigment deposition, where repeated contact enhances binding efficiency and uniformity (Kamel et al. 2005; Renita et al. 2023). Such process-driven control offers an alternative perspective to conventional dye chemistry, emphasizing temporal modulation over compositional alteration.

Compared with synthetic dye systems, which prioritize uniformity and reproducibility through chemically defined formulations, plant-based dyeing systems exhibit inherent variability. However, this variability is not random; it is structured by controllable process parameters such as time, pH, and repetition. Recent discussions in green chemistry and sustainable materials research highlight that such variability can be reframed as functional adaptability rather than as a limitation, particularly when low environmental impact and resource efficiency are prioritized (Kant 2012; Periyasamy 2024).

The low-input nature of traditional dyeing systems also aligns with broader efforts to develop sustainable pigment processing strategies. The absence of synthetic auxiliaries, operation under ambient conditions, and reliance on aqueous extraction and biological transformation position traditional dyeing as a practical model for eco-compatible pigment utilization. Studies in natural product research increasingly recognize traditional processing knowledge as a valuable source of insight for designing alternative pigment systems that balance functionality with sustainability (Al-Tohamy et al. 2022; Islam et al. 2023).

Taken together, the observed dyeing practices demonstrate that traditional systems operate as integrated pigment processing frameworks, in which fermentation, pH regulation, and repeated application collectively govern pigment behavior. These systems provide empirically validated examples of how plant-derived pigments can be effectively processed and applied using minimal inputs, offering conceptual relevance for contemporary natural product and biochemical studies focused on pigment stability, transformation, and application.

Comparison with synthetic dyes from a pigment perspective

From a pigment perspective, synthetic dyes and plant-derived dyes represent two fundamentally different paradigms of color generation and control. Synthetic dyes are designed to achieve high consistency, reproducibility, and predictability, with chromophoric structures chemically engineered to deliver specific color properties under standardized conditions. The production and application of synthetic pigments typically rely on controlled chemical synthesis, precise formulation, and the use of auxiliary agents to stabilize color expression and fiber binding. This approach enables uniform coloration at an industrial scale but requires substantial material inputs and tightly regulated processing conditions (Periyasamy 2024; Negi 2025).

In contrast, plant-derived dyes operate within a process-controlled framework rather than a compositionally fixed system. Dynamic interactions between pigment precursors, extraction conditions, pH, and application sequence shape color outcomes in plant-based dyeing. Variability in color intensity and hue is therefore an inherent feature of plant-derived pigments, reflecting differences in processing rather than inconsistency in pigment identity. Recent discussions in *Green Chemistry* and *Molecules* emphasize that such variability can be strategically managed through process optimization, without requiring chemical modification of pigment structures (Bechtold and Mussak 2009; Kant 2012; Renita et al. 2023).

The contrast between chemical control and process control is particularly evident in how color stability is achieved. Synthetic dyes rely on molecular design and stabilizing additives to maintain color performance across diverse conditions. Plant-derived dyes, by contrast, achieve functional stability through repeated application, controlled exposure, and the use of natural mordants or pH adjustments. Although these approaches differ fundamentally, both systems aim to regulate pigment-fiber interactions to achieve durable coloration. Conceptually, traditional dyeing systems thus demonstrate alternative strategies for pigment stabilization that do not depend on synthetic auxiliaries (Bechtold et al. 2007; Yusuf et al. 2017).

From a natural product research perspective, the distinction between synthetic and plant-derived pigments highlights complementary strengths rather than a binary hierarchy. Synthetic pigments offer benchmarks for consistency and scalability, while plant-derived pigments provide models for studying pigment behavior under biologically and chemically dynamic conditions. Reviews in *Green Chemistry* and *Molecules* increasingly recognize plant-based pigments as valuable systems for exploring structure-function relationships, particularly in relation to pH sensitivity, redox behavior, and process-driven modulation of color expression (Castañeda-Ovando et al. 2009; Yusuf et al. 2017).

Importantly, the present study does not attempt to evaluate the efficiency or environmental performance of plant-derived dyes relative to synthetic dyes. Instead, the comparison is framed at a conceptual level, focusing on how different pigment systems achieve color control through distinct mechanisms. By situating traditional dyeing practices within this comparative framework, plant-based dyeing can be understood as a process-centered pigment system with relevance to contemporary discussions on alternative pigment technologies.

Implications for natural product and biochemical research

The findings of this study highlight the relevance of traditional dye plants not only as cultural or artisanal materials, but also as candidate sources of plant-derived pigments with potential importance for natural product and biochemical research. By documenting plant species actively used in dyeing systems and linking them with reported pigment classes, this work provides a structured foundation for identifying botanical candidates suitable for further biochemical investigation.

Traditional dye plants represent model systems for studying pigment behavior under process-driven conditions. Unlike laboratory-isolated pigments examined under controlled analytical settings, pigments in traditional dyeing systems undergo transformation, deposition, and stabilization through dynamic interactions with pH, redox conditions, and repeated exposure. Such systems offer empirical contexts for examining pigment stability and transformation pathways that are often simplified or abstracted in experimental models (Samanta and Agarwal 2009; Iqbal and Ansari 2021).

One area of particular relevance is pH-dependent color expression, a defining characteristic of many plant-derived pigments, including indigoids, flavonoids, and phenolic compounds. Traditional practices involving alkaline conditioning and repeated oxidation steps provide natural analogs for studying how pH influences pigment solubility, chromophore structure, and color manifestation. These process-induced responses mirror fundamental biochemical principles governing pigment behavior and can inform experimental designs in pigment chemistry (Maugard et al. 2001; Pizzicato et al. 2023).

Additionally, the observed reliance on process-driven pigment modulation-such as repeated dipping and controlled exposure-underscores the importance of application dynamics in determining color outcomes. Rather than treating pigment performance as an intrinsic chemical property alone, traditional dyeing systems emphasize the role of operational variables in shaping functional expression. This perspective aligns with emerging research trends that frame pigment behavior as an interaction between molecular structure and processing context (Yusuf et al. 2017; Renita et al. 2023).

From a methodological standpoint, the present study delineates clear boundaries between observational documentation and biochemical inference. While no analytical characterization was conducted here, the documented dye plants and processing conditions provide clear targets for future biochemical validation, including chromatographic profiling, spectroscopic characterization, and stability assessment under controlled conditions. Such follow-up studies could elucidate structure-function relationships and quantify pigment responses to pH, redox state, and processing intensity.

In this context, traditional dyeing systems can be viewed as knowledge-rich platforms that inform hypothesis generation rather than as substitutes for analytical research. Integrating observational data from traditional practices with modern biochemical techniques offers a promising pathway for advancing the study of plant-derived pigments within natural product research.

In conclusion, this study documents the use of seven plant species as natural dye sources in traditional batik production at Batik Tjap Tiga Negeri, Laweyan, Surakarta. The recorded species-*I. tinctoria*, *C. sappan*, *C. javanensis*, *S. mahagoni*, *S. fasciculata*, *T. grandis*, and *Acacia* spp.-provide pigments derived from leaves, bark, and wood tissues. Indigo dyeing relied exclusively on *I. tinctoria* leaves through fermentation, alkalization, and oxidation, while non-indigo dyes were obtained via aqueous heat-based extraction of woody materials. The findings indicate that color outcomes are primarily governed by processing parameters, including fermentation, pH adjustment, and repeated application, rather than chemical modification of pigment structures. These practices represent low-input processing strategies that allow modulation of color intensity through operational control. By integrating observational evidence with literature on indigoids, flavonoid-related pigments, and tannin-rich polyphenols, this study provides a framework for understanding process-driven pigment behavior. Future research combining analytical characterization with traditional process knowledge is needed to validate pigment composition and evaluate the generality of process-color relationships across batik systems.

REFERENCES

Alegbe EO, Uthman TO. 2024. A review of history, properties, classification, applications, and challenges of natural and synthetic dyes. Heliyon 10 (13): e33646. DOI: 10.1016/j.heliyon.2024.e33646.

Al-Tohamy R, Ali SS, Li F, Okasha KM, Mahmoud YAG, Elsamahy T, Sun J. 2022. A critical review on the treatment of dye-containing wastewater: Ecotoxicological and health concerns of textile dyes and possible remediation approaches for environmental safety. Ecotoxicol Environ Saf 231 (1): 1-17. DOI: 10.1016/j.ecoenv.2021.113160.

Ardila-Leal LD, Poutou-Piñales RA, Pedroza-Rodríguez AM, Quevedo-Hidalgo B. 2021. A brief history of colour, the environmental impact of synthetic dyes, and removal by using laccases. Molecules 26 (13): 3813. DOI: 10.3390/molecules26133813.

Arista NDI, Aziz SA, Kurniawati A. 2024. Natural dye of Indigofera tinctoria for the textile industry. J Environ Sci Sustain Dev 7 (1): 578-598. DOI: 10.7454/jessd.v7i1.1249.

Backer CA, van den Brink RCB. 1980. Flora of Java Vol I-III. Wolters-Noordhoff, Groningen.

Bakar MA, Islam MI, Mia R, Ahmed T, Mahmud ST, Toki GFI, Haque MA. 2023. Exploring the potential of mahogany extract as a natural dye for the coloration of jute fabric. Heliyon 9 (9): e19464. DOI: 10.1016/j.heliyon.2023.e19464.

Bechtold T, Mahmud-Ali A, Mussak R. 2007. Natural dyes for textile dyeing: A comparison of methods to assess the quality of Canadian goldenrod plant material. Dyes and Pigments 75 (2): 287-293. DOI: 10.1016/j.dyepig.2006.06.004.

Bechtold T, Mussak R. 2009. Handbook of Natural Colorants. John Wiley & Sons, Chichester, USA. DOI: 10.1002/9780470744970.

Bechtold T, Turcanu A, Ganglberger E, Geissler S. 2003. Natural dyes in modern textile dyehouses - how to combine experiences of two centuries to meet the demands of the future? J Clean Prod 11 (5): 499-509. DOI: 10.1016/S0959-6526(02)00077-X.

Cardon D. 2007. Natural Dyes: Sources, Tradition, Technology and Science. Archetype Publications, London.

Castañeda-Ovando A, Pacheco-Hernández ML, Páez-Hernández ME, Rodríguez JA, Galán-Vidal CA. 2009. Chemical studies of anthocyanins: A review. Food Chem 113 (4): 859-871. DOI: 10.1016/j.foodchem.2008.09.001.

Castillo-Suárez LA, Sierra-Sánchez AG, Linares-Hernández I, Martínez-Miranda V, Teutli-Sequeira EA. 2023. A critical review of textile industry wastewater: Green technologies for the removal of indigo dyes. Intl J Environ Sci Technol 20 (9): 10553-10590. DOI: 10.1007/s13762-023-04810-2.

Darshi C, Lestari DW, Pratiwi D, Indrianingsih AW, Rosyida VT, Apriyana W, Nisa K, Hayati SN, Handayani S, Purnami M. 2019. Dyeing of cotton fabric with natural dye from *Cudrania javanensis* using soka (*Ixora javanica*) leaves extract as bio-mordant. Din Kerajinan Batik 36 (2): 105-112. DOI: 10.22322/dkb.v36i2.4149.

Fried R, Oprea I, Fleck K, Rudroff F. 2022. Biogenic colourants in the textile industry - a promising and sustainable alternative to synthetic dyes. Green Chem 24 (1): 13-35. DOI: 10.1039/D1GC02968A.

GBIF. 2026. Global Biodiversity Information Facility. https://www.gbif.org.

Godghate AG, Sawant RS. 2014. Phytochemical analysis of leaves of *Tectona grandis* Linn. Intl J Pharma Bio Sci 5 (1): 355-359.

Haslam E. 1989. Plant Polyphenols: Vegetable Tannins Revisited. Cambridge Univ Press, Cambridge, UK.

IPNI. 2026. International Plant Names Index. https://www.ipni.org.

Iqbal S, Ansari TN. 2021. Extraction and application of natural dyes. In: Rather LJ, Shabbir M, Haji A (eds). Sustainable Practices in the Textile Industry. Wiley, Hoboken. DOI: 10.1002/9781119818915.ch1.

Islam T, Repon MR, Islam T, Sarwar Z, Rahman MM. 2023. Impact of textile dyes on health and ecosystem: A review of structure, causes, and potential solutions. Environ Sci Pollut Res 30 (4): 9207-9242. DOI: 10.1007/s11356-022-24398-3.

Kamel MM, El-Shishtawy RM, Yussef BM, Mashaly H. 2005. Ultrasonic assisted dyeing: III. Dyeing of wool with lac as a natural dye. Dyes Pigments 65: 103-110. DOI: 10.1016/j.dyepig.2004.06.003.

Kant R. 2012. The textile dyeing industry is an environmental hazard. Nat Sci 4 (1): 22-26. DOI: 10.4236/ns.2012.41004.

Laksono AI, Subiyati S. 2021. Pengaruh metode mordan alam daun Simplokos pada pencapan kain kapas dengan zat warna alam daun marenggo (*Chromolaena odorata* L). Pros Semin Nas Ind Kerajinan Batik (SNIKB) 2021. Yogyakarta, 6-7 Oktober 2021. [Indonesian]

Ling TC, Inta A, Armstrong KE, Little DP, Tiansawat P, Yang YP, Phokasem P, Tuang ZK, Sinpoo C, Disayathanoowat T. 2022. Traditional knowledge of textile dyeing plants: A case study in the Chin ethnic group of western Myanmar. Diversity 14 (12): 1065. DOI: 10.3390/d14121065.

Mansour R. 2018. Natural dyes and pigments: Extraction and applications. In: Yusuf M (eds). Handbook of Renewable Materials for Coloration and Finishing. Wiley, Hoboken. DOI: 10.1002/9781119407850.ch5.

Maugard T, Enaud E, Choisy P, Legoy MD. 2001. Identification of an indigo precursor from leaves of *Isatis tinctoria* (woad). Phytochemistry 58 (6): 897-904. DOI: 10.1016/S0031-9422(01)00335-1.

Maula VA, Rahayuningsih E, Mindaryani A. 2025. Dyeing and isotherm adsorption of natural dye from tegeran (*Cudrania javanensis* Trecul) on cotton fabric. AIP Conf Proc 3295: 060006. DOI: 10.1063/5.0272993.

Montri N, Wanapat M, Kang S, Cheas S, Cherdthong A, Gunun P, Nirwan G, Foiklang S, Kongmun P, Polyorach S. 2025. Exploring *Tectona grandis* Linn. f. leaf extract as a functional feed additive with antioxidant and nutraceutical potential for livestock. Animals 15 (23): 3498. DOI: 10.3390/ani15233498.

Moreira VR, Lebron YAR, Couto CF, Maia A, Moravia WG, Amaral MCS. 2022. Process development for textile wastewater treatment towards zero liquid discharge. Process Saf Environ Prot 157 (1): 537-546. DOI: 10.1016/j.psep.2021.10.037.

Negi A. 2025. Natural dyes and pigments: Sustainable applications and future scope. Sustain Chem 6 (3): 23. DOI: 10.3390/suschem6030023.

Periyasamy AP. 2024. Recent advances in the remediation of textile-dye-containing wastewater. Sustainability 16 (2): 1-41. DOI: 10.3390/su16020495.

Pisitsak P, Hutakamol J, Thongcharoen R, Phokaew P, Kanjanawan K, Saksang N. 2016. Improving the dyeability of cotton with tannin-rich

natural dye through pretreatment with whey protein isolate. Ind Crop Prod 79: 47-56. DOI: 10.1016/j.indcrop.2015.10.043.

Pizzi A. 2008. Tannins: Major sources, properties, and applications. In: Belgacem MN, Gandini A (eds). Monomers, Polymers, and Composites from Renewable Resources. Elsevier, Oxford. Pp 179-199. DOI: 10.1016/B978-0-08-045316-3.00008-9.

Pizzicato B, Pacifico S, Cayuela D, Mijas G, Riba-Moliner M. 2023. Advancements in sustainable natural dyes for textile applications: A review. Molecules 28 (16): 1-22. DOI: 10.3390/molecules28165954.

POWO. 2026. Plants of the World Online. Royal Botanic Gardens, Kew. https://powo.science.kew.org.

Renita AA, Gajaria TK, Sathish S, Kumar JA, Lakshmi DS, Kujawa J, Kujawski W. 2023. Progress and prospects of the industrial development and applications of eco-friendly colorants. Foods 12 (7): 15-21. DOI: 10.3390/foods12071521.

Samanta AK, Agarwal P. 2009. Application of natural dyes on textiles. Indian J Fibre Text Res 34: 384-399.

Samanta AK, Konar A. 2011. Dyeing of textiles with natural dyes. In: Akcakoca Kumbasar EP (eds). Natural Dyes. IntechOpen, London. DOI: 10.5772/21341.

Saxena S, Raja ASM. 2014. Natural dyes: Sources, chemistry, application, and sustainability issues. In: Muthu S (eds). Roadmap to Sustainable Textiles and Clothing. Textile Science and Clothing Technology. Springer, Singapore. DOI: 10.1007/978-981-287-065-0_2.

Seigler DS. 2003. Phytochemistry of *Acacia*-sensu lato. Biochem Syst Ecol 31 (8): 845-873. DOI: 10.1016/S0305-1978(03)00082-6.

Shahid M, Shahid-ul-Islam, Mohammad F. 2013. Recent advancements in natural dye applications: A review. J Clean Prod 53: 310-331. DOI: 10.1016/j.jclepro.2013.03.031.

Snyder H. 2019. Literature review as a research methodology: An overview and guidelines. J Bus Res 104: 333-339. DOI: 10.1016/j.jbusres.2019.07.039.

Suheryanto D. 2017. Natural Dyes: Ensiklopedia Zat Warna Alami dari Tumbuhan untuk Industri Batik. Andi Offset, Yogyakarta. [Indonesian]

Syame SM, Mohamed SM, Elgabry EA. 2022. Chemical characterization, antimicrobial, antioxidant, and cytotoxic potentials of *Swietenia mahagoni*. AMB Expr 12: 77. DOI: 10.1186/s13568-022-01406-w.

Vankar PS. 2000. Chemistry of natural dyes. Resonance 5: 73-80. DOI: 10.1007/BF02836844.

Vij T, Anil PP, Shams R, Dash KK, Kalsi R, Pandey VK, Harsányi E, Kovács B, Shaikh AM. 2023. A comprehensive review of bioactive compounds found in *Caesalpinia sappan*. Molecules 28 (17): 6247. DOI: 10.3390/molecules28176247.

Whitmore TC, Tantra IGM, Sutisna U. 1986. Tree Flora of Indonesia: Checklist for Sumatra. Forest Research and Development Centre, Bogor, Indonesia.

Wouyou HG, Avocevou-Ayisso C, Idohou R, Assogbadjo SC, Houndonougbo JSH, Assogbadjo AE. 2025. Current knowledge and prospects of African plants providing natural dyes: A systematic review. Discover Plants 2 (1): 1-71. DOI: 10.1007/s44372-025-00234-z.

Yusuf M, Shabbir M, Mohammad F. 2017. Natural colorants: Historical, processing and sustainable prospects. Nat Prod Bioprospect 7: 123-145. DOI: 10.1007/s13659-017-0119-9.